

AD-A016 565

CYLINDRICAL LANGMUIR PROBE MEASUREMENTS FROM ROCKET  
FLIGHTS COVERING THE PERIOD 31 JANUARY 1969 THROUGH  
3 APRIL 1974

Robert C. Wilson

Boston College

Prepared for:

Air Force Cambridge Research Laboratories

30 April 1975

DISTRIBUTED BY:

**NTIS**

National Technical Information Service  
U. S. DEPARTMENT OF COMMERCE

310077

AD A 016565  
AFCRL-TR-75-0265

# Cylindrical Langmuir Probe Measurements from Rocket Flights Covering the Period 31 January 1969 thru 3 April 1974

by

Robert C. Wilson

Space Data Analysis Laboratory

Department of University Research

Boston College

Chestnut Hill, Massachusetts 02167

30 APRIL 1975

SCIENTIFIC REPORT NO. 1 & 2.

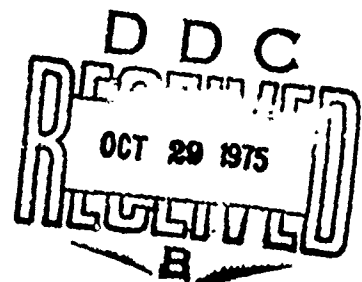
Approved for public release; distribution-unlimited.

AIR FORCE CAMBRIDGE RESEARCH LABORATORIES

AIR FORCE SYSTEMS COMMAND

UNITED STATES AIR FORCE

HANSCOM AFB, MASSACHUSETTS 01731



Reproduced by  
NATIONAL TECHNICAL  
INFORMATION SERVICE  
US Department of Commerce  
Springfield, VA 22151

Qualified requestors may obtain additional copies from the Defense Documentation Center. All others should apply to the National Technical Information Service.

ACCESSION NO.		
NTIS	White Section	<input checked="checked" type="checkbox"/>
DDC	Diff Section	<input type="checkbox"/>
UNANNOUNCED		<input type="checkbox"/>
JUSTIFICATION .....		
BY .....		
DISTRIBUTION/AVAILABILITY CODES		
Dist.	Avail. and/or SPECIAL	
A		

REPORT DOCUMENTATION PAGE		READ INSTRUCTIONS BEFORE COMPLETING FORM
1. REPORT NUMBER AFCRL-TR-75-0265	2. GOVT ACCESSION NO.	3. RECIPIENT'S CATALOG NUMBER
4. TITLE (and Subtitle) CYLINDRICAL LANGMUIR PROBE MEASUREMENTS FROM ROCKET FLIGHTS COVERING THE PERIOD 31 JANUARY 1969 THROUGH 3 APRIL 1974		5. TYPE OF REPORT & PERIOD COVERED Scientific - Interim
7. AUTHOR(s) Robert C. Wilson		6. PERFORMING ORG. REPORT NUMBER Scientific Report No. 1 & 2
9. PERFORMING ORGANIZATION NAME AND ADDRESS Trustees of Boston College Chestnut Hill, Massachusetts 02167		8. CONTRACT OR GRANT NUMBER(s) F19628-72-C-0089
11. CONTROLLING OFFICE NAME AND ADDRESS Air Force Cambridge Research Laboratories Hanscom AFB, Massachusetts 01731 Contract Monitor: John Sandock/OPR		10. PROGRAM ELEMENT, PROJECT, TASK AREA & WORK UNIT NUMBERS 7663-01-01 62101F
14. MONITORING AGENCY NAME & ADDRESS (if different from Controlling Office)		12. REPORT DATE April 30, 1975
		13. NUMBER OF PAGES 121
		15. SECURITY CLASS. (of this report) Unclassified
		15a. DECLASSIFICATION/DOWNGRADING SCHEDULE
16. DISTRIBUTION STATEMENT (of this Report)  Approved for public release; distribution unlimited		
17. DISTRIBUTION STATEMENT (of the abstract entered in Block 20, if different from Report)		
18. SUPPLEMENTARY NOTES		
19. KEY WORDS (Continue on reverse side if necessary and identify by block number)  Cylindrical Langmuir Probe      Electron Current PCA-69      Positive Ion Current Experimental Measurements		
20. ABSTRACT (Continue on reverse side if necessary and identify by block number)  The current measurements made by cylindrical Langmuir probe systems flown on NIRO and Ute-Tomahawk vehicles are described. Particular emphasis is placed on the electron current and positive ion current.  (Cont.)		

~~UNCLASSIFIED~~

~~SECURITY CLASSIFICATION OF THIS PAGE(When Data Entered)~~

20. (Cont.)

Measurements were made over an altitude range extending from 60 kilometers to 145 kilometers, thus, encompassing the D- and E- regions.

The development of the electronic instrumentation is presented.

~~UNCLASSIFIED~~

~~SECURITY CLASSIFICATION OF THIS PAGE(When Data Entered)~~

# TABLE OF CONTENTS

	<u>PAGE</u>
TABLE OF CONTENTS	iii
LIST OF ILLUSTRATIONS	iv
LIST OF TABLES	vii
INTRODUCTION	1
TABLE OF VEHICLES	2
LANGMUIR PROBE THEORY	3
LANGMUIR PROBE INSTRUMENTATION	6
RESULTS	
(1) Results From NIRO AT7.891	8
(2) Results From NIRO AH7.890	9
(3) Results From NIRO AH7.892	10
(4) Results From NIRO A07.902-9	10
(5) Results From NIRO AT7.896	11
(6) Results From NIRO A07.902-6	11
(7) Results From NIRO A07.101-3	13
(8) Results From NIRO A07.101-4	13
(9) Results From NIRO A07.101-2	14
(10) Results From NIRO A07.001-1	14
(11) Results From Ute Tomahawk A09.303-3	15
(12) Results From Ute Tomahawk A09.303-4	16
APPENDIX	18
ILLUSTRATIONS	20
REFERENCES	112

# LIST OF ILLUSTRATIONS

<u>FIGURE</u>		<u>PAGE</u>
1	Theoretical Semi-Log Plot of Electrode Current	21
2	Block Diagram of Langmuir Probe Model LP68B	22
3	Block Diagram of Langmuir Probe Model LP69C	23
4	Block Diagram of Langmuir Probe Model LP70A	24
5	Block Diagram of Langmuir Probe Model LP71B	25
6	Electron Current Amplifier Calibration for LP 68B-4	26
7	Positive Ion Current Amplifier Calibration for LP 68B-4	27
8	Electron Current Amplifier Calibration for LP 68B-5A	28
9	Positive Ion Current Amplifier Calibration for LP 68B-5A	29
10	Electron Current Amplifier Calibration for LP 68B-10A	30
11	Positive Ion Current Amplifier Calibration for LP 68B-10A	31
12	Electron Current Amplifier Calibration for LP 69C-6	32
13	Positive Ion Current Amplifier Calibration for LP 69C-6	33
14	Electron Current Amplifier Calibration for LP 70A-2	34
15	Positive Ion Current Amplifier Calibration for LP 70A-2	35
16	Electron Current Amplifier Calibration for LP 70A-3	36
17	Positive Ion Current Amplifier Calibration for LP 70A-3	37
18	Electron Current Amplifier Calibration for LP 71B-1	38
19	Positive Ion Current Amplifier Calibration for LP 71B-1	39
20	Electron Current Amplifier Calibration for LP 71B-4	40
21	Positive Ion Current Amplifier Calibration for LP 71B-4	41
22	Electron Current Amplifier Calibration for LP 71B-2	42
23	Positive Ion Current Amplifier Calibration for LP 71B-2	43
24	Electron Current Amplifier Calibration for LP 71B-3	44
25	Positive Ion Current Amplifier Calibration for LP 71B-3	45
26	Electron Current Amplifier Calibration for LP 71B-8	46
27	Positive Ion Current Amplifier Calibration for LP 71B-8	47
28	Electron Current Amplifier Calibration for LP 71B-9	48
29	Positive Ion Current Amplifier Calibration for LP 71B-9	49
30	Langmuir Probe Function Generator Waveform LP 68B-4	50
31	Langmuir Probe Function Generator Waveform LP 68B-5A and LP68B-10A	51
32	Langmuir Probe Function Generator Waveform LP 70A and LP 71B-1,2,3,4.	52
33	Langmuir Probe Function Generator Waveform LP 71B-8, 9	53
34	Flight Trajectory for NIRO AT 7.891	54

<u>FIGURE</u>		<u>PAGE</u>
35	Vehicle Potential Measurements for AT 7.891	55
36	Electron Current Versus Altitude AT 7.891	56
37	Positive-Ion Current Measurement at -3 Volts Versus Altitude for AT 7.891	57
38	Positive-Ion Current Measurement at -9 Volts Versus Altitude for AT 7.891	58
39	Flight Trajectory for NIRO AH 7.890	59
40	Positive-Ion Current Measurement at -3 Volts Versus Altitude for AH 7.890	60
41	Strip Chart Data Between 77.6 KM - 81.7 KM for AH 7.890	61
42	Strip Chart Data	62
43	Strip Chart Data at Vehicle Apogee for AH 7.890	63
44	Strip Chart Data on Vehicle Descent Between 90.25KM and 87.3 KM - AH 7.890	64
45	Strip Chart Data on Vehicle Descent Between 61.9 KM and 57.75 KM - AH 7.890	65
46	Strip Chart Data Between $T_0 + 59$ secs and $T_0 + 64$ secs for AH 7.892	66
47	Strip Chart Data Between $T_0 + 90$ secs and $T_0 + 94$ secs for AH 7.892	67
48	Strip Chart Data Between $T_0 + 155$ secs and $T_0 + 159$ secs for AH 7.892	68
49	Strip Chart Data Between $T_0 + 202$ secs and $T_0 + 206$ secs for AH 7.892	69
50	Vehicle Potential Measurement for AH 7.892	70
51	Electron Current Measurement Versus Time After Rocket Launch for AH 7.892	71
52	Positive-Ion Current Measurement at -9 Volts Versus Time After Rocket Launch for AH 7.892	72
53	Positive-Ion Current Measurement At -3 volts Versus Time After Rocket Launch for AH 7.892	73
54	Electron Current Versus Time After Launch for AO 7.902-9	74
55	Strip Chart Data Between $T_0 + 136$ sec and $T_0 + 140$ sec for AO 7.902-9	75
56	Strip Chart Data Between $T_0 + 169$ sec and $T_0 + 173$ sec For AO 7.902-9	76
57	Strip Chart Data Between $T_0 + 201$ sec and $T_0 + 206$ sec for AO 7.902-9	77
58	Strip Chart Data Between $T_0 + 218$ sec and $T_0 + 223$ sec for AO 7.902-9	78
59	Vehicle Trajectory for NIRO AT 7.896	79
60	Vehicle Trajectory for NIRO AO 7.902-6	80
61	Vehicle Potential Measurement for NIRO AO 7.902-6	81
62	Strip Chart Data Near Rocket Apogee for NIRO AO 7.902-6	82
63	Strip Chart Data Between 96.46 KM and 102.35 Kilometers for AO 7.902-6	83
64	Strip Chart Data Between 109.85 KM and 105.46 KM for AO 7.902-6	84
65	Strip Chart Data Between 93.89 KM and 86.7 KM for AO 7.902-6.	85
66	Positive-Ion Current Measurements at -3 Volts for NIRO AO 7.902-6	86
67	Positive-Ion Current Measurements at -8 Volts for NIRO AO 7.902-6.	87
68	Vehicle Trajectory for NIRO AO 7.101-4	88
69	Vehicle Potential Measurements for NIRO AO 7.101-4	89
70	Electron Current Measurements for NIRO AO 7.101-4	90
71	Positive-Ion Current Measurements at -9 Volts for NIRO AO 7.101-4	91



<u>FIGURE</u>		<u>PAGE</u>
72	Positive-Ion Current Measurements at -3 Volts for NIRO AO 7.101-4	92
73	Vehicle Trajectory for NIRO AO 7.001-1	93
74	Strip Chart Data Between $T_0 + 123$ sec and $T_0 + 128$ sec for NIRO AO 7.001-1	94
75	Strip Chart Data Between $T_0 + 155$ sec and $T_0 + 159$ sec for NIRO AO 7.001-1	95
76	Electron Current Measurements for NIRO AO 7.001-1	96
77	Vehicle Trajectory for Ute-Tomahawk AO 9.303-3	97
78	Vehicle Potential Measurements for Ute-Tomahawk AO 9.303-3	98
79	Electron Current Measurements for AO 9.303-3	99
80	Positive-Ion Current Measurement at -9 Volts for AO 9.303-3	100
81	Positive-Ion Current Measurement at -3 Volts for AO 9.303-3	101
82	Vehicle Trajectory for Ute-Tomahawk AO 9.303-4	102
83	Vehicle Potential Measurements for Ute-Tomahawk AO 9.303-4	103
84	Electron Current Measurements for AO 9.303-4	104
85	Positive-Ion Current Measurements at -9 Volts for Ute-Tomahawk AO 9.303-4	105
86	Positive-Ion Current Measurements at -3 Volts for Ute-Tomahawk AO 9.303-4	106
87	Strip Chart Data Between 75.7 KM and 80.6 KM on Vehicle Ascent for AO 9.303-4	107
88	Strip Chart Data Between 97.6 KM and 101.3 KM on Vehicle Ascent for AO 9.303-4	108
89	Strip Chart Data Between 124.3 KM and 125.5 KM on Vehicle Ascent for AO 9.303-4	109
90	Strip Chart Data Between 126.67 KM and 125.72 KM on Vehicle Descent for AO 9.303-4	110
91	Strip Chart Data Between 103.96 KM and 101.17 KM on Vehicle Descent for AO 9.303-4	111

## LIST OF TABLES

TABLE		PAGE
1	Langmuir Probes	2
2	Rocket Vehicle and Probe Configuration	5
3	Rocket Vehicle and Corresponding Langmuir Probe	6

## INTRODUCTION

An examination of the ionosphere was made by rocketborne cylindrical Langmuir probes under various disturbed ionospheric conditions. It is the purpose of this report to present the electron currents, positive ion currents and vehicle potentials measured by the probe.

In total, twelve rocket flights were examined, ten of the NIRO type and two of the Ute-Tomahawk type. The flights were flown over a period extending from 31 January 1969 through 3 April 1974. The rockets considered in this report are listed in Table 1.

TABLE 1

## LANGMUIR PROBES

<u>VEHICLE NO.</u>	<u>DATE</u>	<u>TIME (Z)</u>	<u>PLACE</u>	<u>PROB I.D.</u>	<u>EVENT</u>
AT 7.891	31 Jan 69	17-30-00	Wallops	LP68B-4	Winter Anomaly
AH 7.890	11 Oct 69	2-00-00	Churchill	LP68B-5A	PCA-69 Certification
AI 7.892	7 Nov 69	2-51-00	Churchill	LP68B-10A	Post PCA-69
AO 7.902-9	7 Mar 70	18-37-30	Wallops	LP69C-6	Eclipse
AT 7.896	20 Nov 70	23-23-14	Eglin	LP70A-2	Aladdin Prog. I
AO 7.902-6	6 Oct 71	10-00-00	Wallops	LP70A-3	Pre-Sunrise Program
AO 7.101-3	6 Oct 71	10-11-00	Wallops	LP71B-1	Sunrise Program
AO 7.101-4	6 Oct 71	10-44-00	Wallops	LP71B-4	Post-Sunrise Program
AO 7.101-2	6 Oct 71	11-05-00	Wallops	LP71B-2	Post-Sunrise Program
AO 7.001-1	6 Feb 72	17-15-00	Wallops	LP71B-3	Negative Ion Twilight Studies
AO 9.303-3	28 Mar 74	4-05-00	Churchill	LP71B-8	Auroral Studies
AO 9.303-4	3 Apr 74	19-18-00	Churchill	LP71B-9	Auroral Studies

## LANGMUIR PROBE THEORY

The Langmuir Probe is a useful instrument for determining electron density, positive ion density and electron temperature. Basically, the probe operates by applying a programmed voltage to an electrode immersed in a plasma and then measures the current which flows to the electrode. Analysis of the resulting current-voltage relationships provides information directly related to the electron density, positive ion density and electron temperature. The basic technique in a rarified regime has been described in detail by Langmuir and Mott-Smith (1924)<sup>1</sup> and Smith (1964).<sup>2</sup>

The Langmuir probe described here is a rocket-borne instrument used to measure the following ionospheric parameters:

- (1) Electron density
- (2) Positive-ion density
- (3) Electron temperature
- (4) Vehicle to plasma potential

The Langmuir probe consists of an electrode of known geometry which is immersed in the ionospheric plasma, and an electronics box which applies a voltage waveform to the probe and monitors the current-voltage relationship. The desired parameters can then be calculated from the current-voltage curve such as the one shown in Figure 1 as follows:

- (1) Electron density is proportional to the electrode current in the electron accelerating region.
- (2) Positive-ion density is proportional to the electrode current in the positive ion accelerating region.
- (3) Electron temperature can be found from the expression describing the curve in the exponential part of the electron retarding region. The expression describing the region is

$$i = I_0 \exp\left(\frac{eV}{kT}\right)$$

where

$V$  = negative electrode to plasma voltage

$I_0$  = electron current when the electrode is at space potential  
(point of inflection)

$e$  = electronic charge

$k$  = Boltzmann constant

$T$  = electron temperature

By taking the logarithm of the above expression, the electron temperature is found to be

$$T = \frac{e}{k} \frac{V}{\ln(i/I_0)}$$

- (4) Vehicle to plasma potential is given by the voltage at the point of inflection in the current-voltage curve.

The Langmuir probe electrode is mounted on a pivot parallel to the length of the rocket and is held against a door by a spring. During ascent, when the rocket reaches altitude, the door ejects, allowing the electrode to pivot  $90^\circ$  so that it is perpendicular to the rocket major axis and is immersed in the ionospheric plasma. For those vehicles which employed dual electrodes (Table 2) the probes were mounted  $180^\circ$  apart on the side of the rocket.

TABLE 2

## POCKET VEHICLE AND PROBE CONFIGURATION

<u>VEHICLE</u>	<u>PROBE I.D.</u>	<u>DESIGNER</u>	<u>PROBE CONFIGURATION</u>
AT 7.891	68B-4	Upper Air Research Lab. Univ. of Utah	Dual Electrodes
AH 7.890	68B-5	"	Dual Electrodes
AO 7.902-9	69C-6	"	Dual Electrodes
AH 7.892	68B-10A	Upper Air Research Lab. Univ. of Utah	Dual Electrodes
AT 7.896	70A-2	Space Science Lab. Utah State Univ.*	Single Electrode
AO 7.902-6	70A-3	" *	"
AO 7.101-3	71B-1	" *	"
AO 7.101-4	71B-4	" *	"
AO 7.101-2	71B-2	" *	"
AO 7.101-1	71B-5	" *	"
AO 7.001-1	71B-3	" *	"
AO 9.303-3	71B-8	" *	"
AO 9.303-4	71B-9	Space Science Lab. Utah State Univ.*	Single Electrode

\* Formerly Upper Air Research Lab. Univ. of Utah

# LANGMUIR PROBE INSTRUMENTATION

Four different Langmuir probe models were employed on the rocket vehicles presented in this study, Model LP68B (3 rockets), Model LP69C (1 rocket), Model LP70A (2 rockets) and Model LP71B (6 rockets). These probes were included on each vehicle in accordance with Table 3.

TABLE 3

## ROCKET VEHICLE AND CORRESPONDING LANGMUIR PROBE

<u>VEHICLE NO.</u>	<u>LANGMUIR PROBE S/N</u>
AH 7.890	LP68B-5A
AT 7.891	LP68B-4
AH 7.892	LP68B-10A
AO 7.902-9	LP69C-6
AT 7.896	LP70A-2
AO 7.902-6	LP70A-3
AO 7.101-3	LP71B-1
AO 7.101-2	LP71B-2
AO 7.001-1	LP71B-3
AO 7.101-4	LP71B-4
AO 9.303-3	LP71B-8
AO 9.303-4	LP71B-9

The theory of operation for the various Langmuir probe models is essentially similar. One significant difference, however, was the condition of the output signal prior to transmission to the telemetry system. The block diagrams for each of Langmuir probe models is shown in Figures 2,3,4, and 5. The calibration curves peculiar to each of



the Langmuir probe models is illustrated in Figures 6 through 29. The calibration curves indicate the electron current output and the positive ion current output as a function of the output voltage from the Langmuir probe system. The function generator waveforms employed by the Langmuir probe systems are shown in Figures 30 through 33.

For each of the Langmuir probe models the electrode configuration was essentially the same. The sensing electrode for each of the models was cylindrical in geometry and had an exposed area of  $10.5 \text{ cm}^2$ , the diameter of the electrode was  $3/32$  inches and the length was  $5\frac{1}{2}$  inches. For the probe Models LP68B and LP69C flown on the NIRO vehicles 7.890, 7.891, 7.892 and 7.902-9 the total effective area was  $21 \text{ cm}^2$  since these two probe models utilized dual electrodes which were mounted diametrically opposite on the side of the rocket.

## RESULTS

The Langmuir probes described in this report were launched at the times and locations outlined in Table 1. Analysis of the rocket flights and brief evaluation of the results obtained will be presented in the following sections.

### RESULTS FROM NIRO AT 7.891

NIRO AT 7.891 was launched from Wallops Island at 1730Z (1230 LT) on 31 January 1969. The rocket payload reached a peak altitude of 137.1 kilometers as shown by the trajectory plotted in Figure 34. Langmuir probe erection occurred 55.5 secs after launch at an altitude of approximately 58 kilometers. The vehicle potential measured during the rocket flight is shown in Figure 35. The potential measured was approximately constant at -0.75 volts for both rocket ascent and descent.

The Langmuir probe system functioned satisfactorily during the course of the flight. However, because of the limited range of the telemetry system, the electrometer saturated, and thereby indicated a saturated electron current early in the flight at  $T_0 + 77.2$  sec. Figure 36 shows the electron current measured at an applied probe voltage of +3 volts. On rocket ascent data was obtained from 60.5 kilometers to 78 kilometers; on descent, data was obtained from 79 kilometers down to 56 kilometers. In the attitude regime of 78 kilometers (ascent) to 79 kilometers (descent) the electron current saturated. According to the Langmuir probe electron amplifier calibration curve, Figure 6, the saturated current was in excess of  $2 \times 10^{-7}$  amps.

The positive ion current measured at an applied probe voltage of -3 volts is illustrated as a function of altitude in Figure 37. The currents measured on ascent and descent are in good agreement with each other. Between the altitudes of 94 kilometers and 118 kilometers the positive ion current reaches a maximum of approximately  $1.3 \times 10^{-7}$  amps. Above 118 kilometers up to apogee, the positive ion current was  $10^{-7}$  amps. Below 94 kilometers, down to 65 kilometers, the current goes from  $10^{-7}$  amps to  $3.5 \times 10^{-10}$  amps.

The positive ion current measured at an applied probe voltage of -9 volts is illustrated in Figure 38 . The current profile agrees favorably with that measured at -3 volts, the values of current at -9 volts being a factor of 1.5 greater than those measured at -3 volts.

#### RESULTS FROM NIRO AH 7.890

NIRO AH 7.890 was launched from the Churchill Research Range at 0200Z on 11 October 1969. This rocket flight constituted part of the certification measurements for PCA-69. A plot of the vehicle trajectory is illustrated in Figure 39 and shows that the peak altitude reached during the flight was 117.8 kilometers. Langmuir probe erection occurred 60 seconds after launch at 0201Z at an altitude of 58.6 kilometers.

The only measurements obtained on this rocket flight were for the positive ion current at an applied probe voltage of -3 volts. Figure 40 shows the positive ion current measured as a function of altitude during rocket ascent and descent.

No other measurements were obtained from the Langmuir probe experiment because of the erratic behavior of the current. Figures 41 thru 45 show portions of the strip chart data. It will be noticed in Figures 41 -- 45 that there was no electron current measurement in the electron channel. As for the positive ion current measured at an applied probe voltage of -9 volts, the strip chart results were close to saturation. This indicates a positive ion current on the order of  $2.0 \times 10^{-5}$  amps, which is three orders of magnitude greater than the positive ion current measured at a probe voltage of -3 volts.

#### RESULTS FROM NIRO AH 7.892

NIRO AH 7.892 was launched from the Churchill Research Range at 0251Z on 7 November 1969. This vehicle was launched as part of a post certification round for PCA-69. The payload reached a peak altitude of 122 kilometers. The Langmuir probe model used for the measurement of electron current and positive ion current was LP68B-10A. The Langmuir probe amplifier calibration curve for the positive ions is shown in Figure 11 and for the electrons in Figure 10.

No trajectory data was obtained for this flight. The Langmuir probe measurements for both the positive ions and electrons are shown as functions of time after launch. Figures 46 thru 49 show segments of the strip chart recordings.

The vehicle potential measured during the rocket flight is shown in Figure 50. Throughout the flight, the potential is nearly constant at -1.25 volts.

The electron current measured at an applied probe voltage of +3 volts is shown in Figure 51. The electron current reaches a maximum of  $5.6 \times 10^{-6}$  amps at approximately 150 seconds after launch.

The positive ion currents measured at an applied probe voltage of -9 volts and -3 volts are shown in Figures 52 and 53 respectively. For an applied probe voltage of -9 volts the current has a maximum of  $1.2 \times 10^{-7}$  amps at 145 seconds after launch. Similarly for an applied probe voltage of -3 volts the current has a maximum of  $3.8 \times 10^{-8}$  amps at 142 seconds after launch.

#### RESULTS FROM NIRO AO 7.902-9

NIRO AO 7.902-9 was launched from Wallops Island at 18-37-30Z on 7 March 1970. This rocket was launched during a solar eclipse. Totality occurred during the rocket flight. The Langmuir probe used on this rocket flight for the measurement of positive ion current and electron current was LP69C-6. The amplifier output calibration curves for the electrons and positive ions is shown in Figure 12 and 13 respectively.

The electron current measured during the solar eclipse event at an applied probe voltage of +3 volts is shown in Figure 54. The results are shown as a function of time after launch; there was no trajectory data available for this flight. Referring to Figure 54 we see that the current increases from  $10^{-8}$  amps at  $T_0 + 100$  secs to  $1.2 \times 10^{-7}$  amps at  $T_0 + 140$  secs, it then remains constant up to  $T_0 + 160$  seconds. At approximately  $T_0 + 170$  seconds, the current decreases to  $9.5 \times 10^{-8}$  seconds, after this time the current gradually increases to  $2.7 \times 10^{-7}$  amps at  $T_0 + 222$  seconds. After  $T_0 + 222$  seconds, the electron current falls off rapidly to  $3.3 \times 10^{-8}$  amps at  $T_0 + 244$  seconds. Figures 55 through 58 show portions of the strip chart data for this flight. It will be noticed in Figures 55 through 58 that there is a continuous current present in the electron channel and that the positive ion channel shows no response to the applied voltage at -3 volts and -8 volts.

#### RESULTS FROM NIRO AT 7.896

NIRO AT 7.896 was launched from Eglin at 23-23-14.048Z (18-23-14.048 LT) on 20 November 1970. The vehicle payload reached a peak altitude of 137.43 kilometers as shown by the trajectory plotted in Figure 59. The Langmuir probe model used for the positive ion current and electron current measurements as LP70A-2. The amplifier calibration curves for this probe for the positive ion output and electron output are shown in Figures 14 and 15 respectively.

No measurements of positive ion current or electron current were obtained during this rocket flight.

#### RESULTS FROM NIRO AO 7.902-6

NIRO AO 7.902-6 was launched from Wallops Island, Virginia at 1000Z (0500 LT) on 6 October 1971. This rocket launching was a part of a sunrise program and was the first in a series of four rockets to be fired during the program. The payload reached a peak altitude of 118.1 kilometers as shown by the trajectory plotted in Figure 60. The Langmuir probe employed on this rocket

flight for the measurement of electron current and positive ion current was LP70A-3. The amplifier calibration curves for the electron output and positive ion output are shown in Figures 16 and 17 respectively. For currents less than  $10^{-10}$  amps, the amplifier calibration data was considered unreliable.

The vehicle potential measured during rocket ascent and descent is plotted in Figure 61. On ascent, the potential was found to be substantially more negative than on rocket descent. The potential measured on ascent was on the order of  $-3/4$  to  $-1\frac{1}{4}$  volts.

The electron current measurements were made at an applied probe voltage +3 volts. However, the values of current that were measured were very small, on the order of  $2 \times 10^{-10}$  amps and were considered unrealistic. Figure 62 shows a portion of the strip chart data near apogee. It will be noticed in Figure 62 that the electron current undergoes a periodic interruption in current-value when the applied probe voltage is at +3 volts. The period associated with the changing electron current is 0.54 seconds. Concurrently with the reduction in the electron current, the positive ion current shows an increase. The increase in the positive ion current approximates the positive ion current measured at an applied probe voltage of -3.0 volts. Figures 63, 64 and 65 show segments of the strip chart data obtained during the flight.

According to the strip chart data obtained from this flight, the electron current first experiences the interruption in value at about 112 seconds after launch (100 kilometers) during rocket ascent. At this time, the period is 1.08 seconds, Figure 63. On descent, it is noticed that the reduction in the electron current becomes less pronounced. Figure 65, which is at the end of the measurable data for this flight, shows that the positive ion current begins to experience a variation in current.

The positive ion current profiles measured at -3 volts and -8 volts during the rocket ascent and descent are shown in Figures 66 and 67. In both cases, the ascent current is greater than the descent current due to the fact that the vehicle potential is more negative on rocket ascent.

#### RESULTS FROM NIRO AO 7.101-3

NIRO AO 7.101-3 was launched from Wallops Island at 1011Z (0511 LT) on 6 October 1971. This vehicle was the second of four rockets launched during the program.

There was no measurable Langmuir probe data obtained on this flight.

#### RESULTS FROM NIRO AO 7.101-4

NIRO AO 7.101-4 was launched from Wallops Island at 1044Z (0544 LT) on 6 October 1971. This rocket launching was a post sunrise launching and was the third of the four rockets launched during the program. The vehicle payload reached a peak altitude of 117.4 kilometers, a plot of the vehicle trajectory is shown in Figure 68. The Langmuir probe system employed for the positive ion current and electron current measurements was LP71B-4. The amplifier calibration curves for this probe model are shown in Figure 21 for the positive ion current output and in Figure 20 for the electron current output.

The vehicle potential measured on rocket ascent and descent during this flight is illustrated in Figure 69. At altitudes above 90 kilometers the measured potential was on the order of  $-1/2$  volts at 70 kilometers.

In Figure 70 the electron current measured for an applied probe voltage of +3 volts is illustrated. The measured current is plotted as a function of altitude for rocket ascent and descent. Between the altitudes of 70 and 105 kilometers the measured current for ascent and descent show reasonably good agreement. Above 105 kilometers up to apogee (117.4 kilometers) the descent current is slightly greater than that measured on ascent. At 110 kilometers, a large increase in current was measured. The magnitude of the current was  $3 \times 10^{-6}$  amps and was experienced on both ascent and descent.

The positive ion currents measured for applied probe voltages of -8 volts and -3 volts is shown in Figure 71 and 72 respectively. At an applied probe voltage of -8 volts the positive ion current measured at altitudes above 80 kilometers show reasonably good agreement

between ascent and descent. At altitudes below 80 kilometers, the positive ion current is enhanced as a result of shock ionization arising from the increase in vehicle velocity. Examination of the currents measured above 90 kilometers to 110 kilometers indicates that the positive ion current is nearly constant at  $7 \times 10^{-8}$  amps (-8 volts) and approximately  $3.5 \times 10^{-8}$  amps (-3 volts). Above 110 kilometers the positive ion current measured at -8 volts decreases to about  $5$  to  $5.5 \times 10^{-8}$  amps and to  $3 \times 10^{-8}$  amps at -3 volts. Below 90 kilometers during rocket ascent the current falls off roughly by a factor of 5 to  $1.5 \times 10^{-8}$  amps (-8 volts) and  $5 \times 10^{-9}$  amps at -3 volts at 75 kilometers.

#### RESULTS OF NIRO AO 7.101-2

NIRO AO 7.101-2 was launched from Wallops Island at 1105Z (605 LT) on 6 October 1971. This vehicle was the last of four rockets launched during the sunrise program.

There was no measurable Langmuir probe data obtained on this flight.

#### RESULTS OF NIRO AO 7.001-1

NIRO AO 7.001-1 was launched from Wallops Island on 6 February 1972 at 17-15-00Z. The rocket reached a peak altitude of 91.8 kilometers at 153.76 seconds after launch. A plot of the vehicle trajectory is shown in Figure 73. The Langmuir probe model used for the measurement of the positive ion current and electron current was LP71B-3. The amplifier calibration curves for the electron output and positive ion output are shown in Figures 24 and 25 respectively. Probe erection occurred at 56.8 seconds after launch at an altitude of 47.6 kilometers.

The Langmuir probe measurements made during this flight were strongly influenced by the effects of vehicle potential. No estimate of the vehicle potential was obtained during this flight due to the absence of the positive ion current. Figures 74 and 75 show portions of the strip chart data obtained during the flight.



Figures 74 and 75 are typical of the strip chart data obtained over the course of the rocket flight. It will be noticed in the Figures that the electron current shows up as a slight increase in current when the applied probe voltage is at +3 volts. Near the end of the flight, at times greater than  $T_0 + 247$  secs., both positive ion measurements and electron measurements show a response to the applied probe voltage. However, at this time, both currents saturate.

The electron current measured by the probe at an applied probe voltage of +3 volts is shown in Figure 76. Only a few measurements were possible due to the vehicle potential problems noted above.

#### RESULTS FROM UTE-TOMAHAWK AO 9.303-3

Ute-Tomahawk AO 9.303-3 was launched from the Churchill Research Range at 4-05-50Z on 28 March 1974. The rocket payload reached a peak altitude of 128.8 kilometers as shown by the trajectory plotted in Figure 77. The Langmuir probe used on this rocket flight for the measurement of positive ion current and electron current was LP71B-8. The amplifier output calibration for the electron and positive ions is shown in Figures 26 and 27 respectively.

The vehicle potential measured as a function of altitude during rocket ascent and descent is shown in Figure 78. On the ascent portion of the flight, the potential is slightly more negative than during descent. At an altitude of 90 kilometers the vehicle potential on ascent measures -2 volts while on descent it was measured at -1 volt. At higher altitudes the vehicle potential during rocket ascent is only about 0.1 volt more negative than during descent.

The electron current measured at an applied probe voltage of +3 volts is shown in Figure 79. The ascent and descent current profiles show reasonably good agreement. On rocket ascent the first measurable electron current has a value of  $2.9 \times 10^{-8}$  amps occurring at an altitude of approximately 90 kilometers. Above this altitude the current gradually increases to  $4.6 \times 10^{-7}$  amps at 98 kilometers from 100 kilometers to

112 kilometers the electron current decreased to  $2.5 \times 10^{-7}$  amps. Between 112 kilometers and apogee (128.8 kilometers) the current increased from  $2.5 \times 10^{-7}$  amps to  $3 \times 10^{-6}$  amps, nearly a factor of 10. On rocket descent, the current shows a steady decrease from  $3 \times 10^{-6}$  amps at apogee to  $1.5 \times 10^{-9}$  amps at 79 kilometers.

The positive ion current measured at an applied probe voltage of -9 volts and -3 volts are shown in Figures 80 and 81 respectively. For both sets of measurements the ascent and descent currents show good agreement. For an applied probe voltage of -3 volts the current exhibits a maximum of about  $2.8 \times 10^{-8}$  amps at 100 kilometers and then decreases to approximately  $6 \times 10^{-9}$  amps at 110 kilometers, above 110 kilometers the current gradually increases to  $2.5$  to  $3 \times 10^{-8}$  amps at apogee (128.8 kilometers). The positive ion currents measured at an applied probe voltage of -9 volts exhibit a similar behavior. The measured currents are approximately a factor of 2.5 greater than those measured at -3 volts.

#### RESULTS FROM UTE-TOMAHAWK AO 9.303-4

Ute-Tomahawk AO 9.303-4 was launched from Fort Churchill at 19-18-00Z on 3 April 1974. The rocket payload reached a peak altitude of 128 kilometers as illustrated by the trajectory plotted in Figure 82. The Langmuir probe model used for the measurements of the electron current and positive ion current was designated LP71B-9. The amplifier calibration curves for the electron output and positive ion output are shown in Figures 28 and 29 respectively. Probe erection occurs at 19-19-05, 65 seconds after launch.

The vehicle potential measured during this flight for rocket ascent and descent is shown in Figure 83. Measurements between 78 kilometers and 100 kilometers were unattainable because the probe was always measuring a positive ion current in this region. Above 100 kilometers during rocket ascent, the potential gradually goes from -2 volts to -1.1 volts at apogee. On the descent portion of the flight the vehicle potential is approximately -1 volt from apogee (128 km) down to 100 kilometers. Below 100 kilometers the potential gradually becomes more negative measuring -2.5 volts at 72.5 kilometers.

The electron current profile measured at an applied probe voltage of +3 volts is shown as a function of altitude for rocket ascent and descent in Figure 84 . There were no electron current measurements made in the altitude regime of 78 kilometers to 100 kilometers. The ascent and descent currents show good agreement with the ascent current being slightly less than that measured during descent. This difference being attributed to the vehicle potential being slightly more negative during rocket ascent.

The positive ion currents measured for applied probe voltages of -9 volts and -3 volts is shown in Figures 85 and 86 respectively. In both cases the measured currents are in good agreement.

Figures 87 and 91 are portions of the strip chart data obtained during the rocket flight.

APPENDIX

## APPENDIX I

### MEASUREMENT OF VEHICLE POTENTIAL

Ideally, the vehicle potential can be read from the current-voltage characteristic curve similar to the one shown in Figure 1. This requires reading the applied sweep voltage at the "breakpoint" which is also known as the plasma potential. The applied voltage corresponding to the breakpoint is equal in magnitude and opposite in sign to the vehicle potential.

In practice, however, the breakpoint is usually not as well defined as illustrated in Figure 1, and would necessitate drawing a straight line along the slope of the current curve in the retarding region and locating the point where the curve deviates from linearity. As an alternative to this approach the applied sweep voltage was determined when the positive ion current fell to zero on the +3 volt to -3 volt sweep. The value of the sweep voltage corresponding to zero positive ion current is then called the vehicle potential.

Using the above method the vehicle potential is measured directly and is generally found to be only slightly less negative, i.e., ( $< \frac{1}{4}$  volt) then if measured by the breakpoint technique.

ILLUSTRATIONS

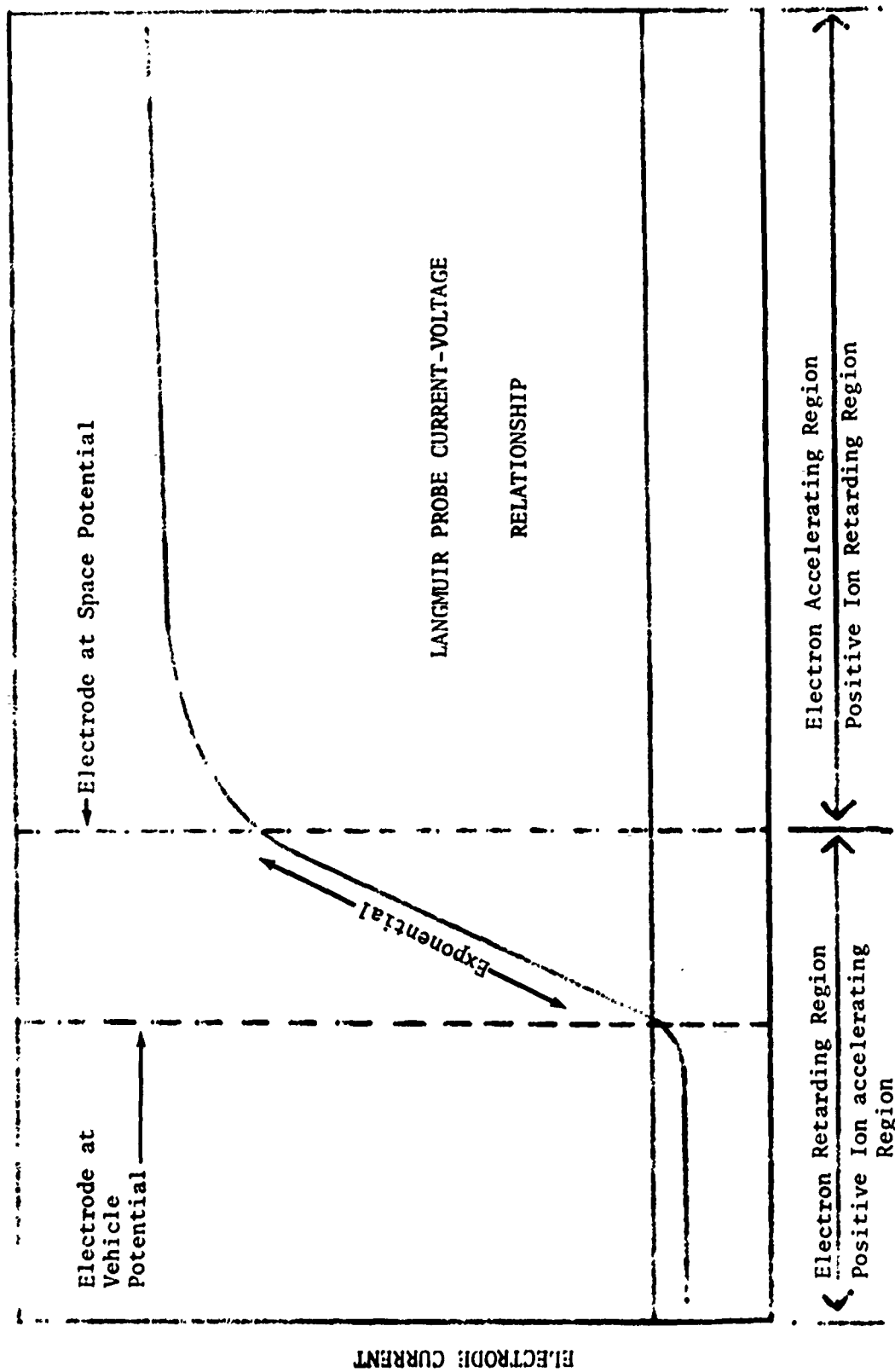


Figure 1 Theoretical Semi-Log Plot of Electrode Current.

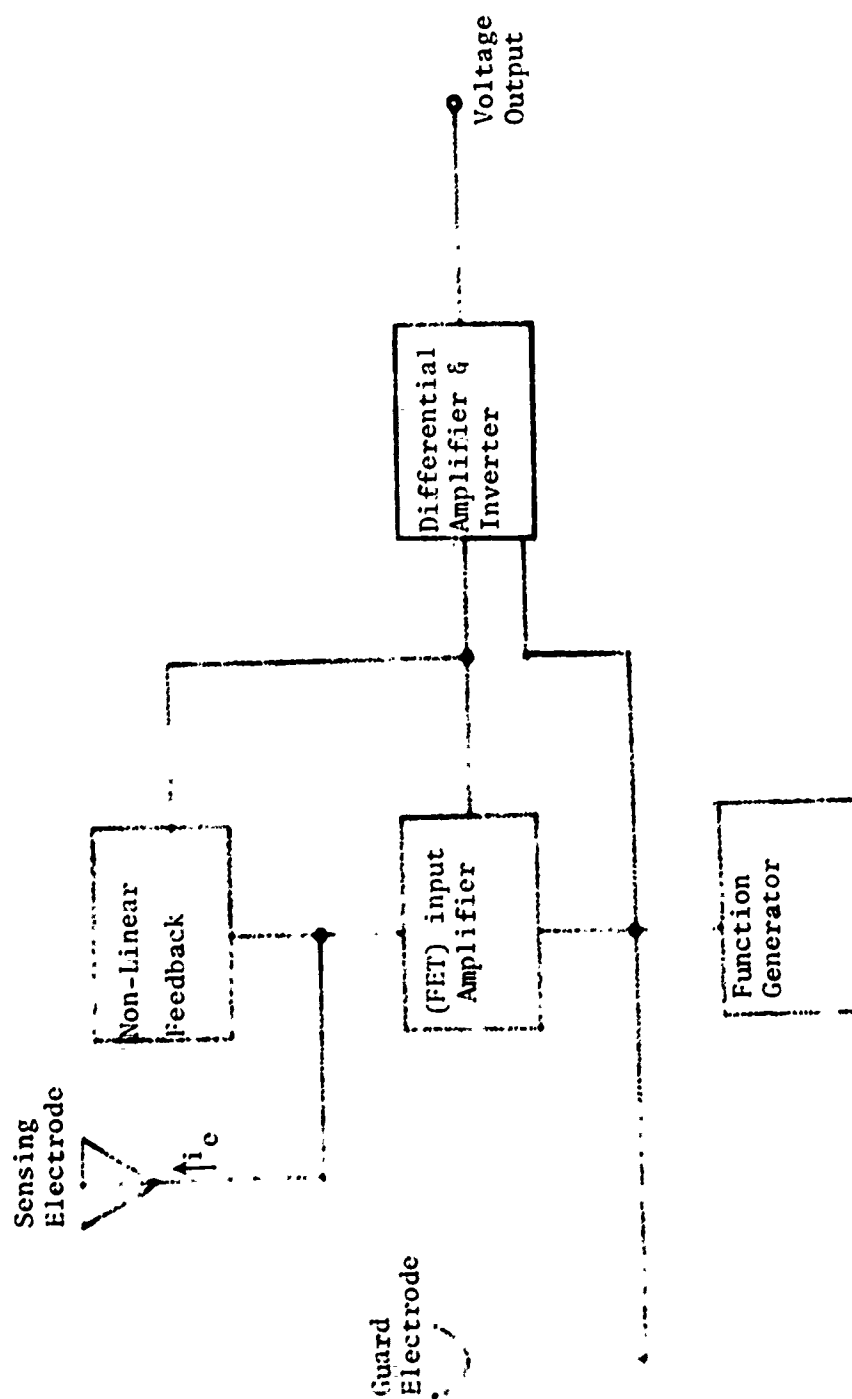


Figure 2 Block Diagram of Langmuir Probe Model LP68B.



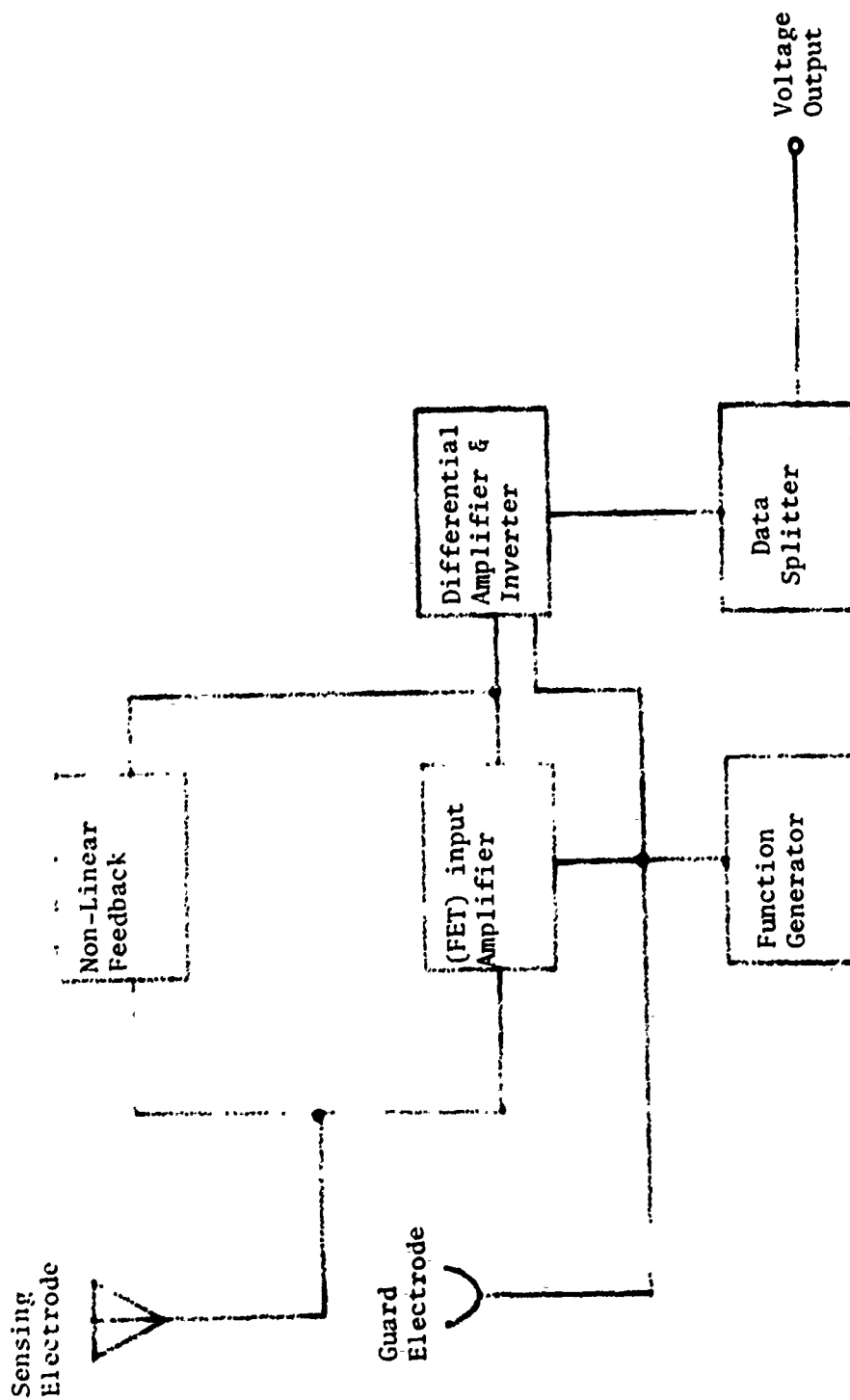


Figure 3 Block Diagram of Langmuir Probe Model LP69C.

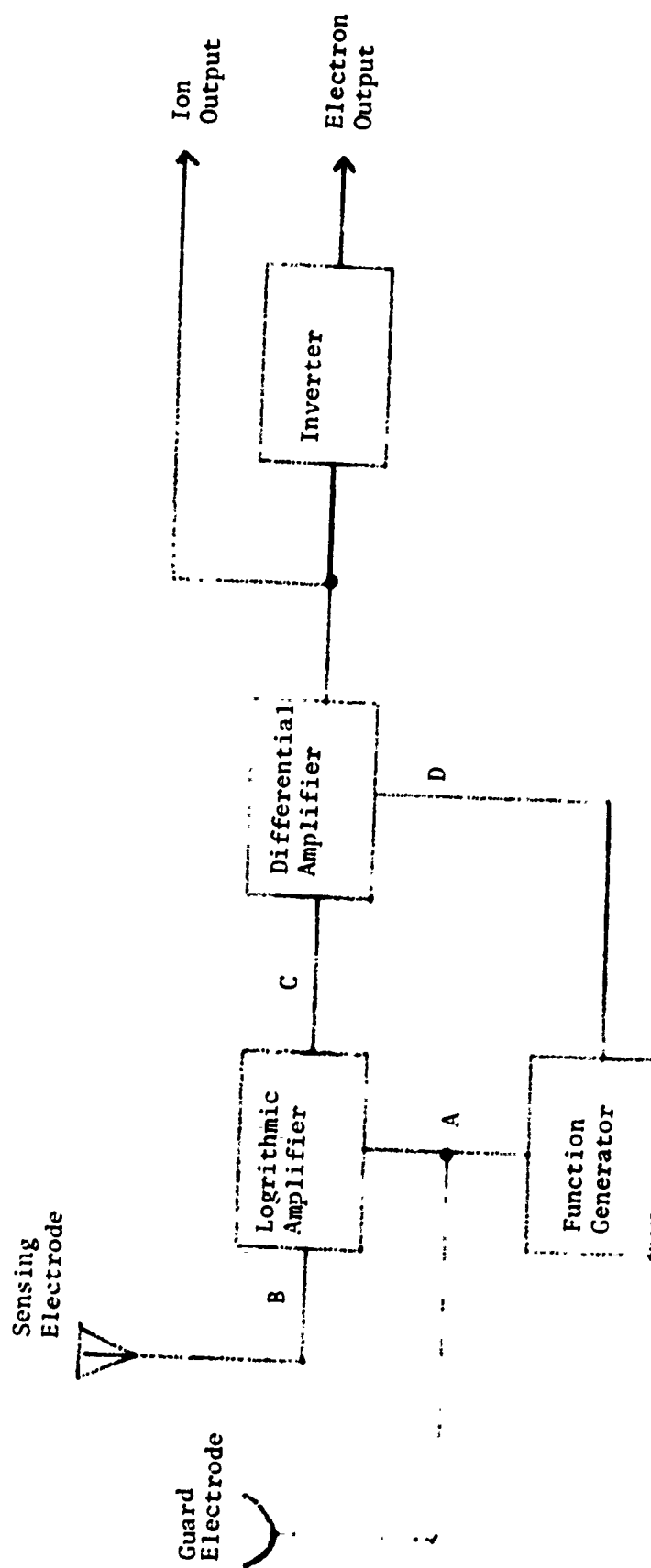


Figure 4 Block Diagram of Langmuir Probe Model LP70A

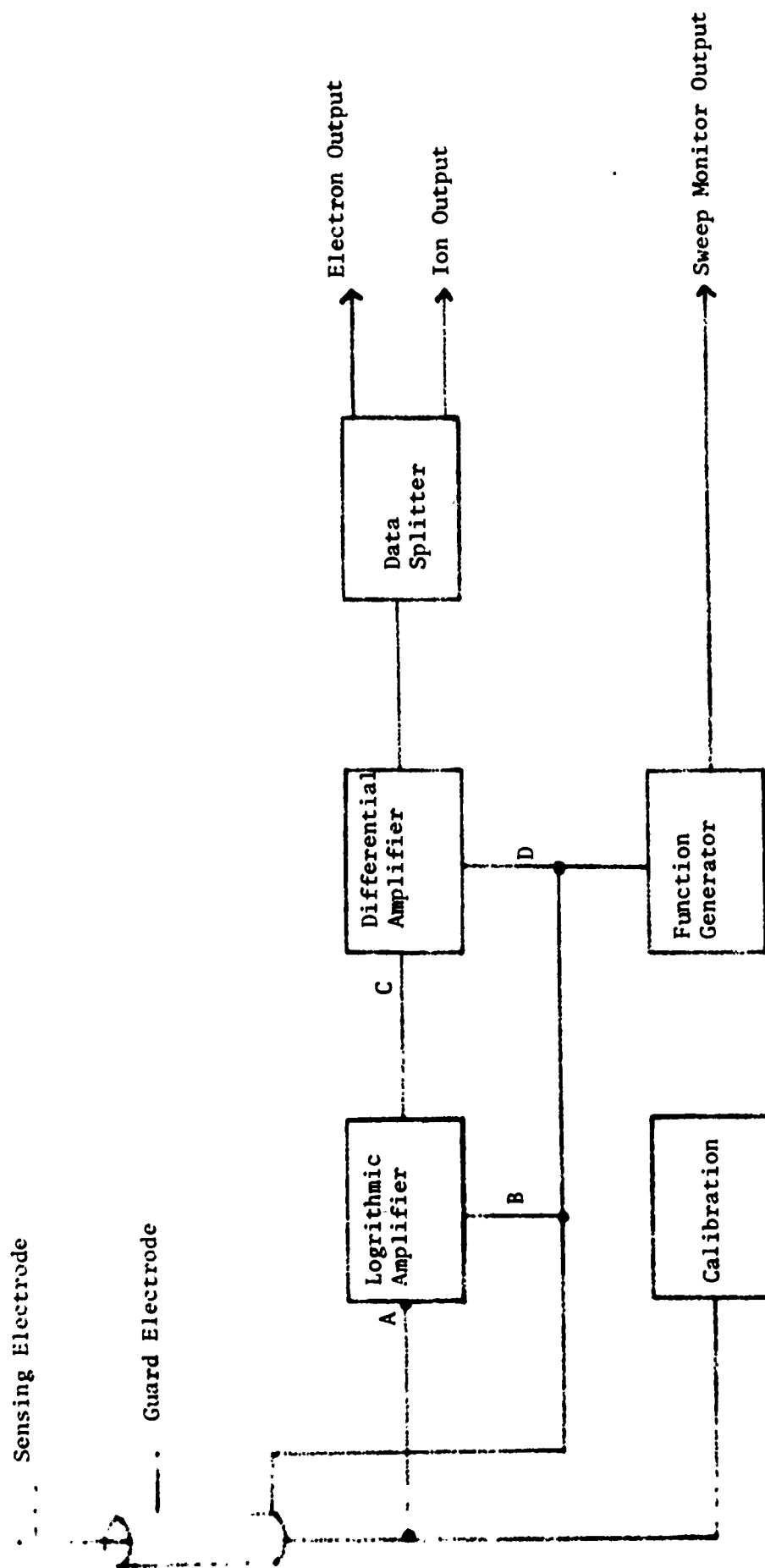


Figure 5 Block Diagram of Langmuir Probe Model 1 LP71B.

7.891

Electron Current

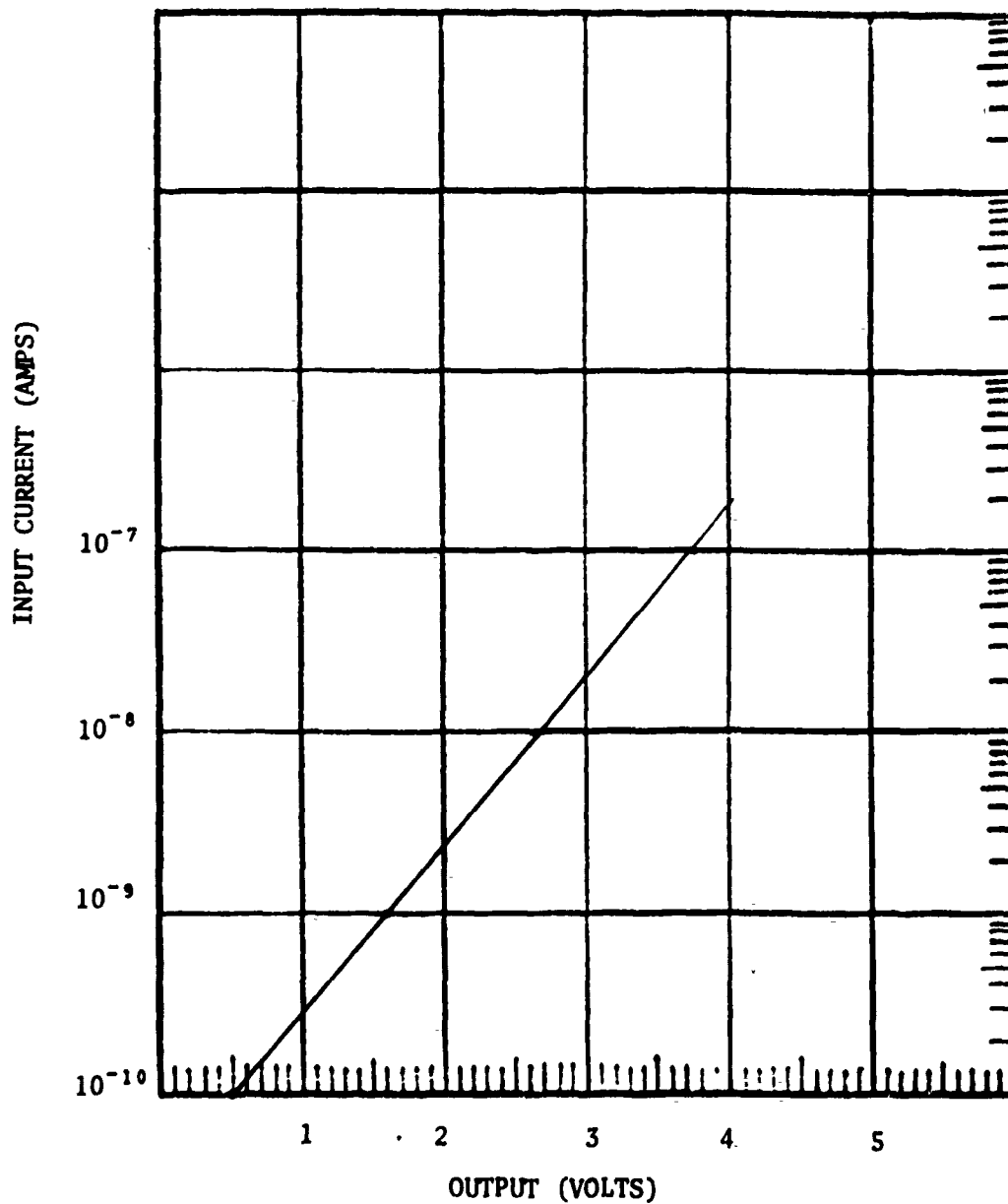


Figure 6 Electron Current Amplifier Calibration for LP68B-4

7.891

LP68B-4

Ion Current

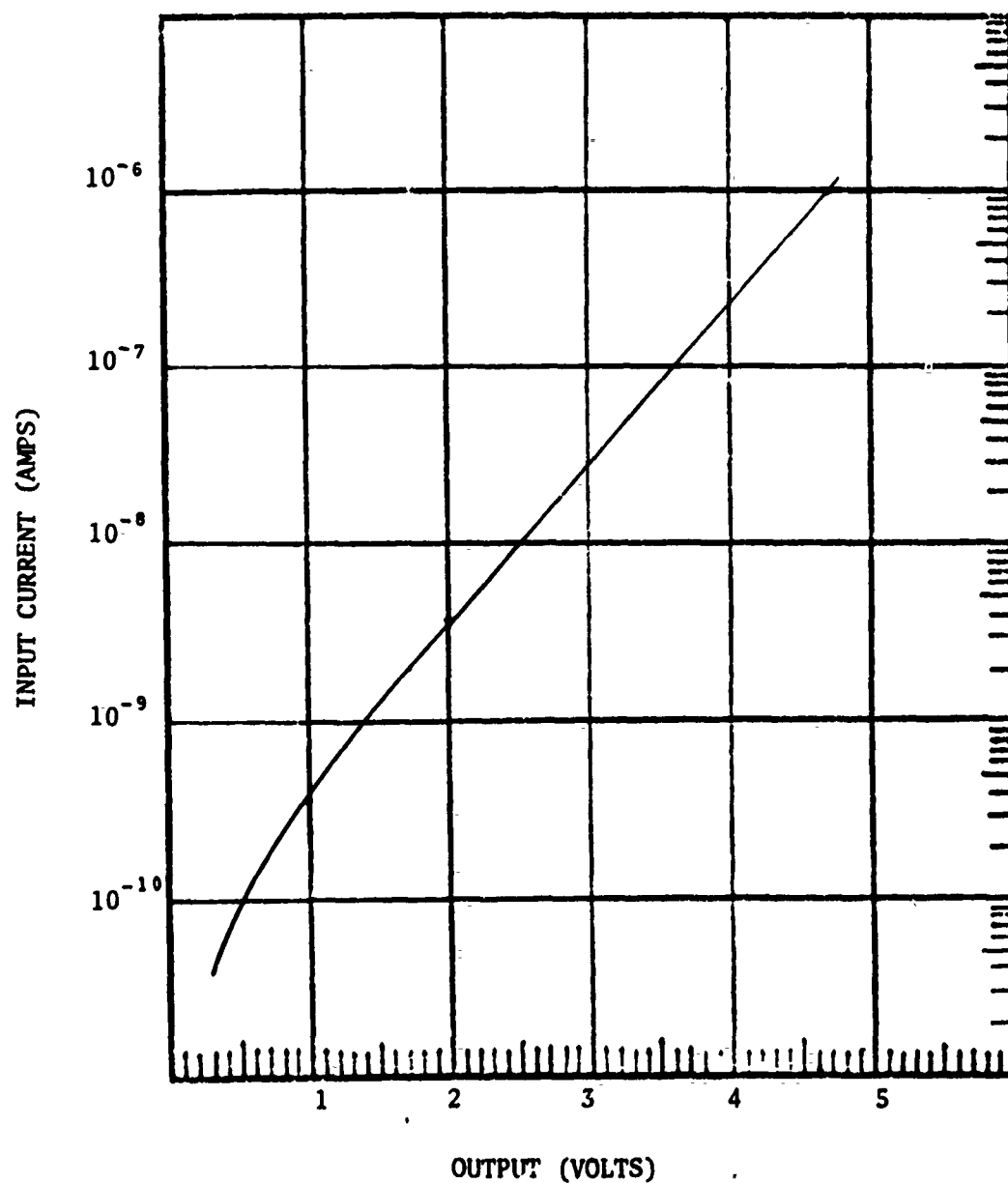


Figure 7 Positive Ion Current Amplifier Calibration for Model LP68B-4

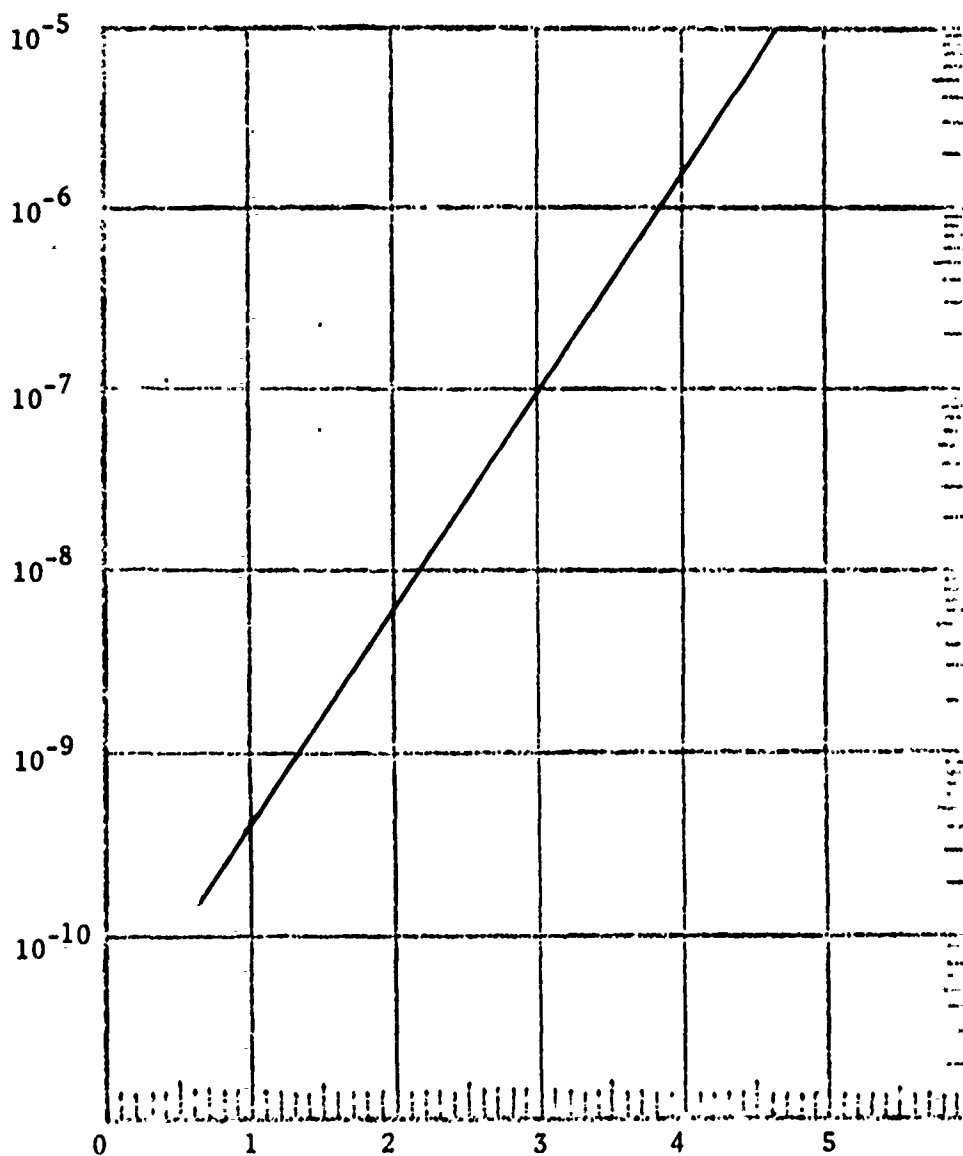


Figure 8 Electron Current Amplifier Calibration for LP68B-5A

7.890

Positive Ion Current

Calibration

68B-5A

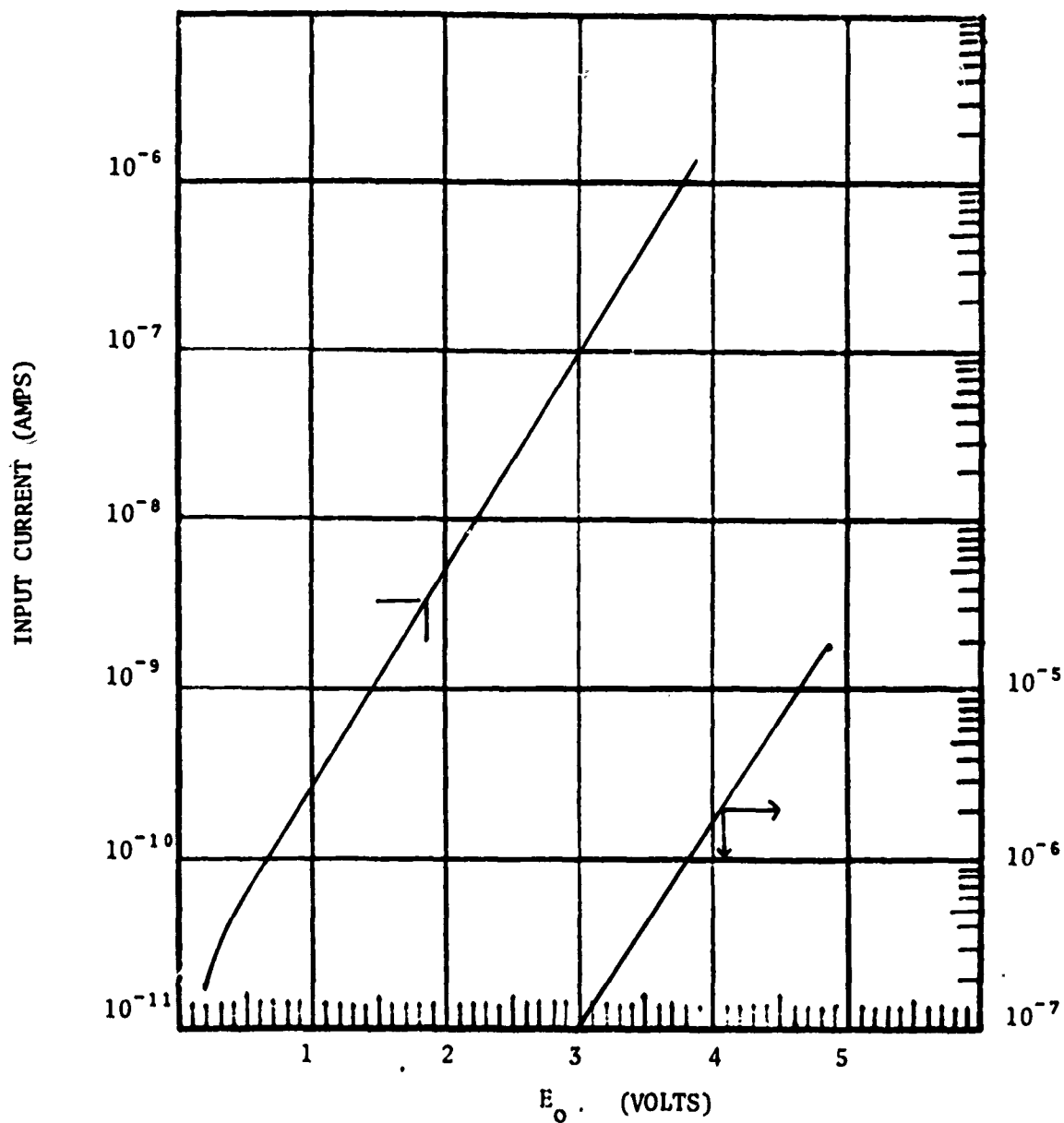


Figure 9 Positive Ion Current Amplifier Calibration For LP68B-5A

Electron Current Calibration

LP68B-10A + 50°C

7.892

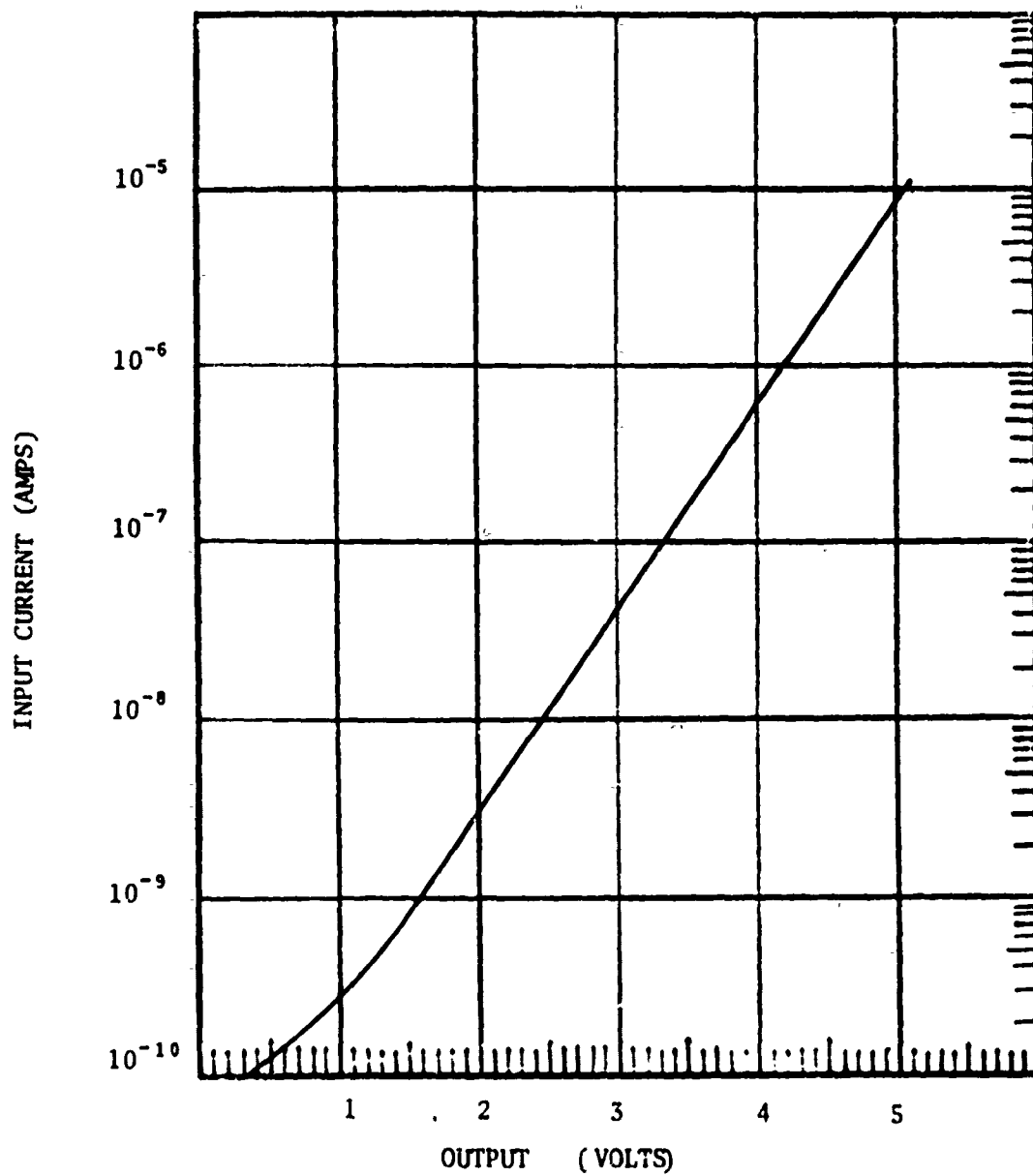


Figure 10 Electron Current Amplifier Calibration for LP68B-10A



Positive Ion Current

LP68B-10A + 50°C

7.892

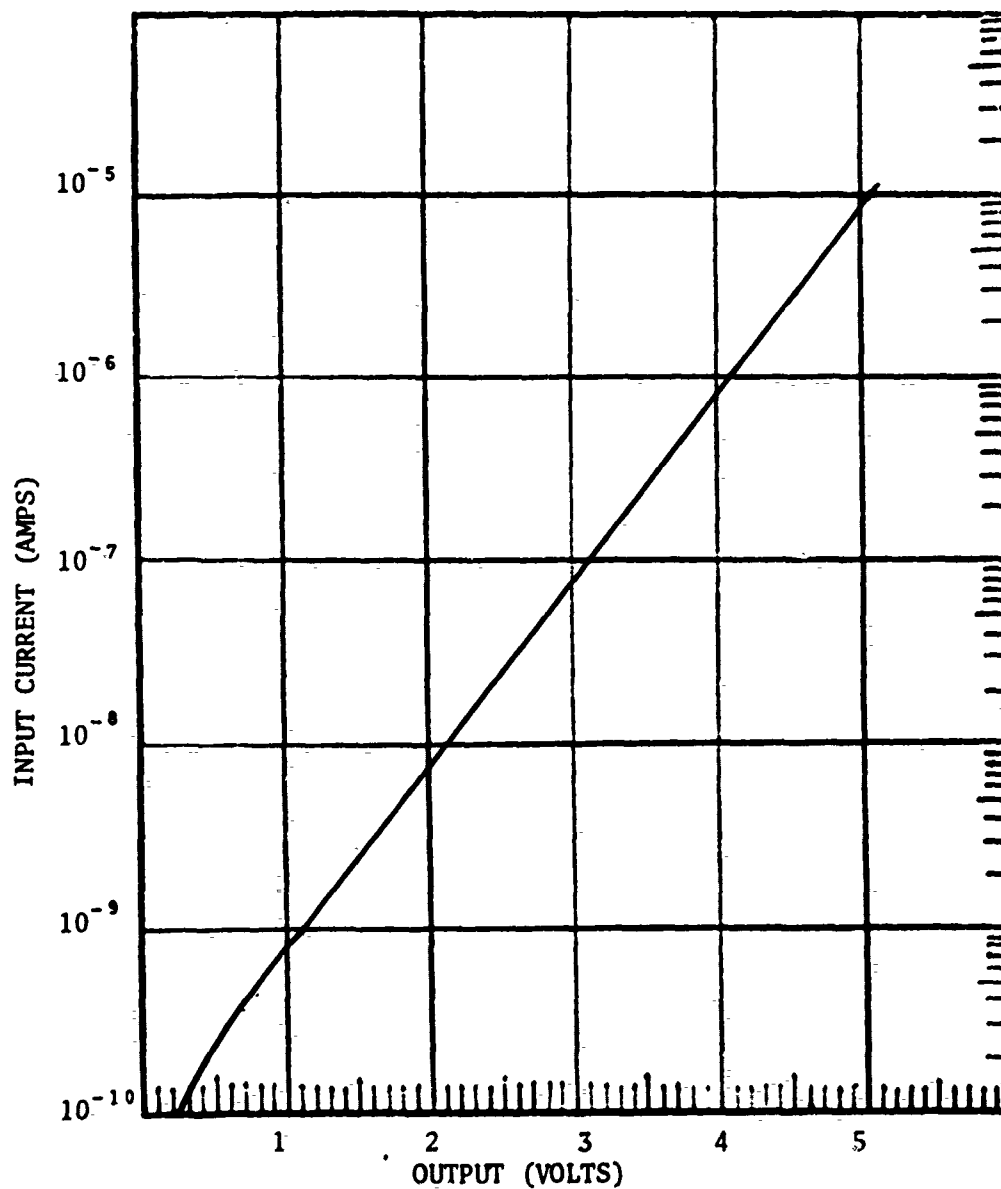


Figure 11 Positive Ion Current Amplifier Calibration for LP68B-10A

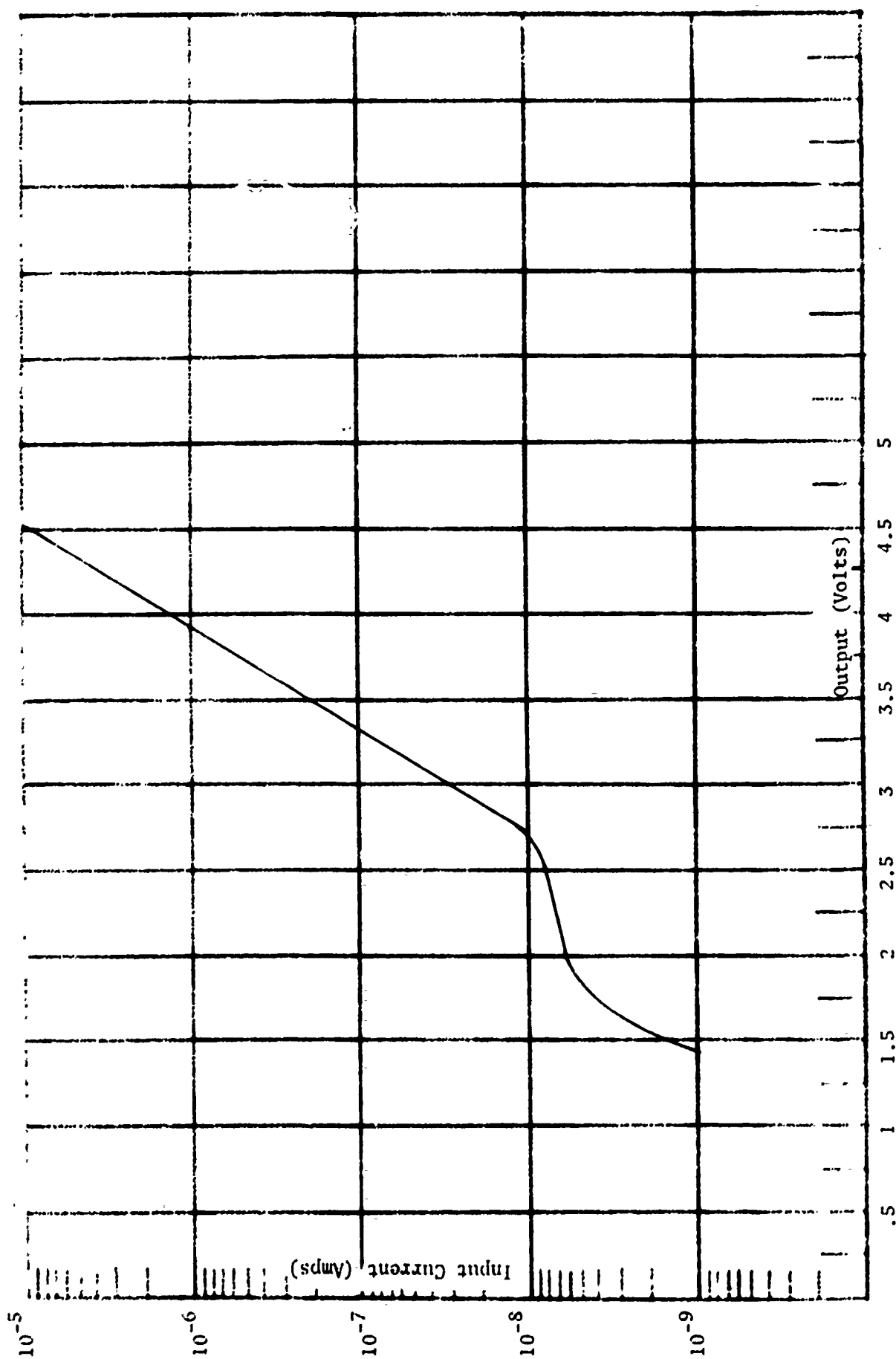


Figure 12 Electron Current Amplifier Calibration for LP69C-6

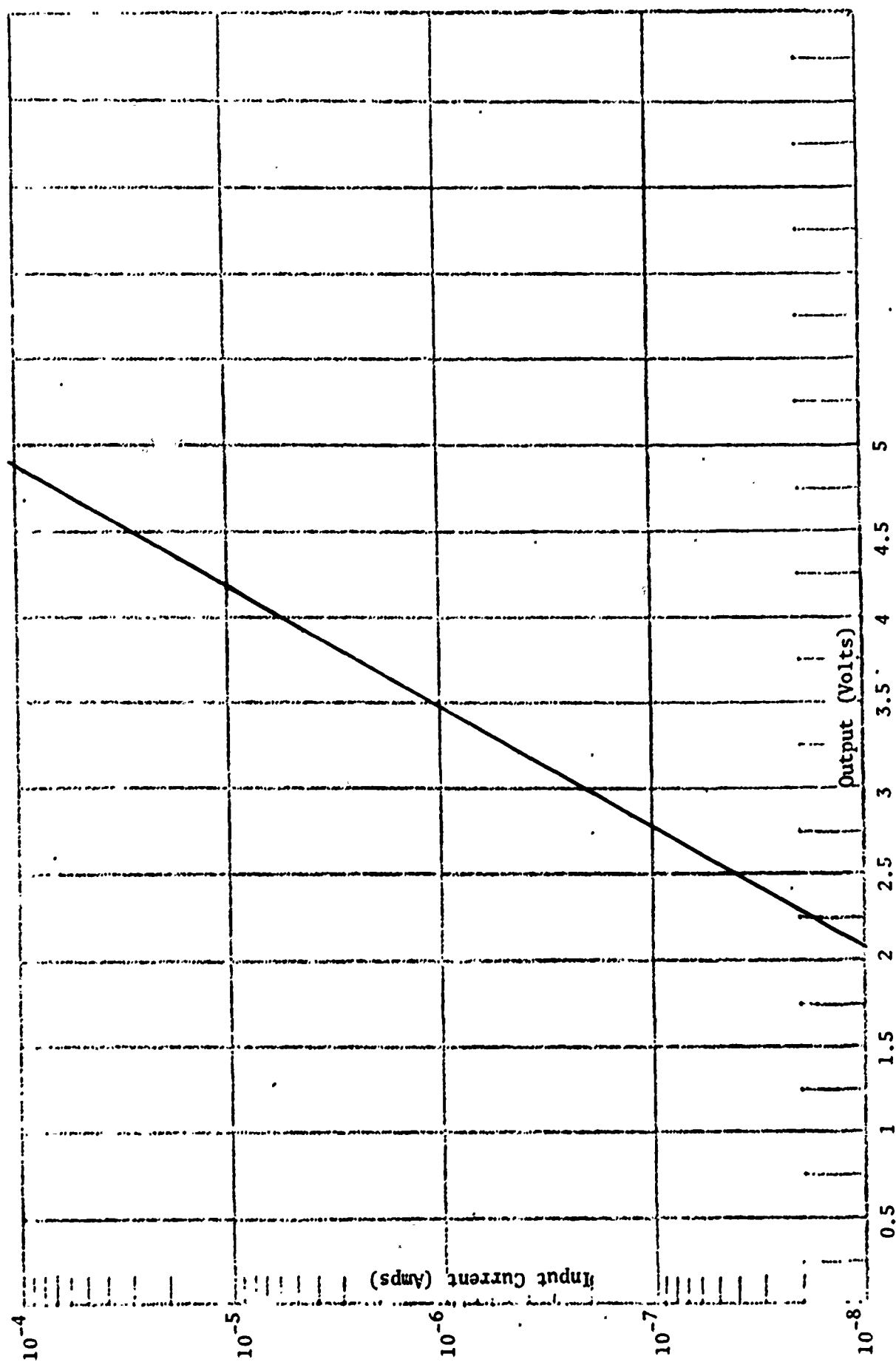


Figure 13 Positive Ion Current Amplifier Calibration LP69C-6

7.896

Electron Output

LP 70-A-2

20°C

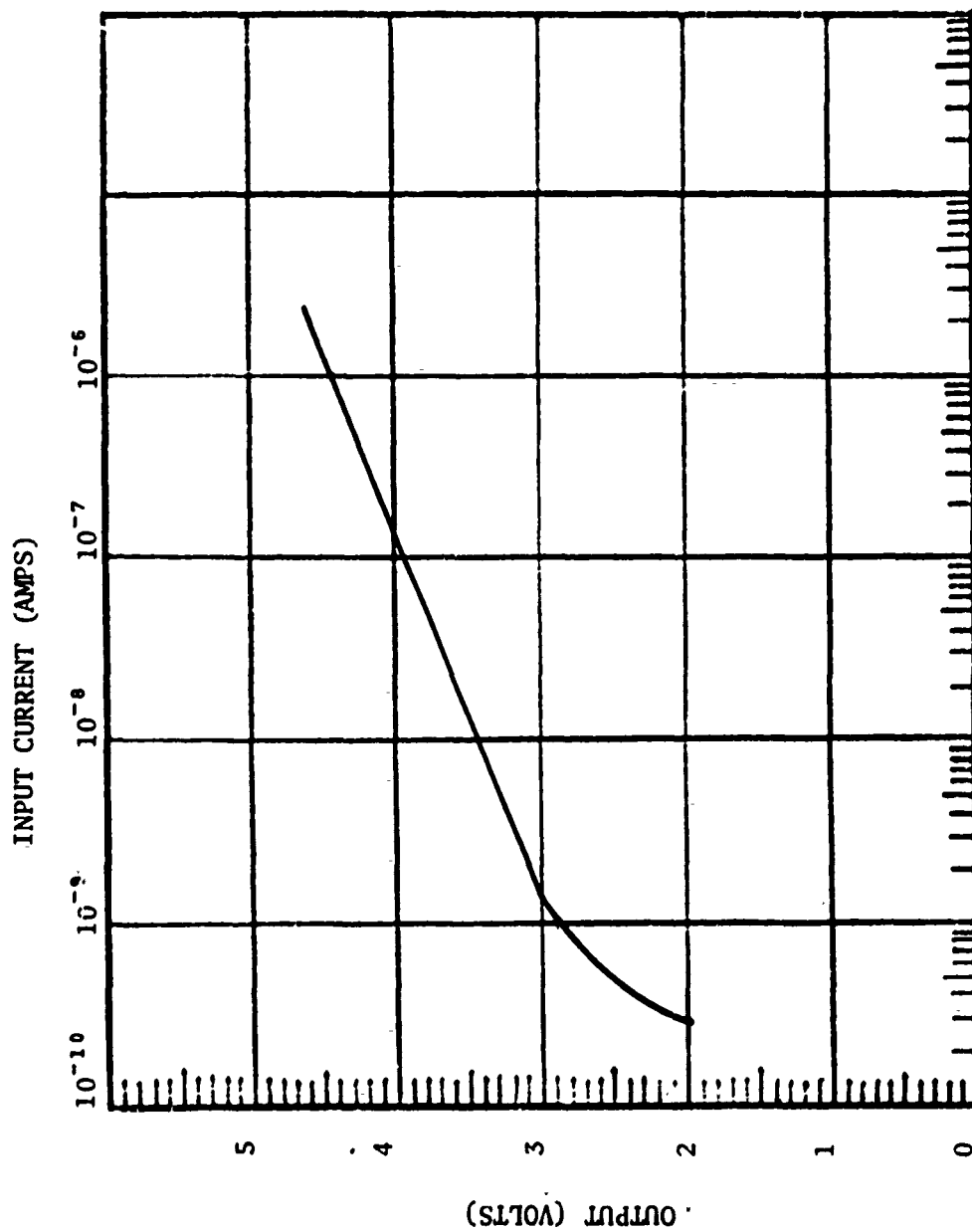


Figure 14 Electron Current Amplifier Calibration for LP70A-2

7.896

Positive Ion Output

LP70-A-2

20°C

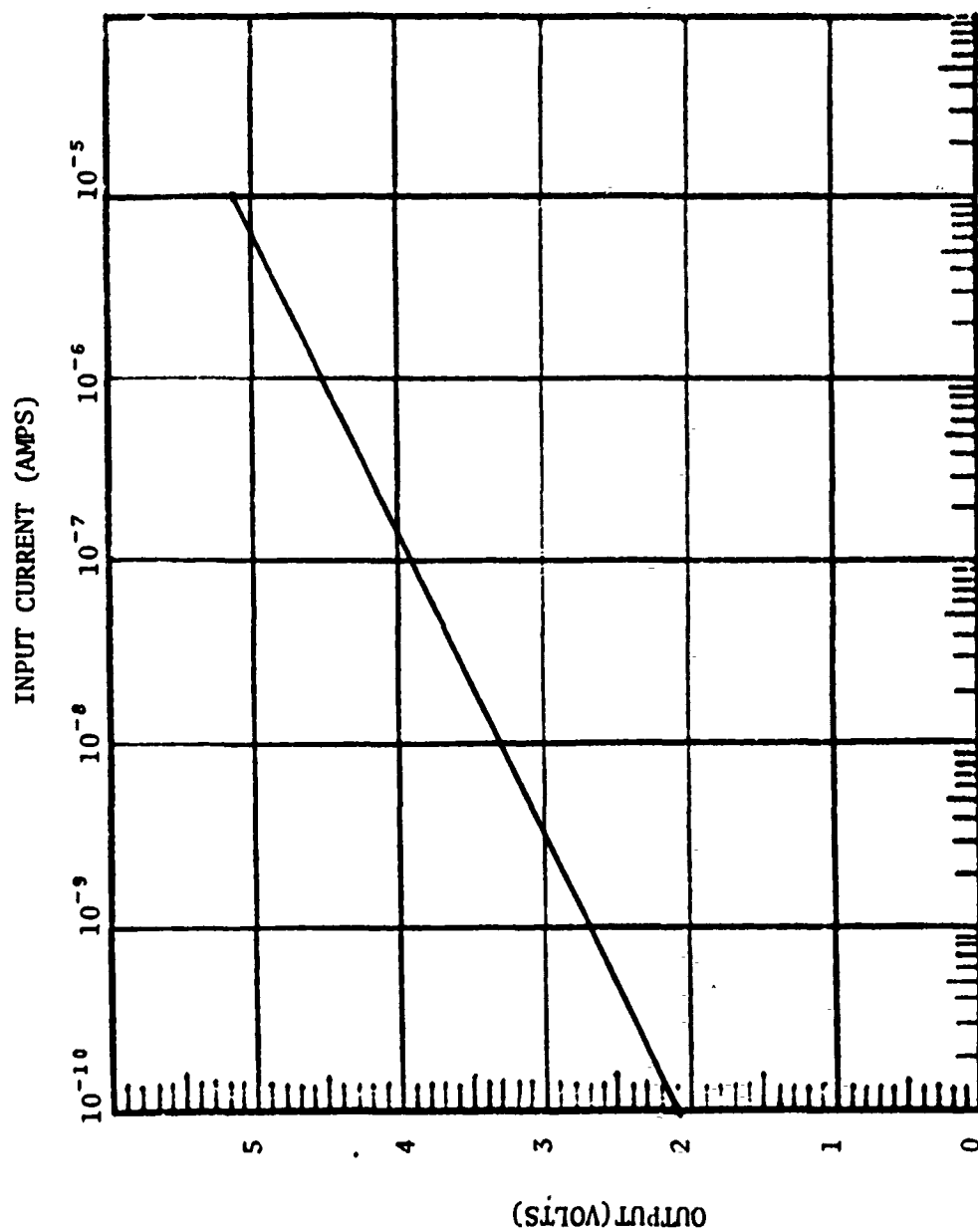


Figure 15 Positive Ion Current Amplifier Calibration for LP70A-2

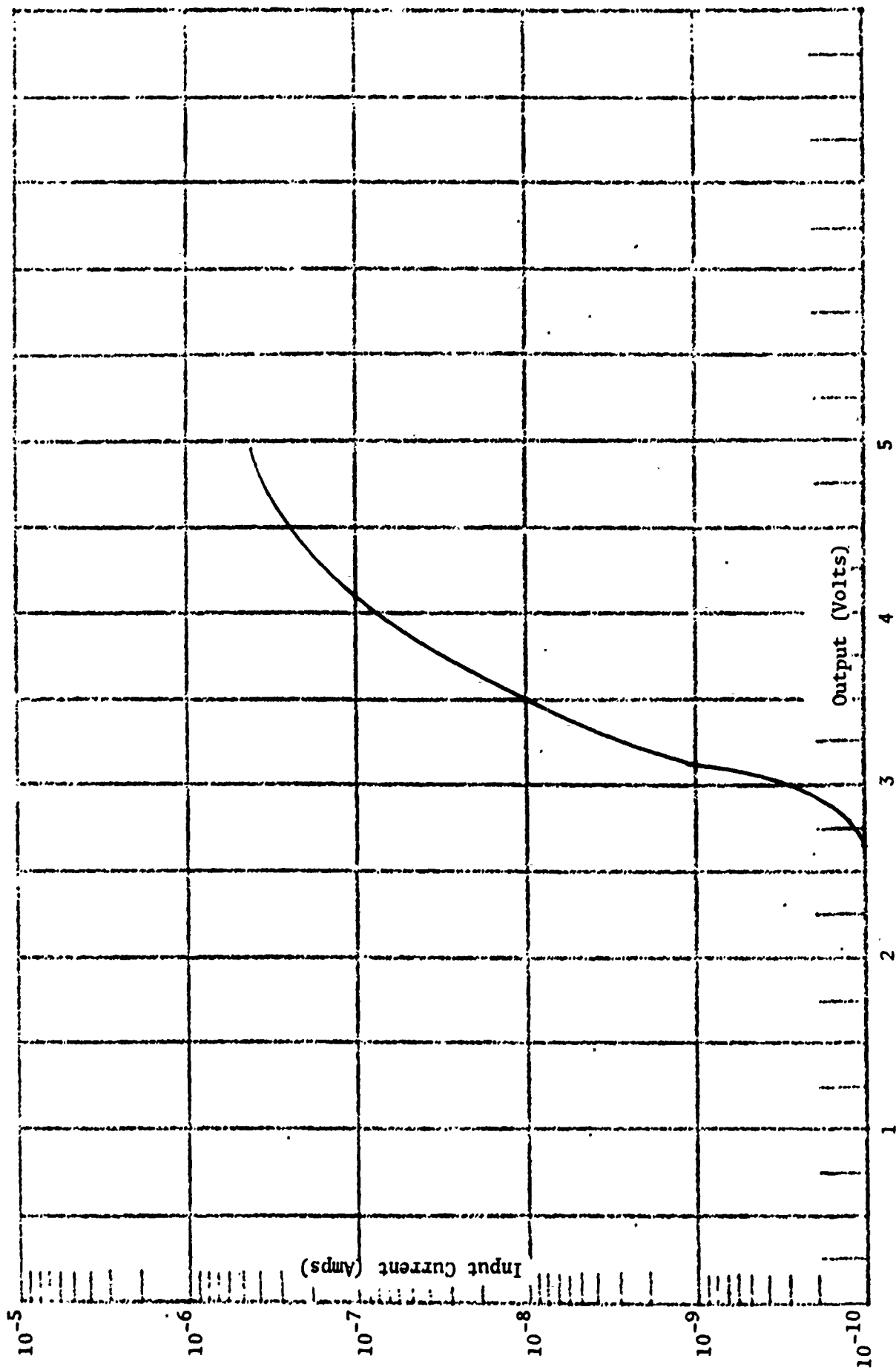


Figure 16 Electron Current Amplifier Calibration for LP70A-3

Positive Ion Calibration

7.902-6

LP70A-3

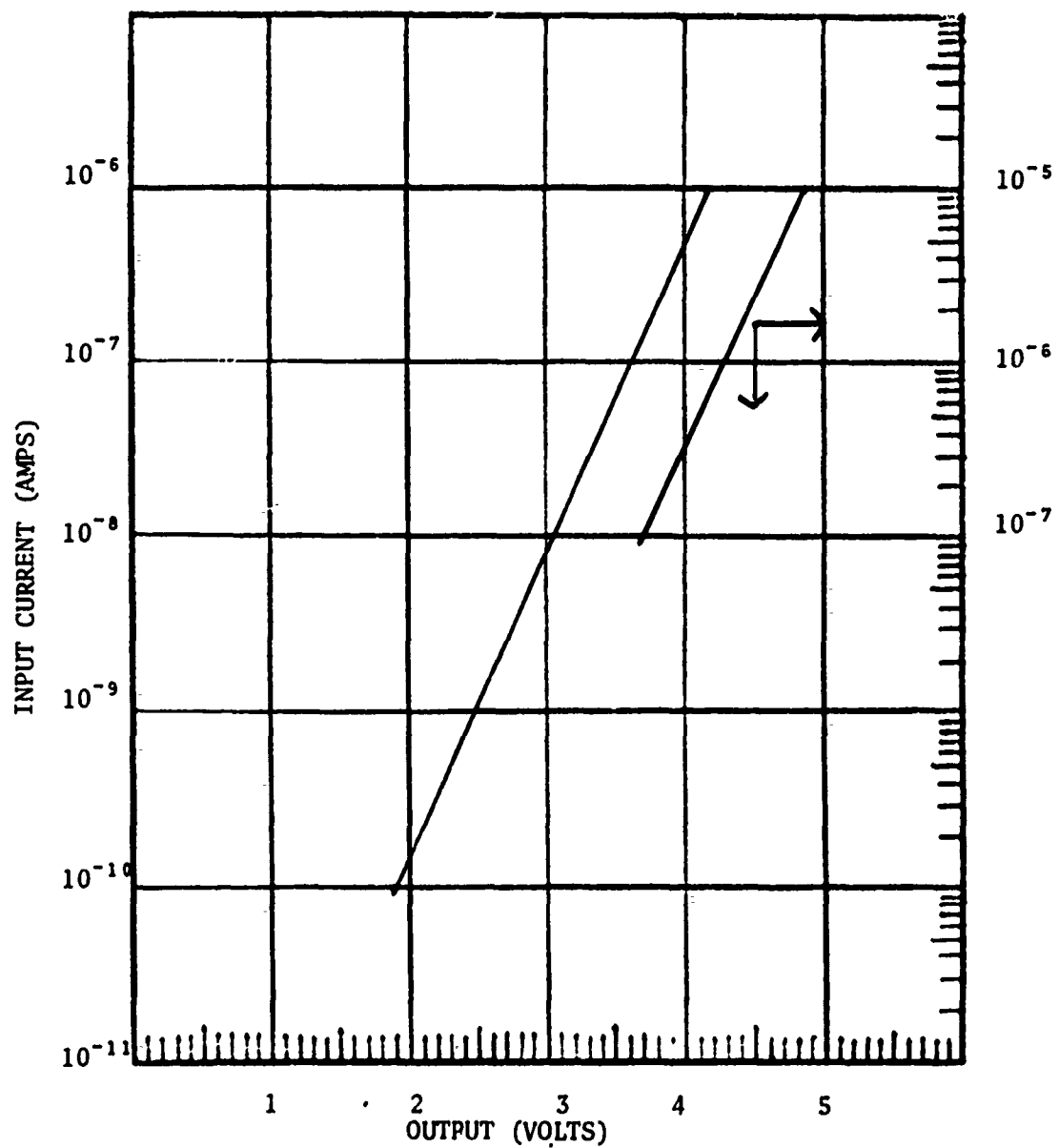


Figure 17 Positive Ion Current Amplifier Calibration for LP70A-3

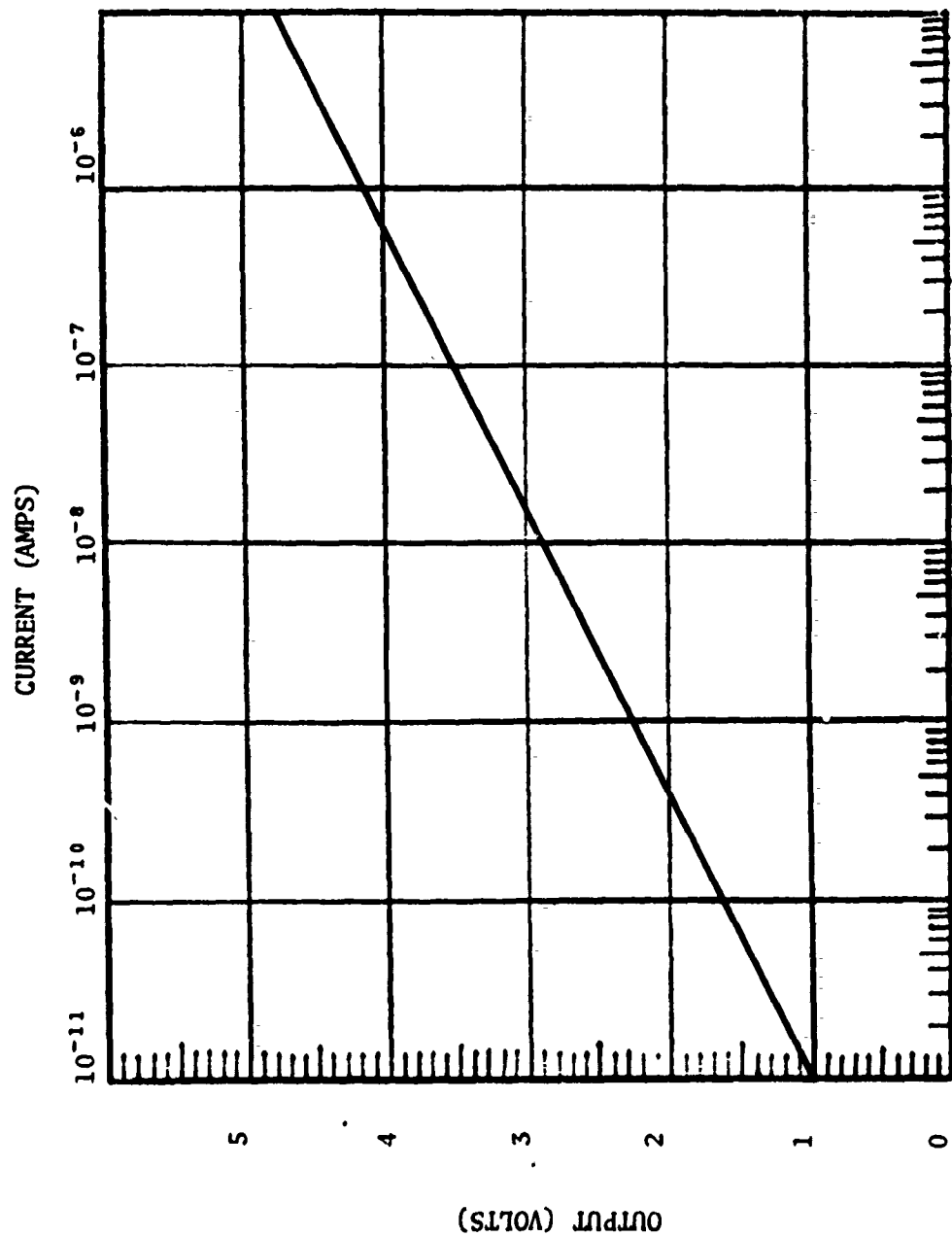


Figure 18 Electron Current Amplifier Calibration for LP71B-1



Positive Ion Output

LP 71B-1

7.101-3

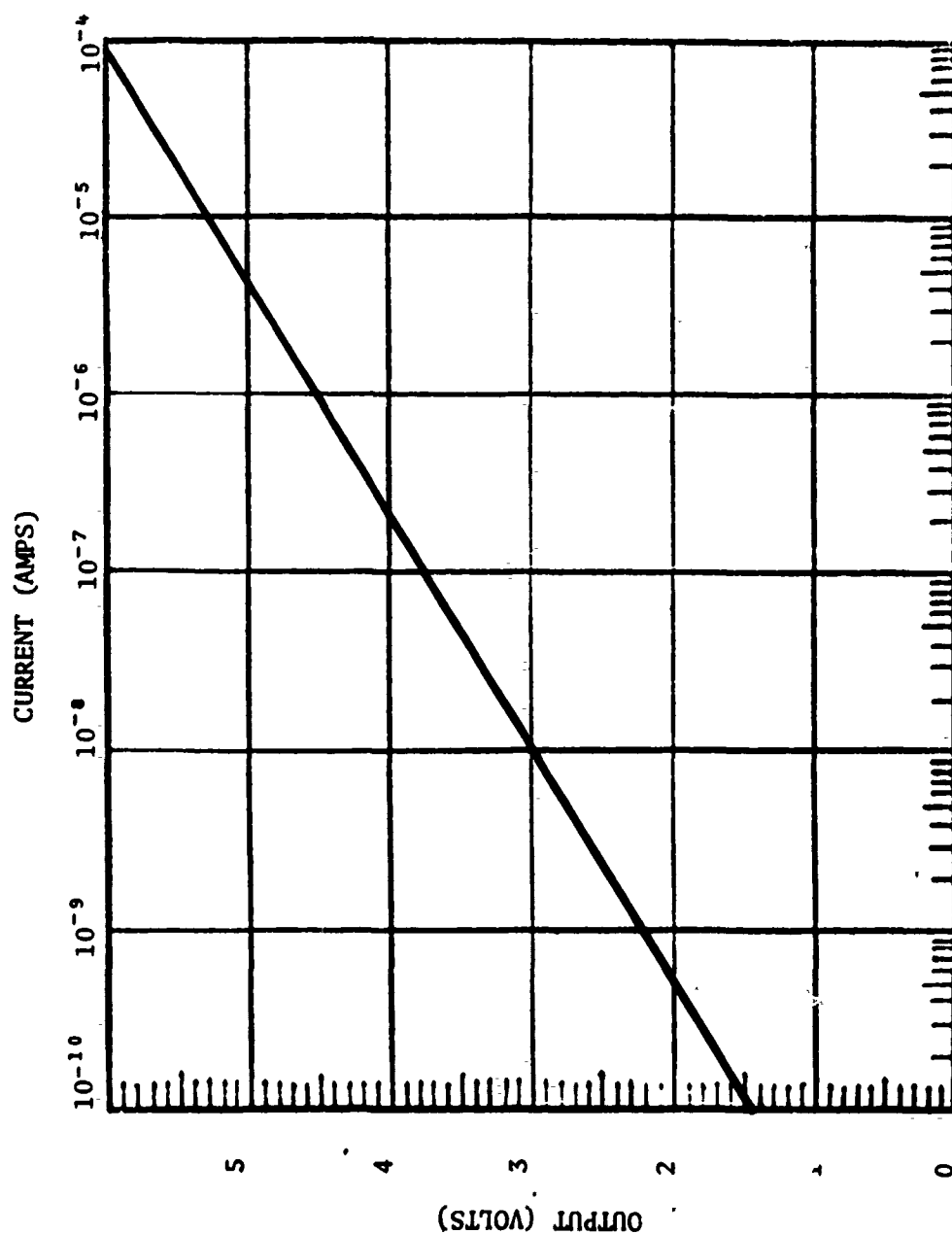


Figure 19 Positive Ion Current Amplifier Calibration for LP71B-1

LP71-B-4

Electron Output

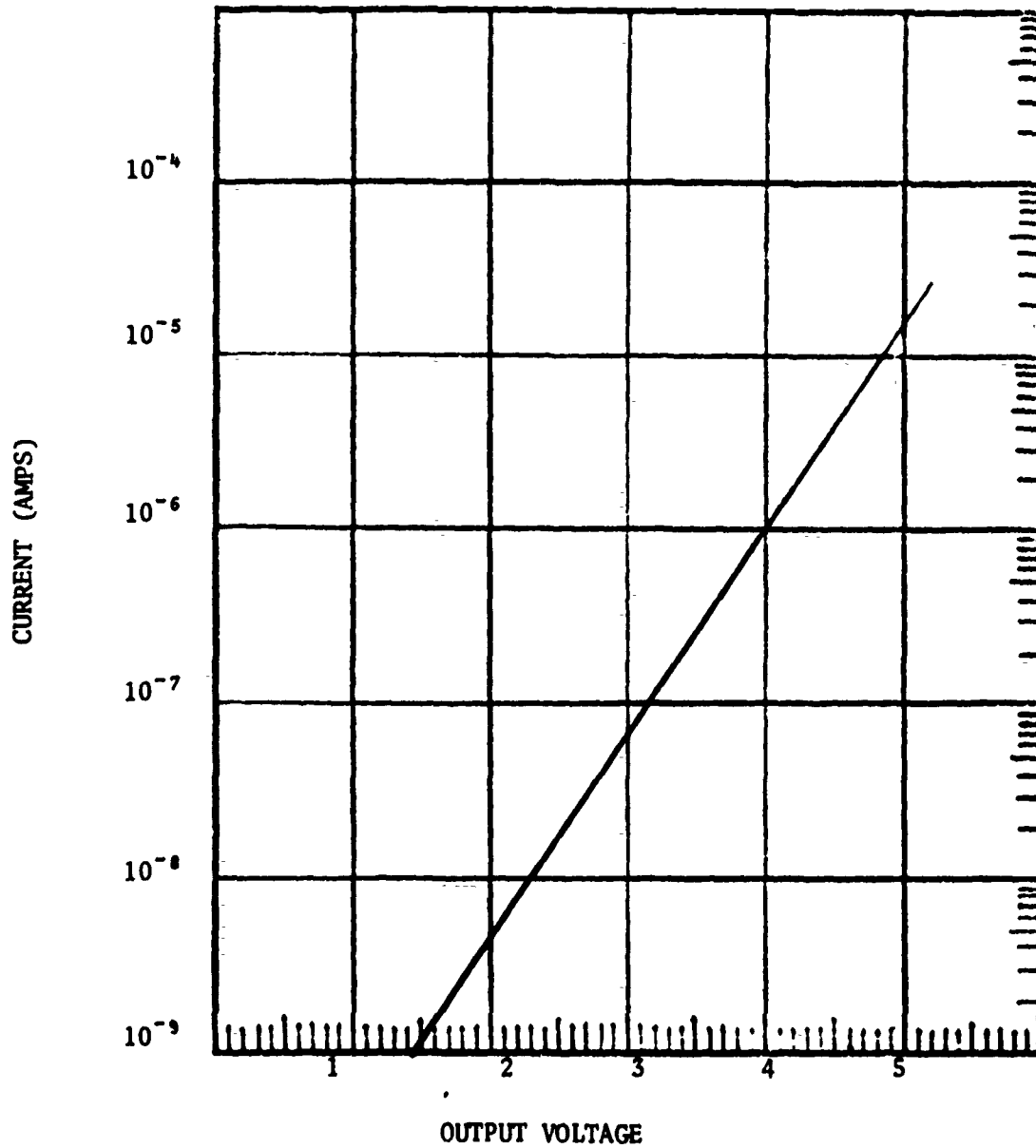


Figure 20 Electron Current Amplifier Calibration for LP71B-4

Positive Ion Current

LP71B-4

7.101-4

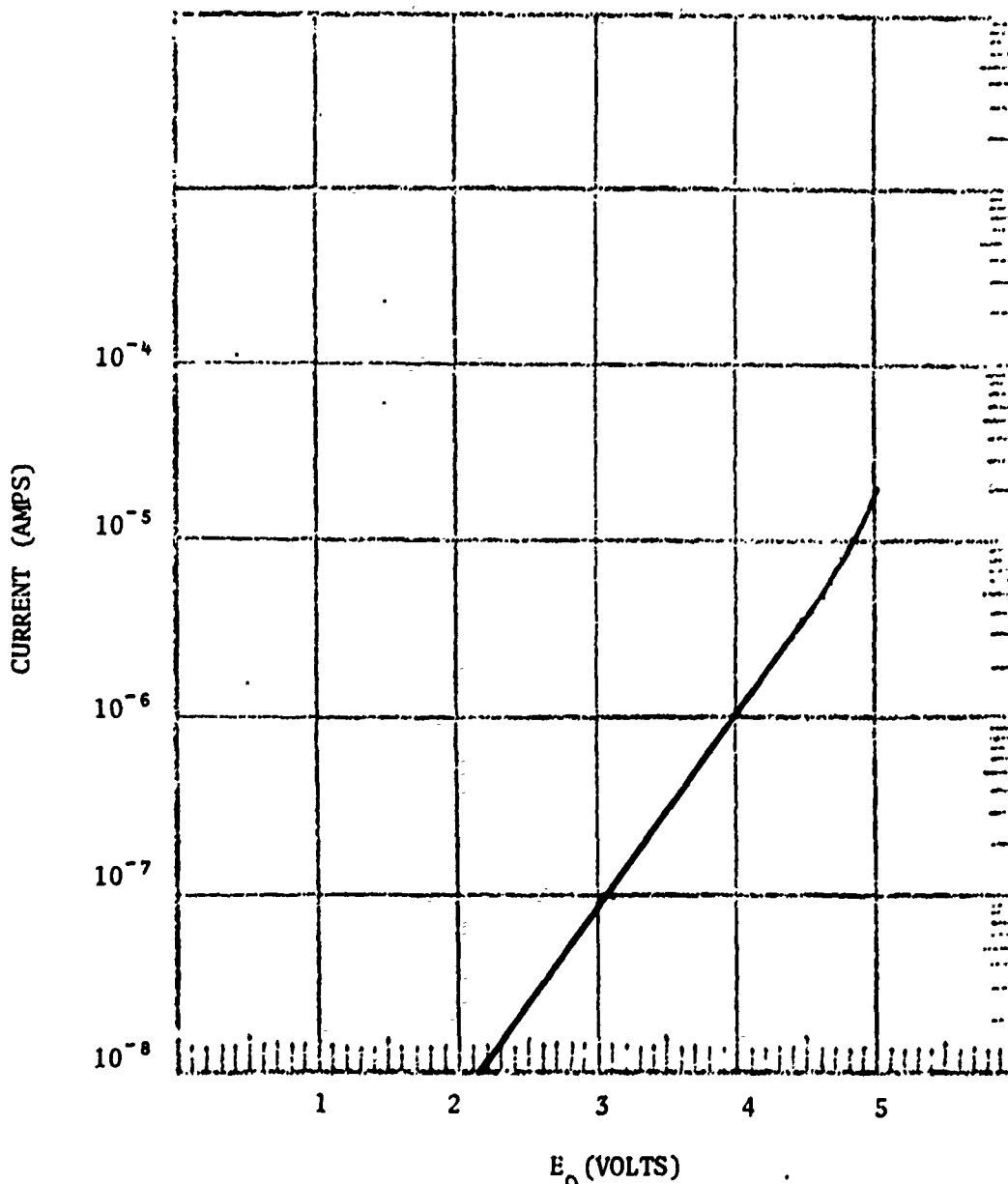


Figure 21 Positive Ion Current Amplifier Calibration  
for LP71B-4 .

LP 71-B2  
 Niro 7.101-2  
 Electron Output

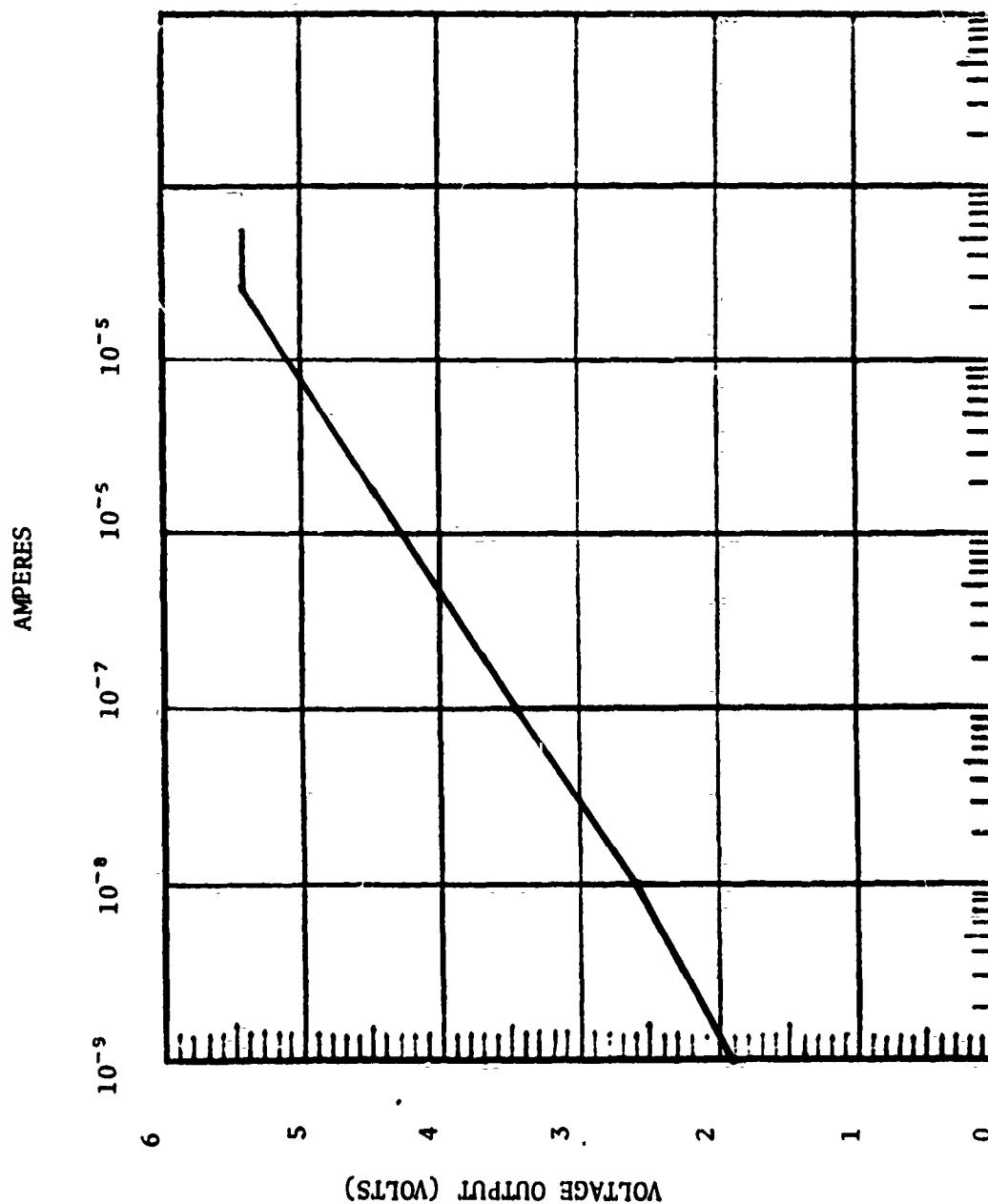


Figure 22 Electron Current Amplifier Calibration for LP71B-2

LP71B-2  
Niros 7.101-2  
Positive Ion Output

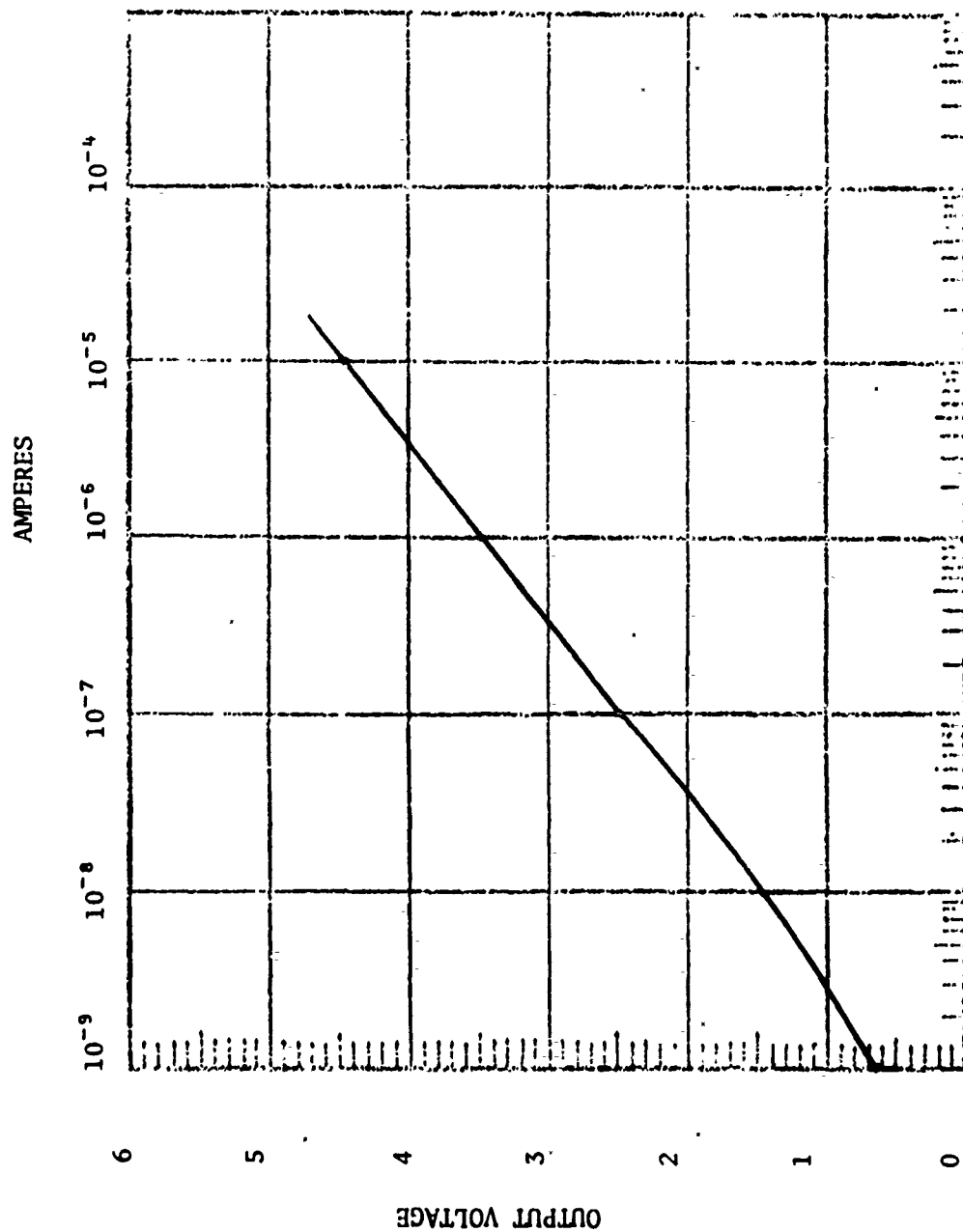


Figure 23 Positive Ion Current Amplifier Calibration for LP71B-2

Electron Output  
LP71B-3  
7.001-1

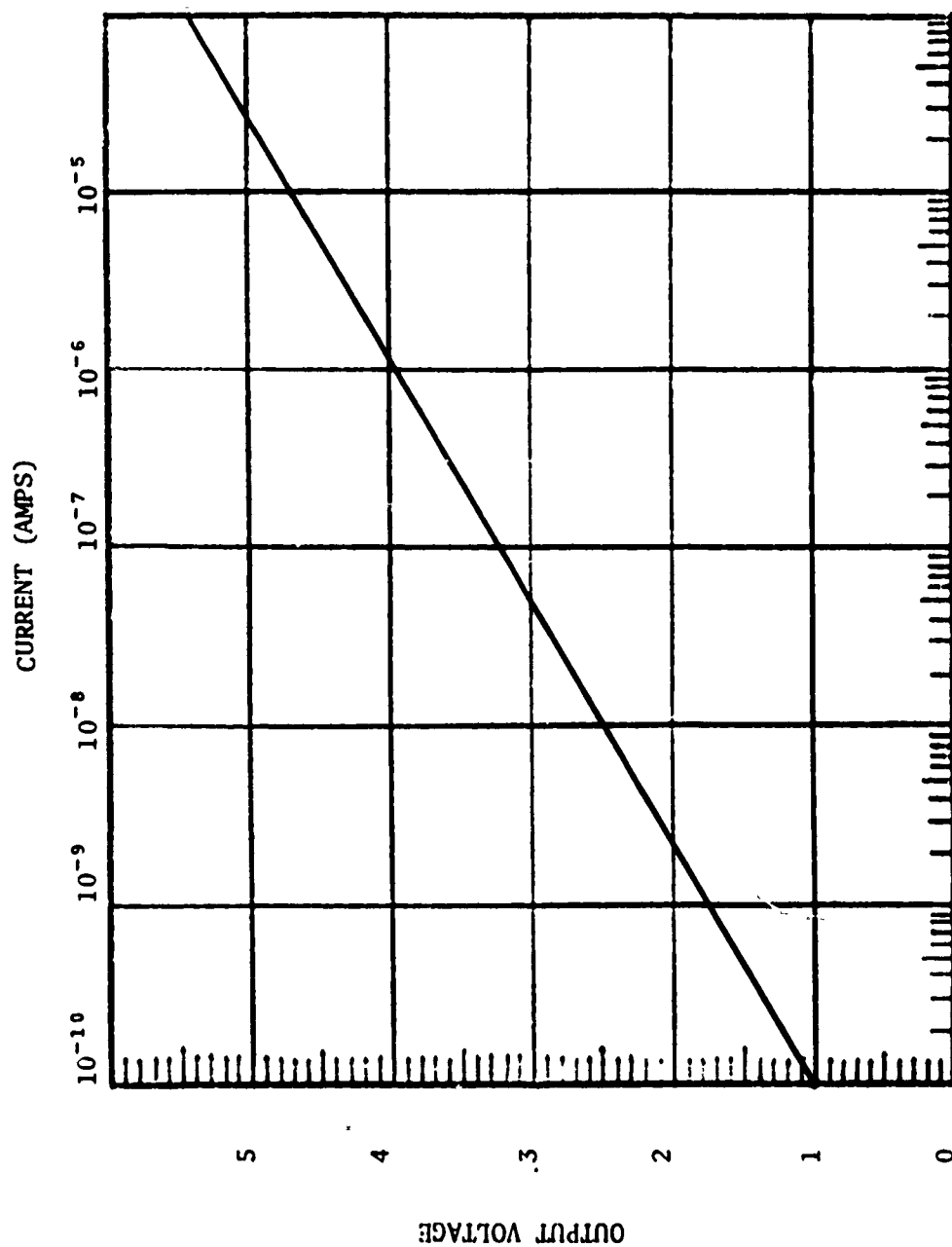


Figure 24 Electron Current Amplifier Calibration For LP71B-3

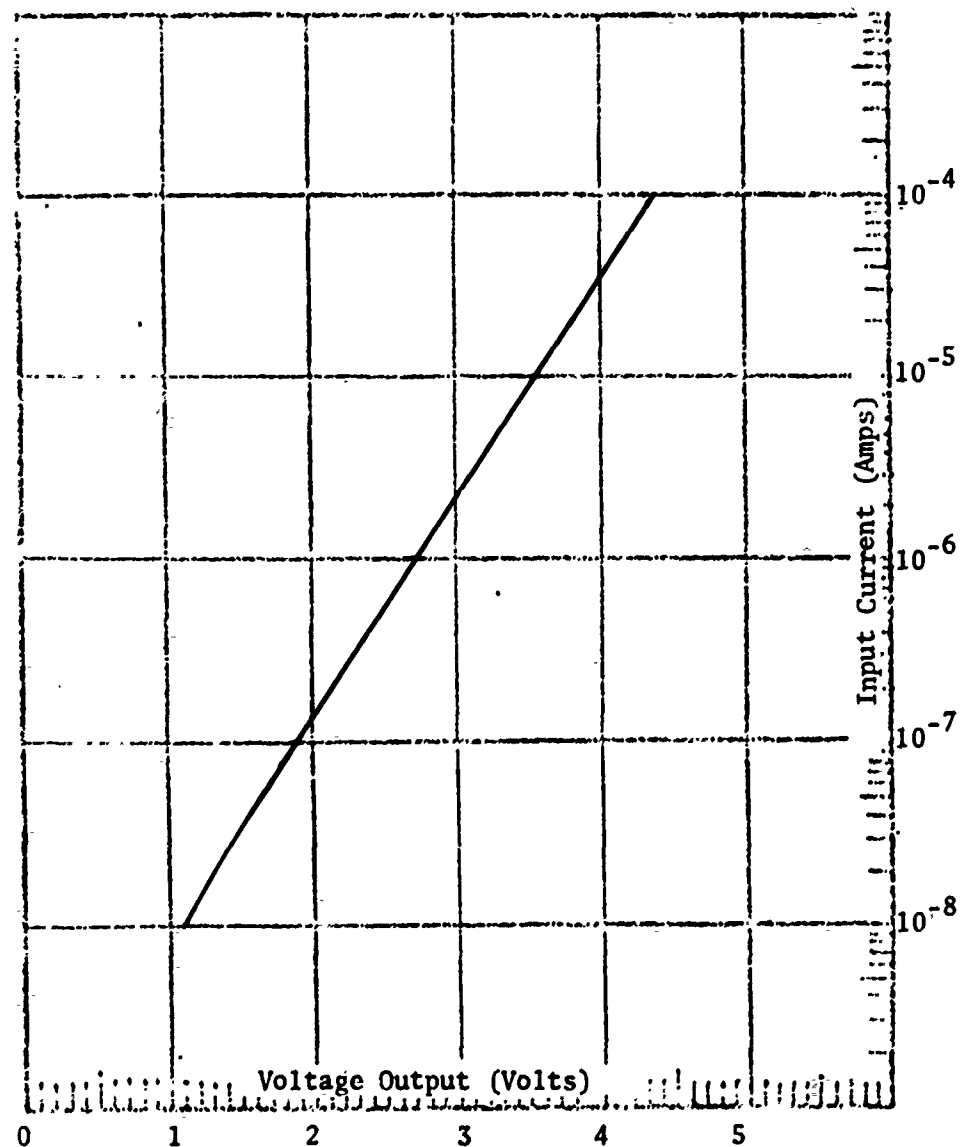


Figure 25 Positive Ion Current Amplifier Calibration for LP71B-3

9.303-3  
LP71B-8

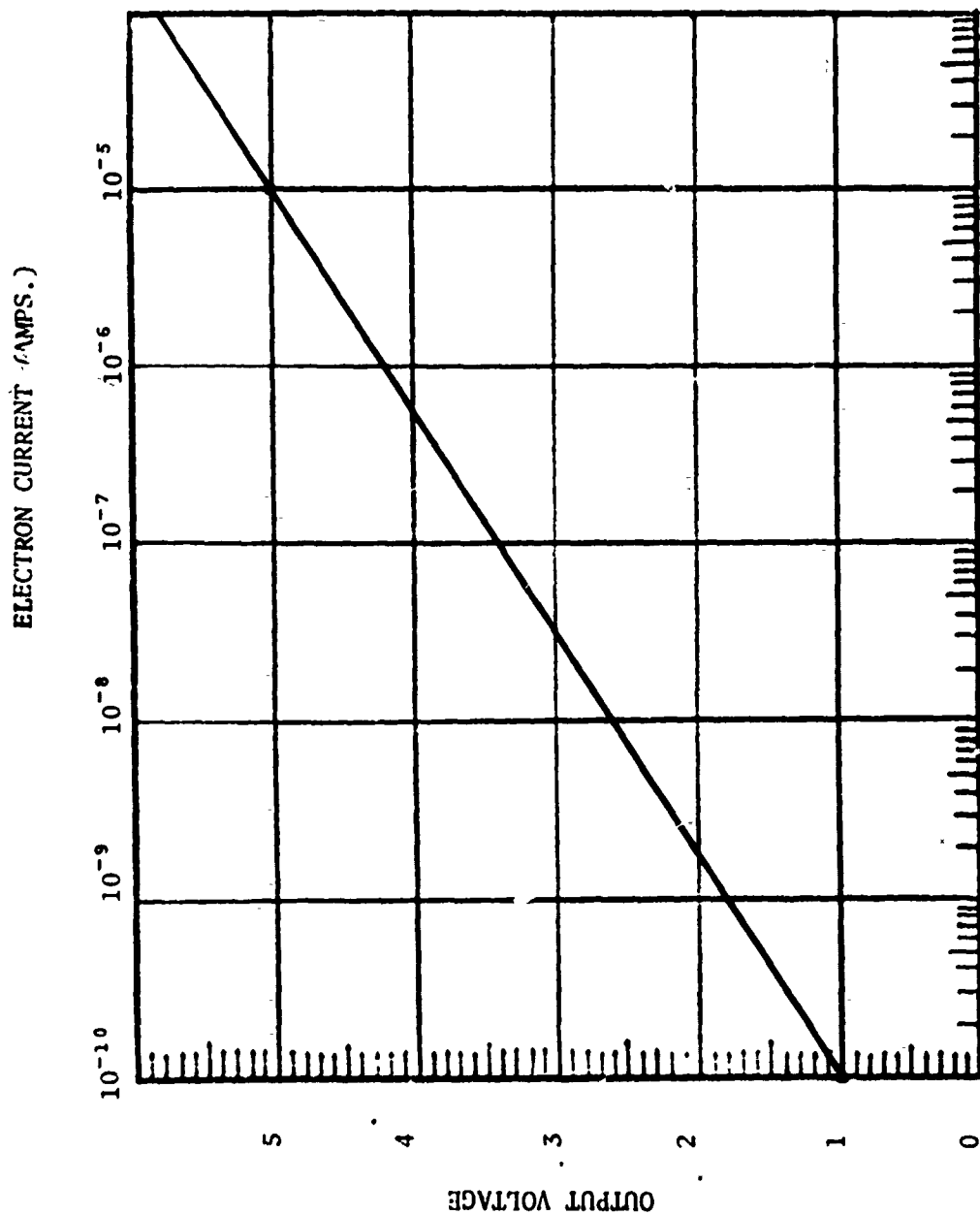


Figure 26 Electron Current Amplifier Calibration for LP71B-8



9.303-3  
LP71B-8

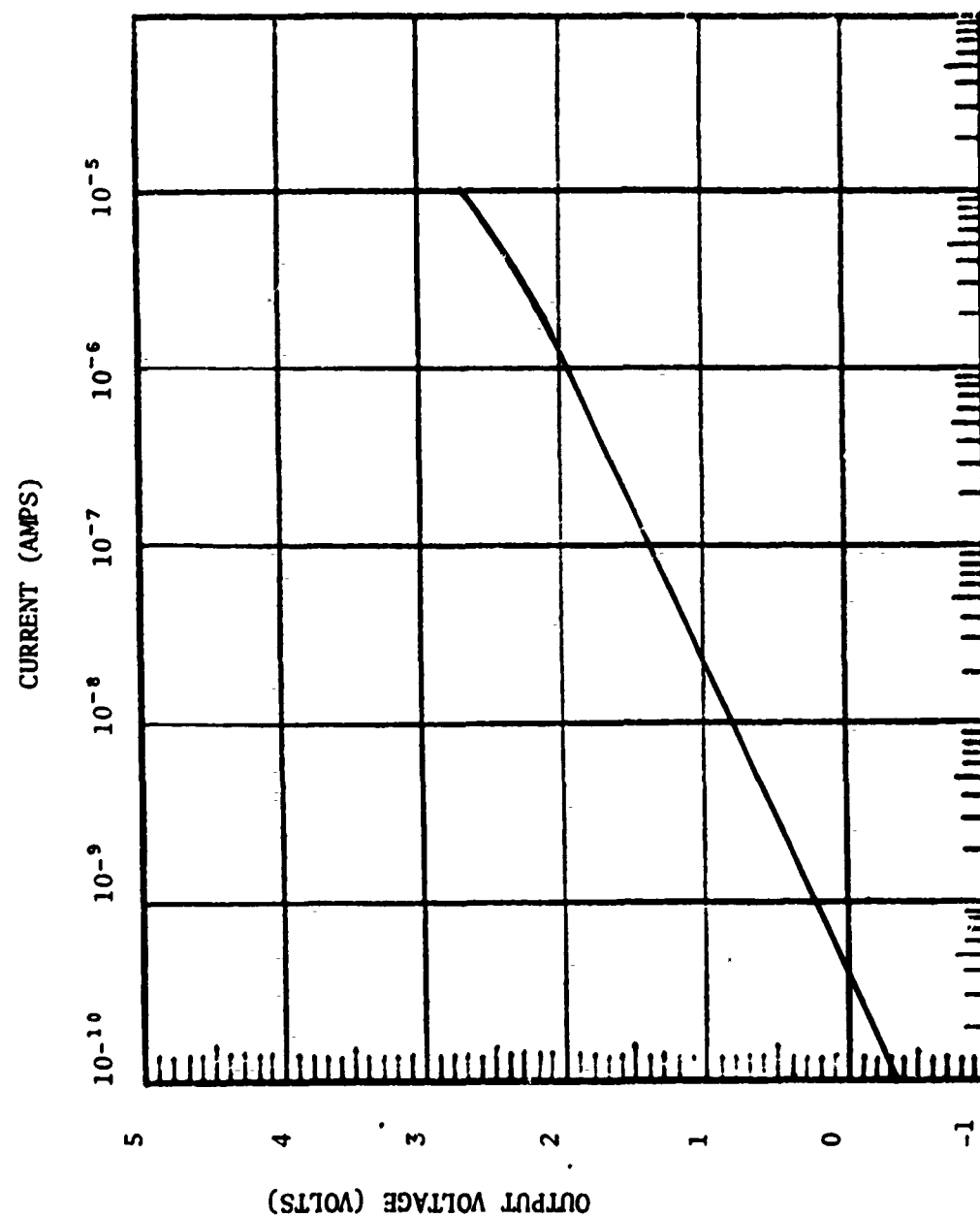


Figure 27 Positive Ion Current Amplifier Calibration for LP71B-8

9.303-4  
LP71B-9

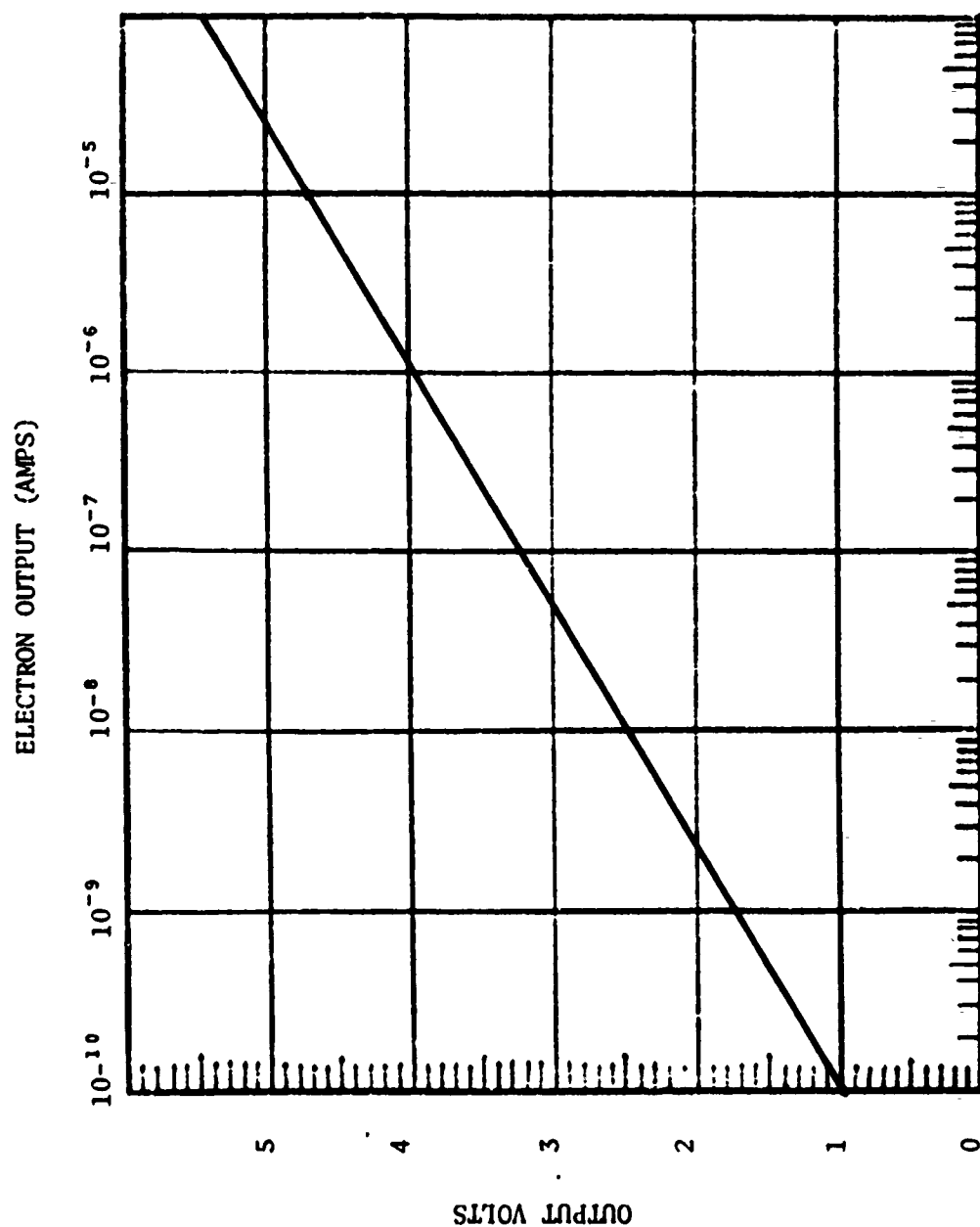


Figure 28 Electron Current Amplifier Calibration for LP71B-9

9.303-4  
LP71B-9

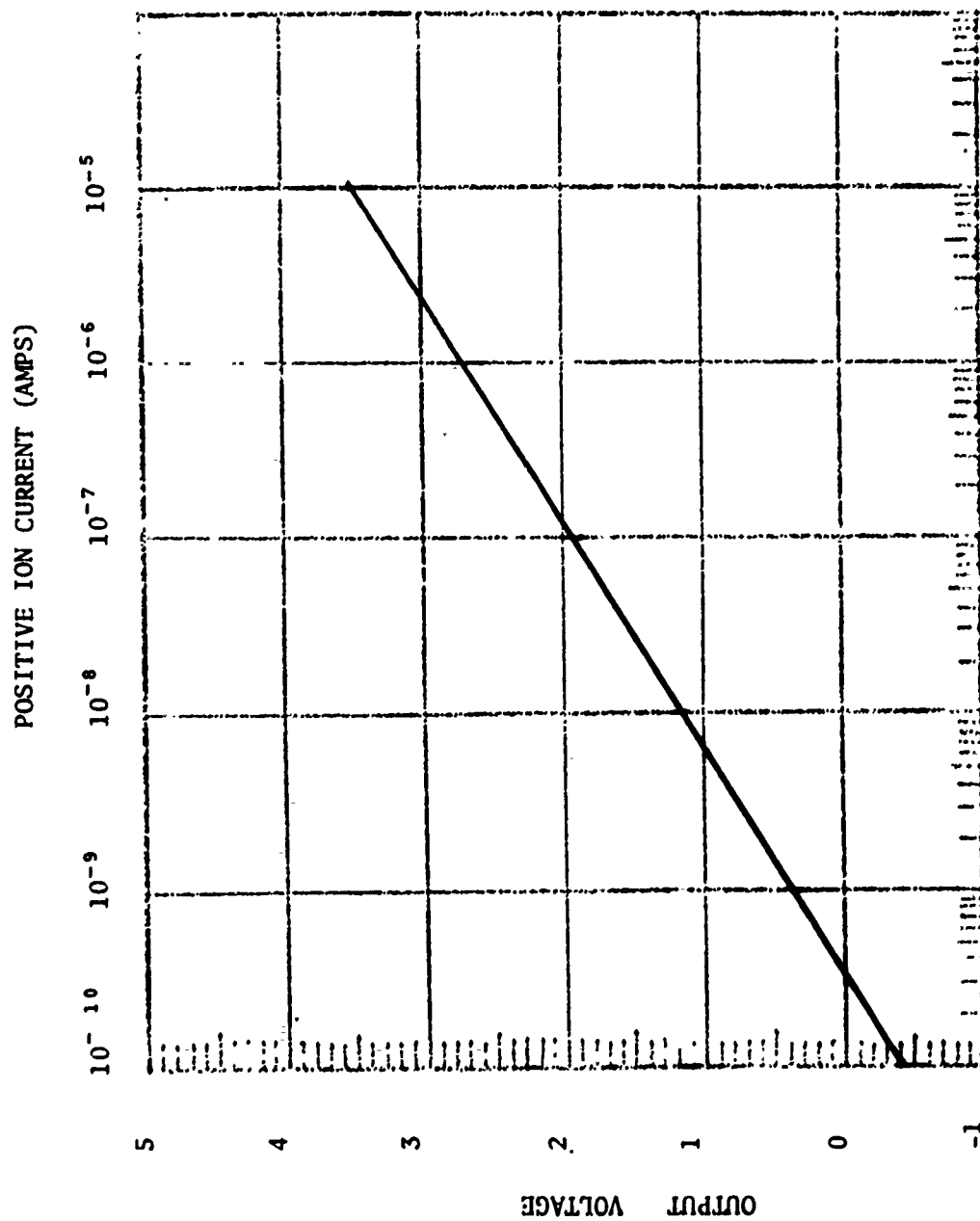


Figure 29 Positive Ion Current Amplifier Calibration for LP71B-9

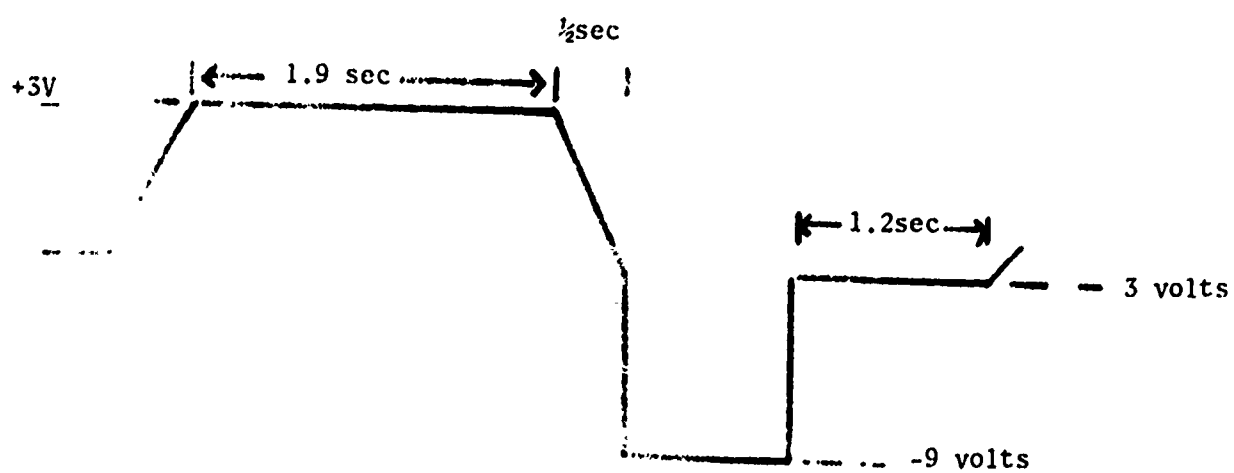


Figure 30 Langmuir Probe Function Generator Waveform for LP68B-4

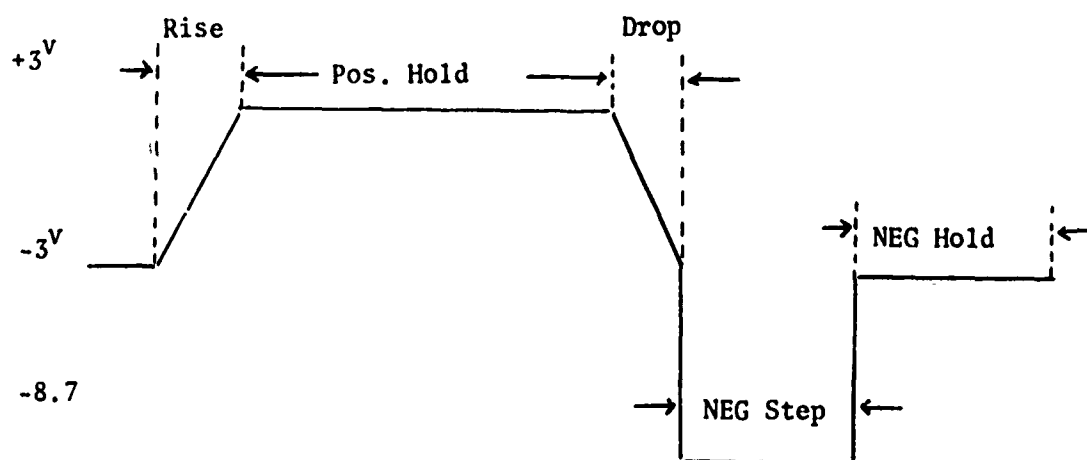


Figure 31 Langmuir Probe Function Generator Waveform for LP68-B5A and LP68-B-10A.

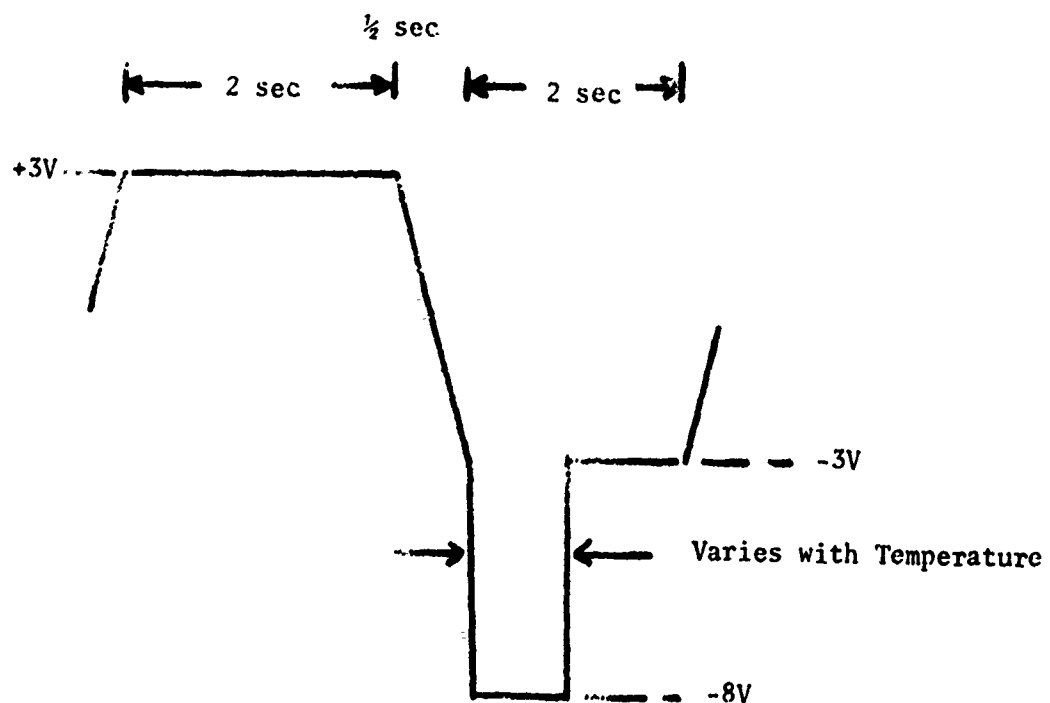


Figure 32 Langmuir Probe Function Generator Waveform for LP70A-2,-3  
and LP71B-1, 2, 3, 4.

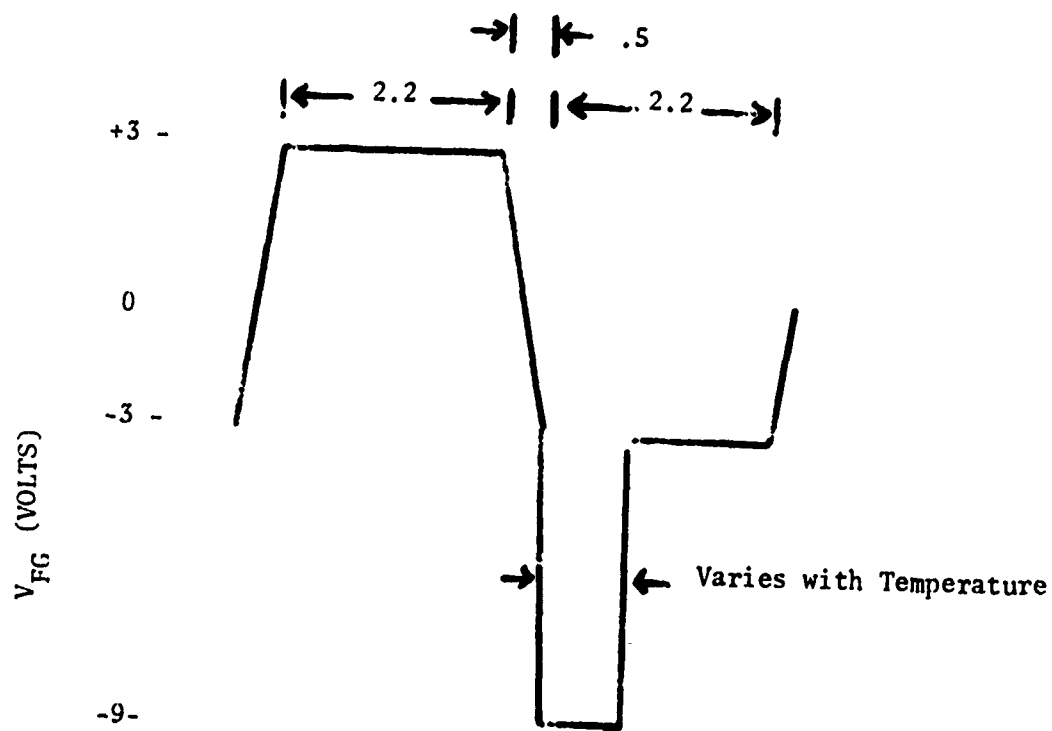


Figure 33 Langmuir Probe Function Generator Waveform for Langmuir Probes LP71B-8 and LP71B-9

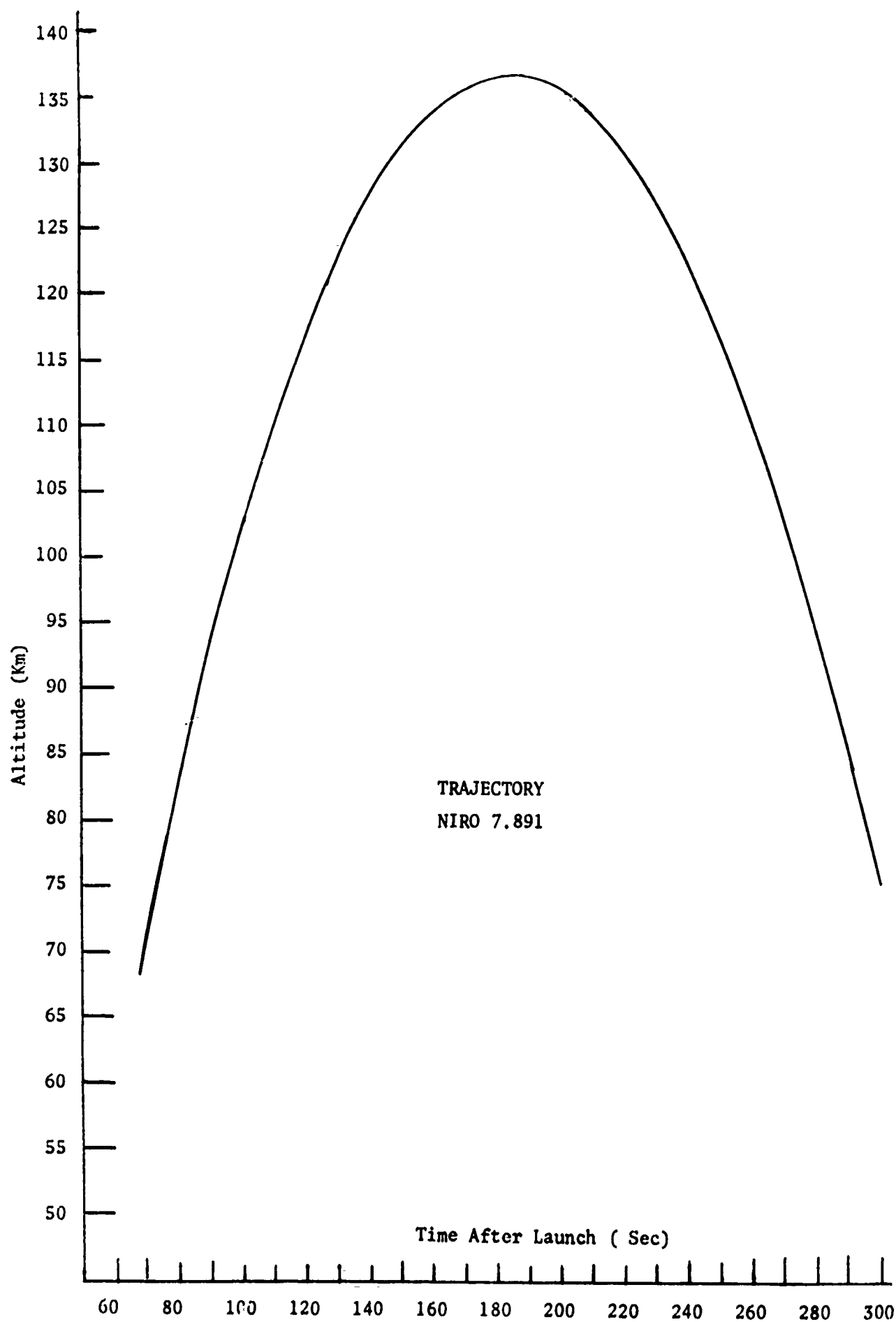


Figure 34 Flight Trajectory for NIRO AT 7.891



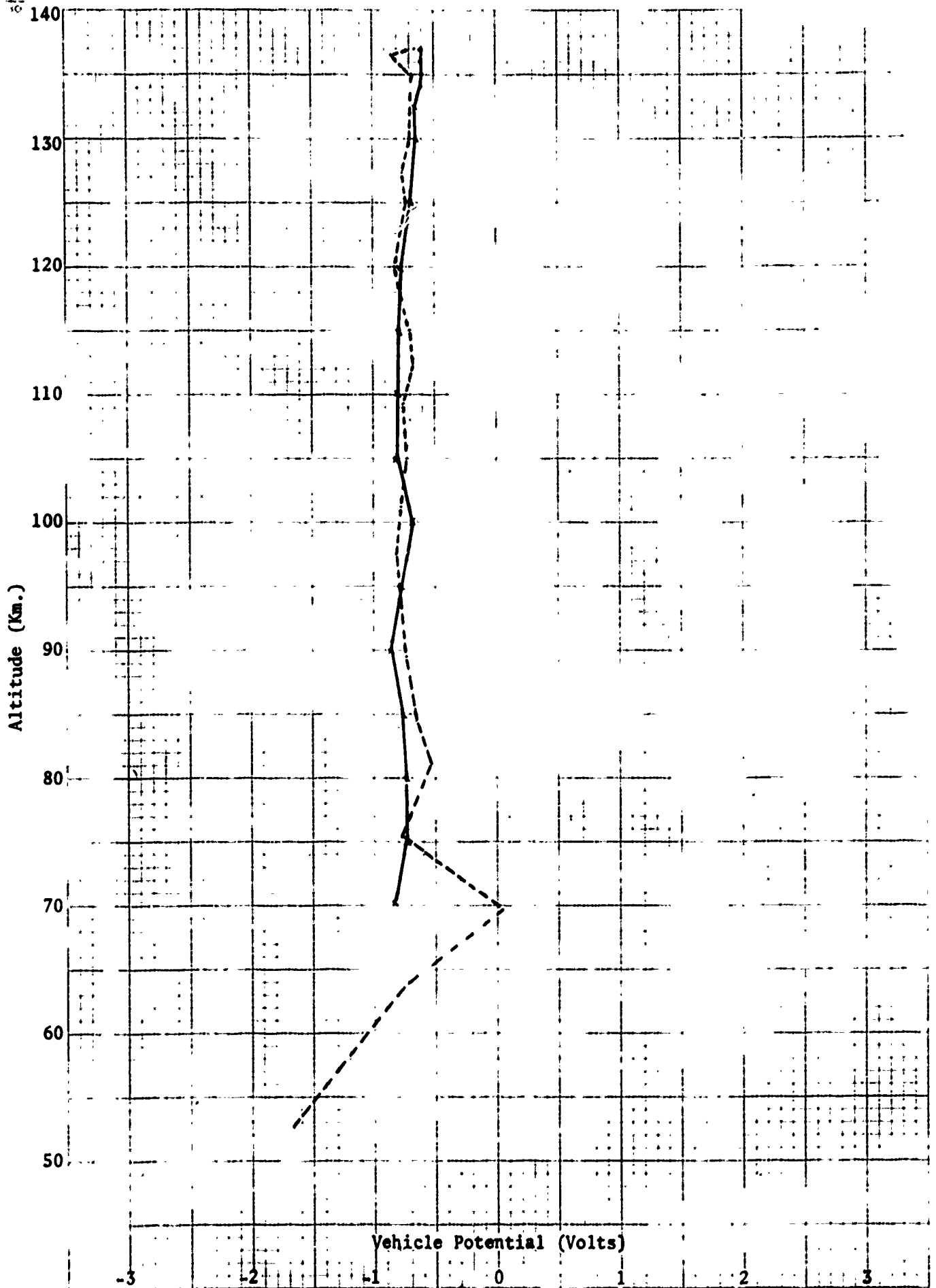


Figure 35 Vehicle Potential Measurements for AT 7.891

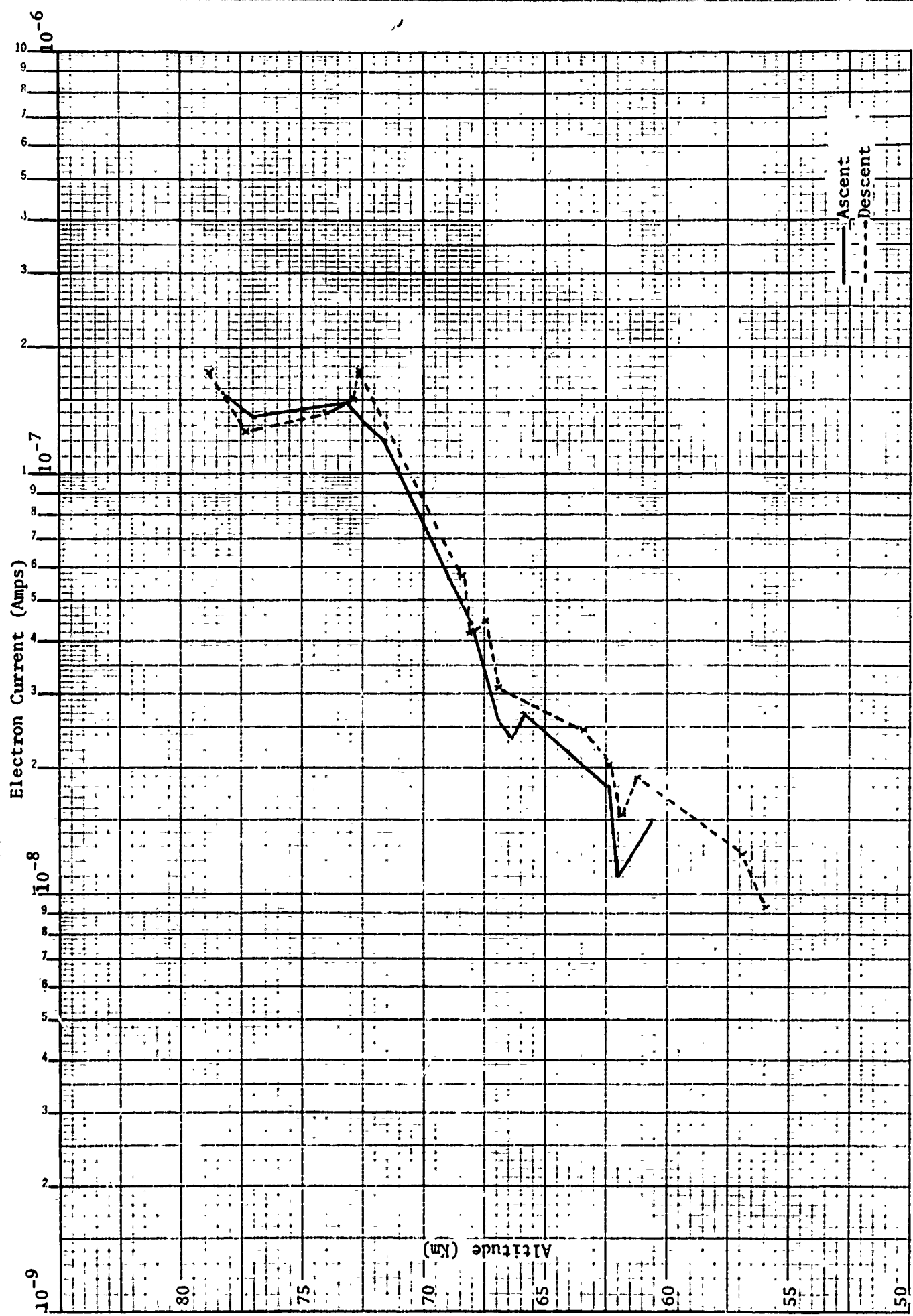


Figure 36 Electron Current versus Altitude AT 7.891

KOE SEMILOGARITHMIC 4G 6012  
4 CYCLES X JASON  
MEUFFEL & ESSER CO

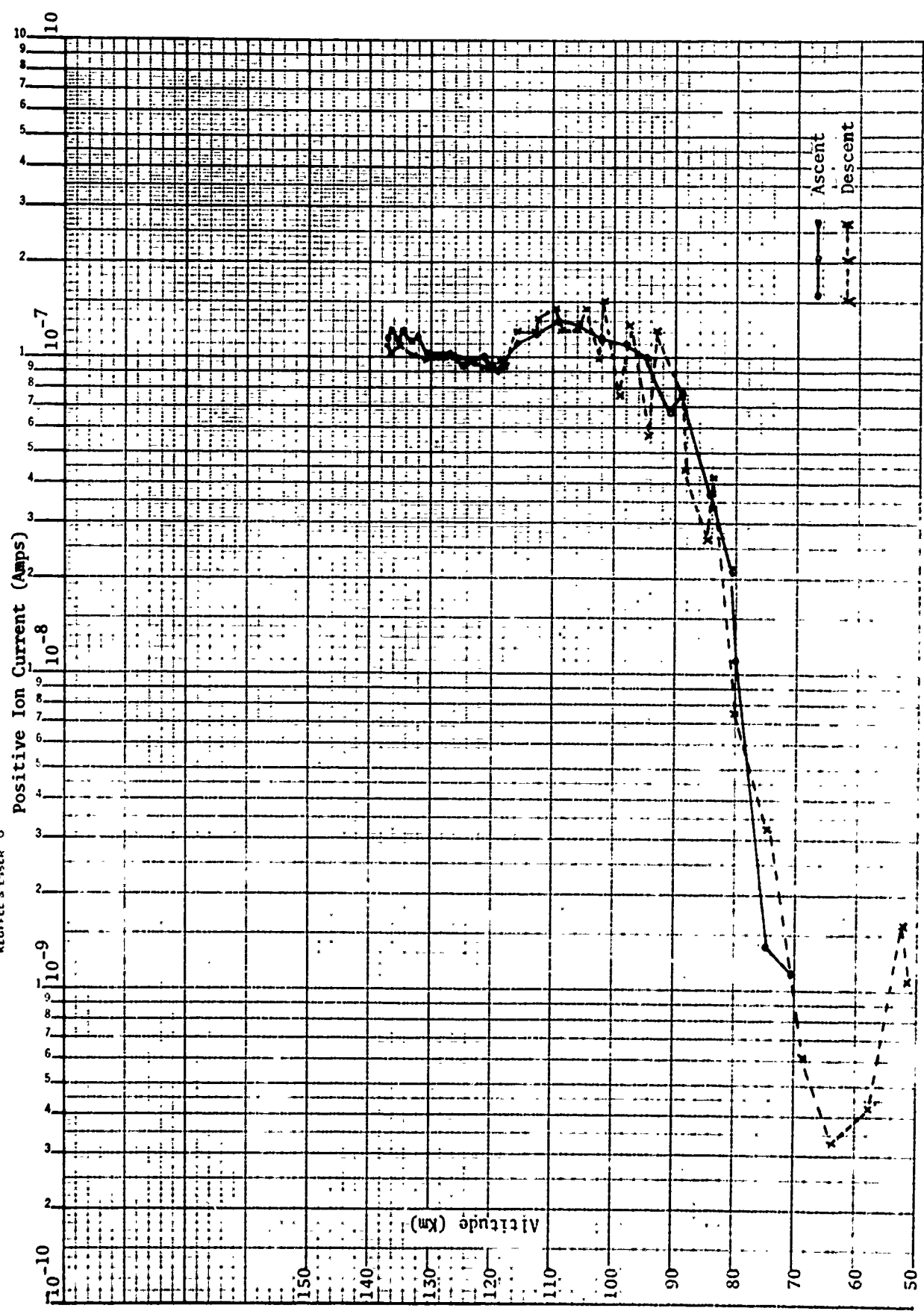


Figure 37 Positive Ion Current Measurements at -3 volts versus Altitude for AT 7.891

K<sub>0</sub>Σ SEMILOGARITHMIC 46 6312  
NEUPRESENTATION

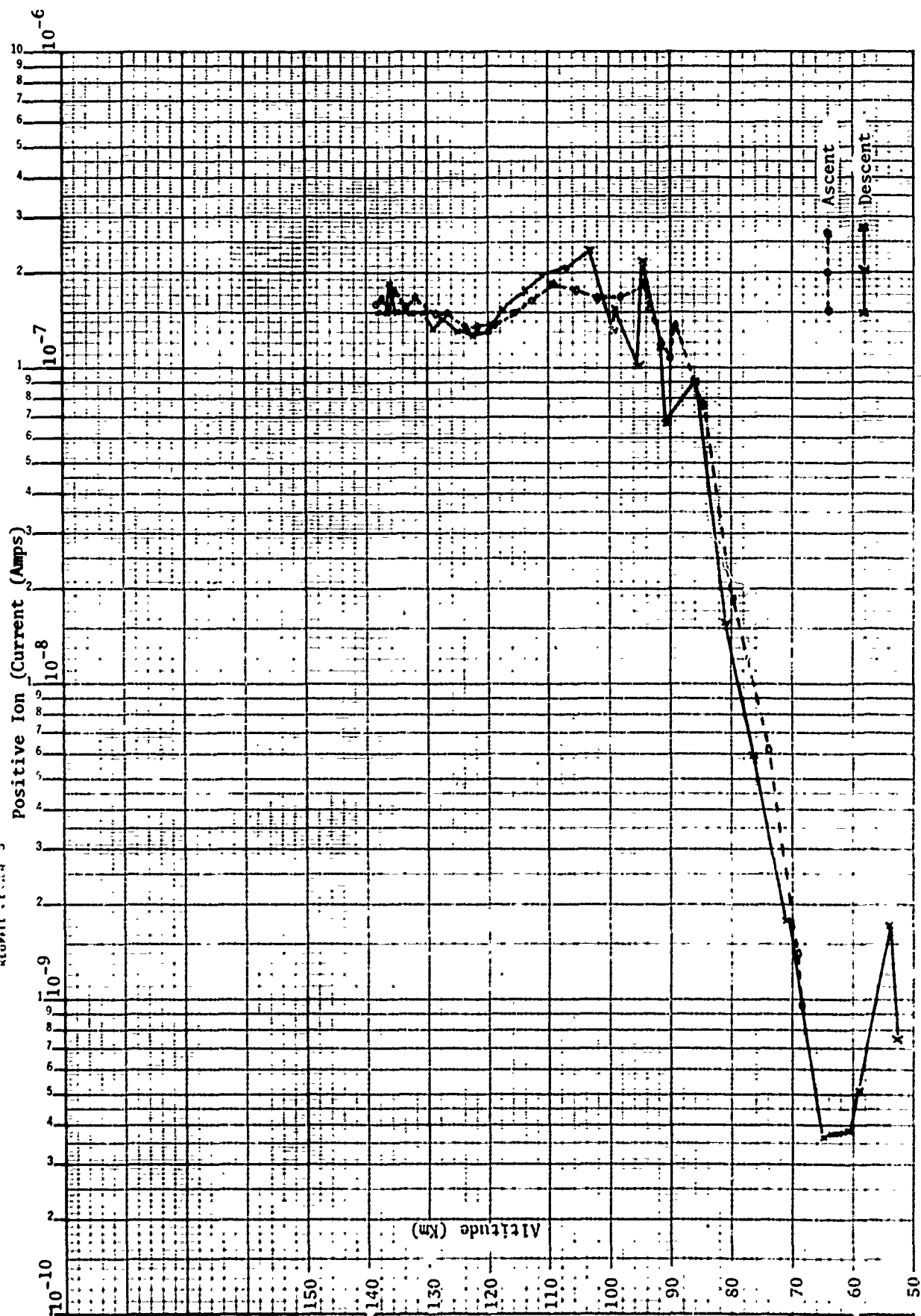


Figure 38 Positive Ion Current Measurements at -9 volts versus Altitude for AT 7.891

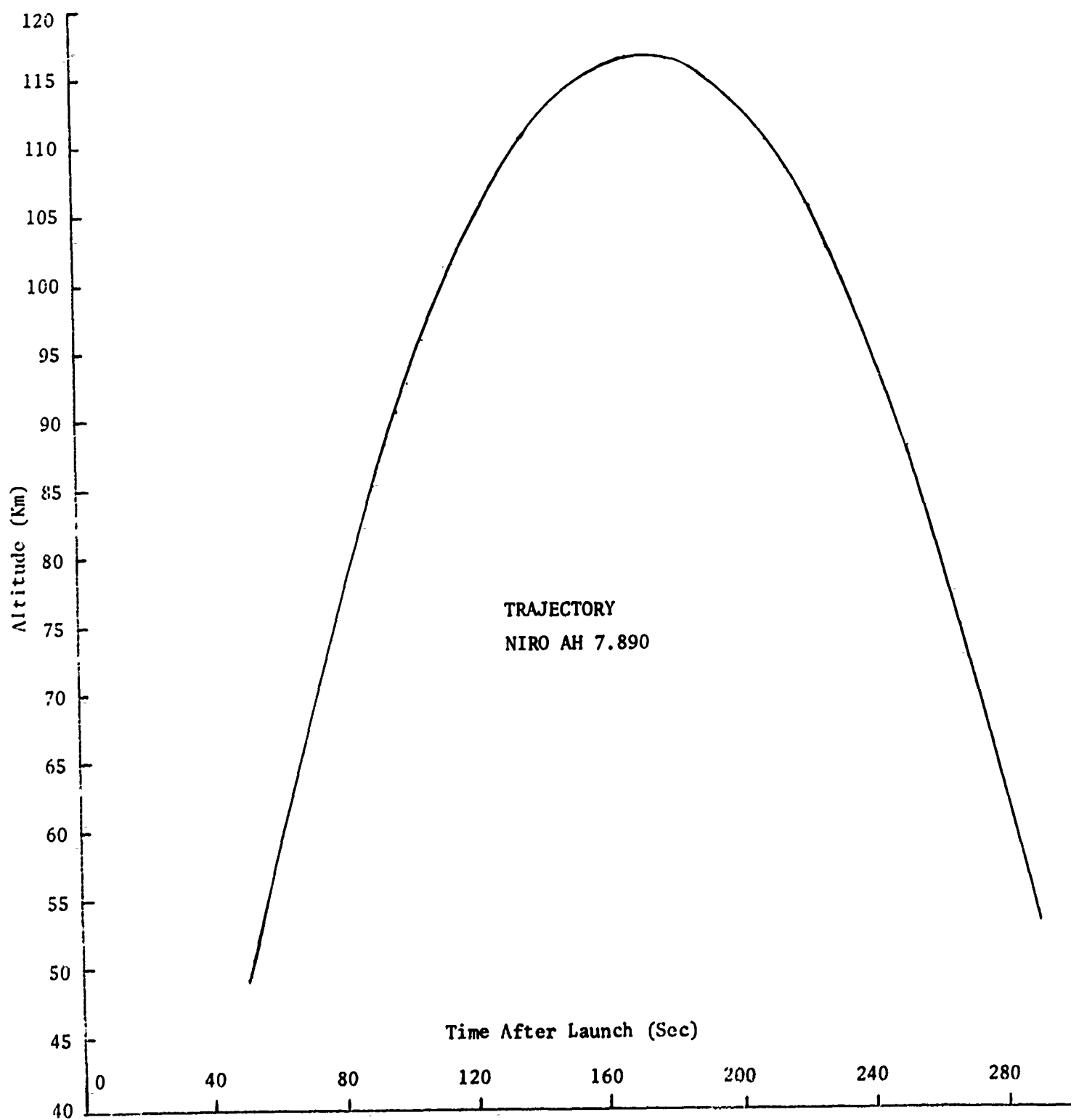


Figure 39 Flight Trajectory for NIRO AH 7.890

K&E SEMI LOGARITHMIC 46 5492  
 3 CYCLES X 70 DIVISIONS  
 KEUFFEL & ESSER CO.

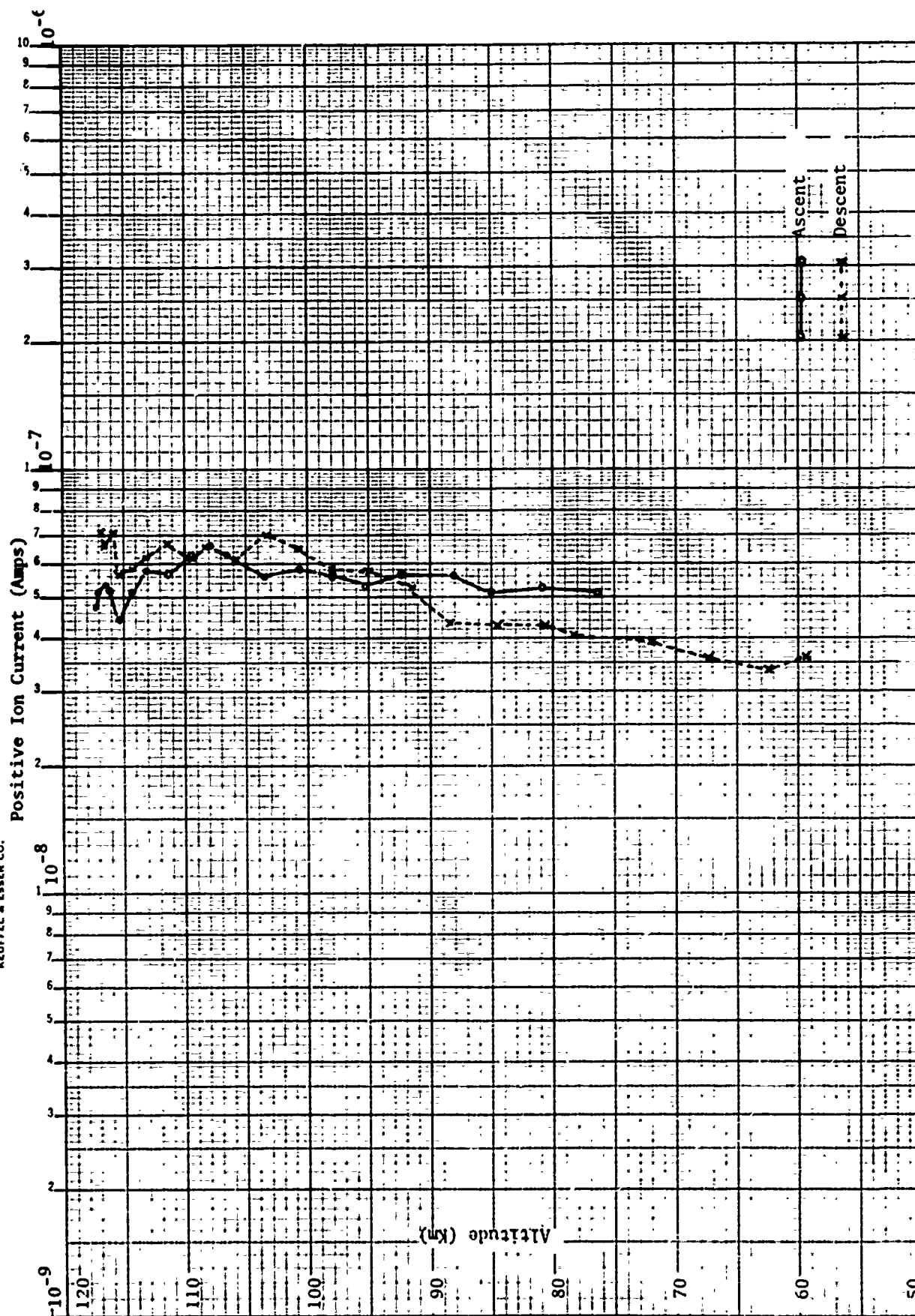


Figure 40 Positive Ion Current Measurement at -3 volts vs. Altitude for AH 7.890

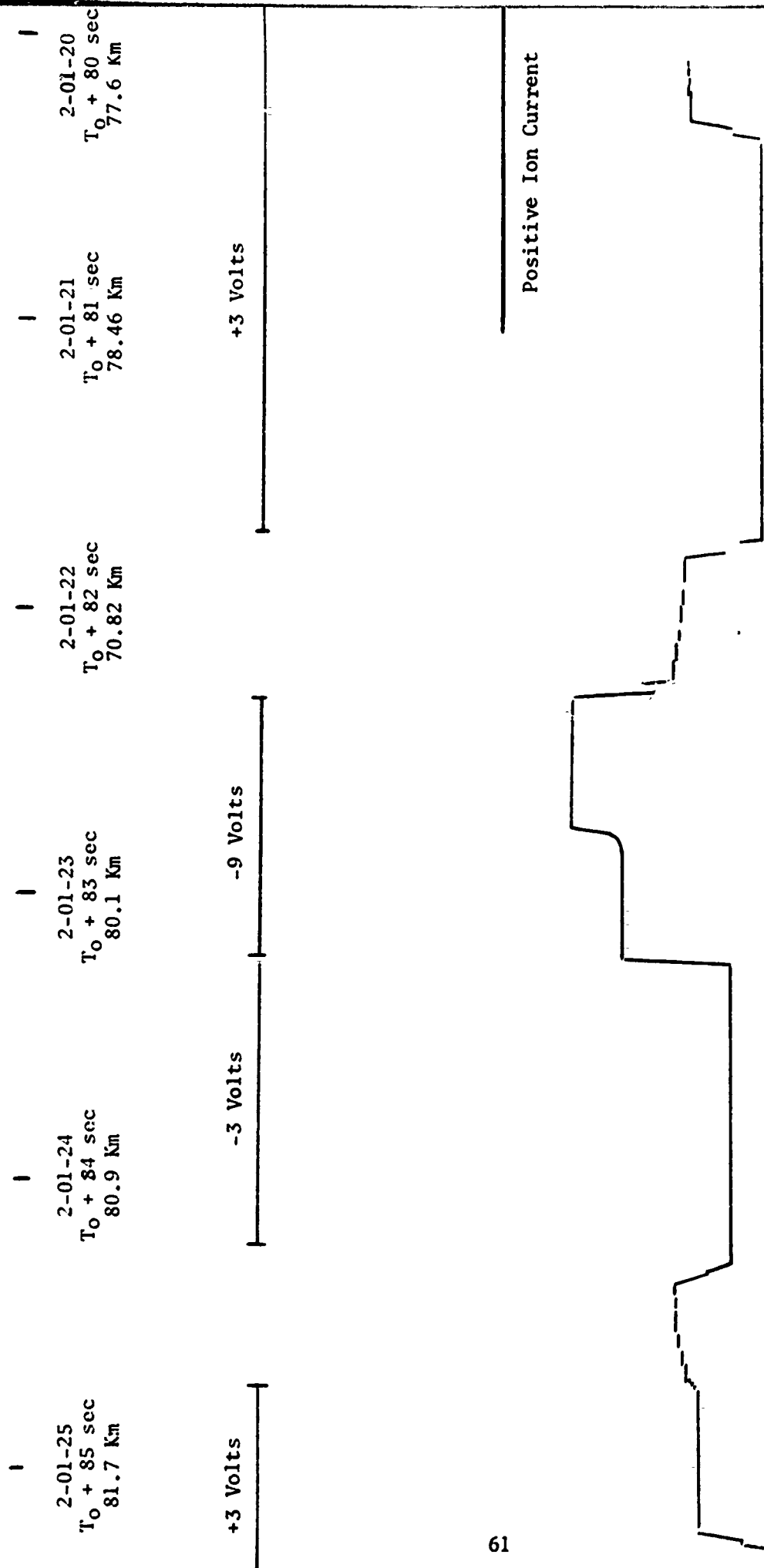


Figure 41 Strip Chart Data Between 77.6 km and 81.7 km for AH 7.890

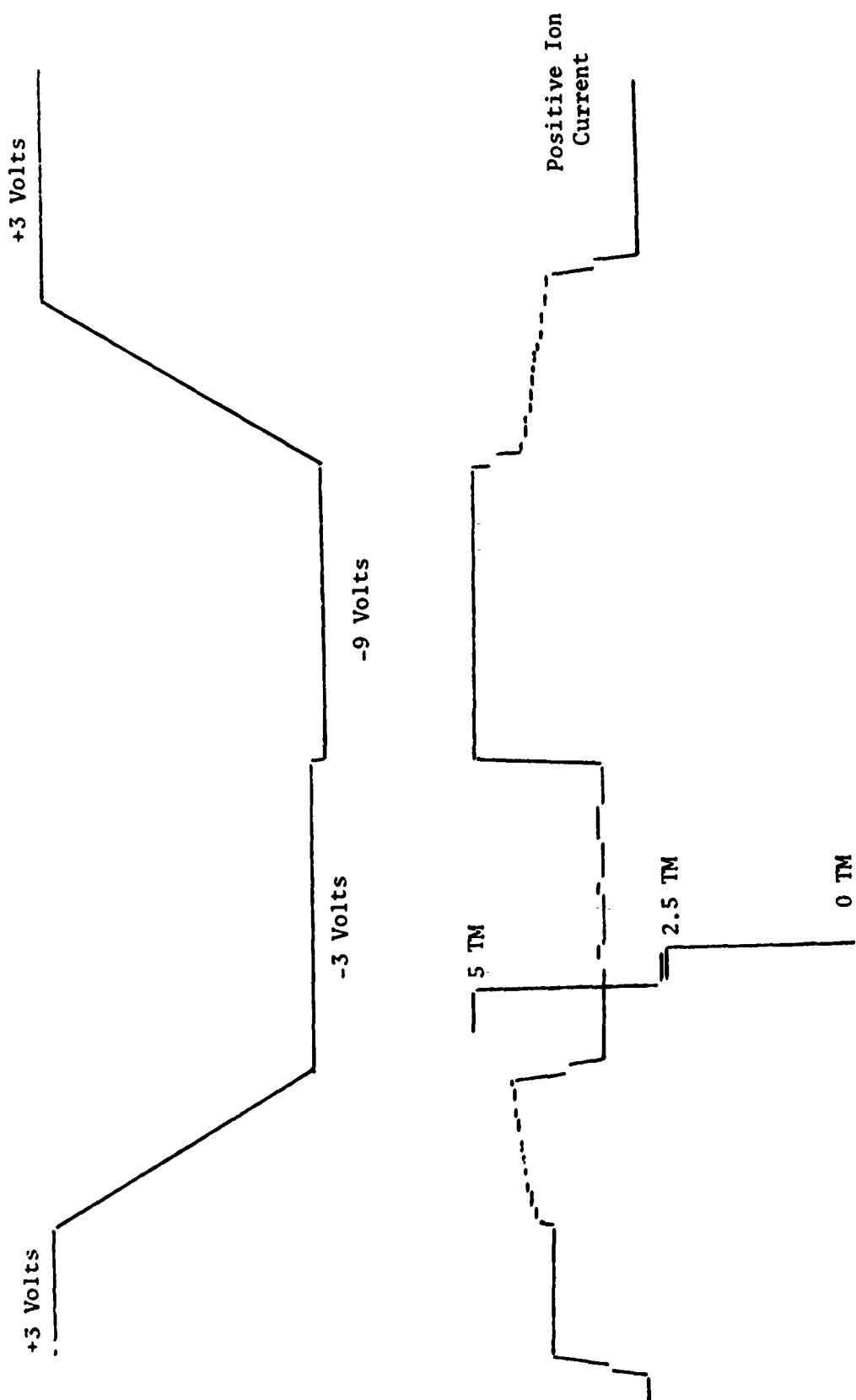


Figure 42 Strip Chart Data



2-02-54 T <sub>0</sub> + 174 sec 117.03 km	2-02-53 T <sub>0</sub> + 173 sec 117.04 km	2-02-52 T <sub>0</sub> + 172 sec 117.04 Km	2-02-51 T <sub>0</sub> + 171 sec 117.04 km	2-02-50 T <sub>0</sub> + 170 sec 117.02 km
+3 Volts	+3 Volts	-3 Volts	-9 Volts	+3 Volts

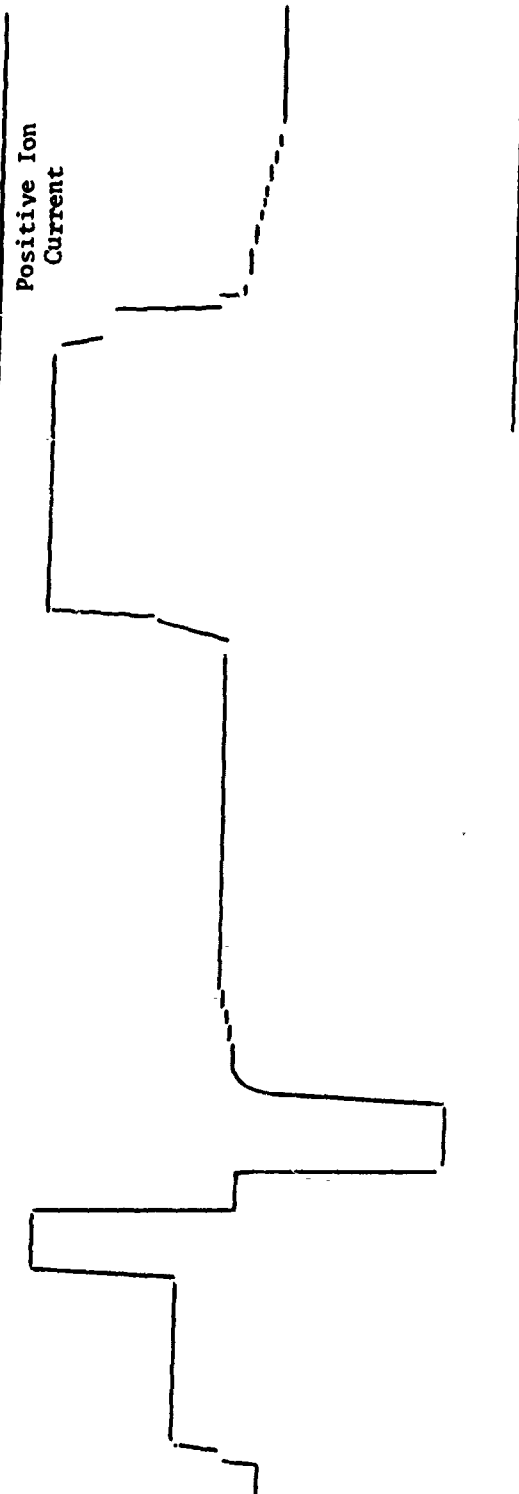


Figure 43 Strip Chart Data at Vehicle Apogee for AH 7.890

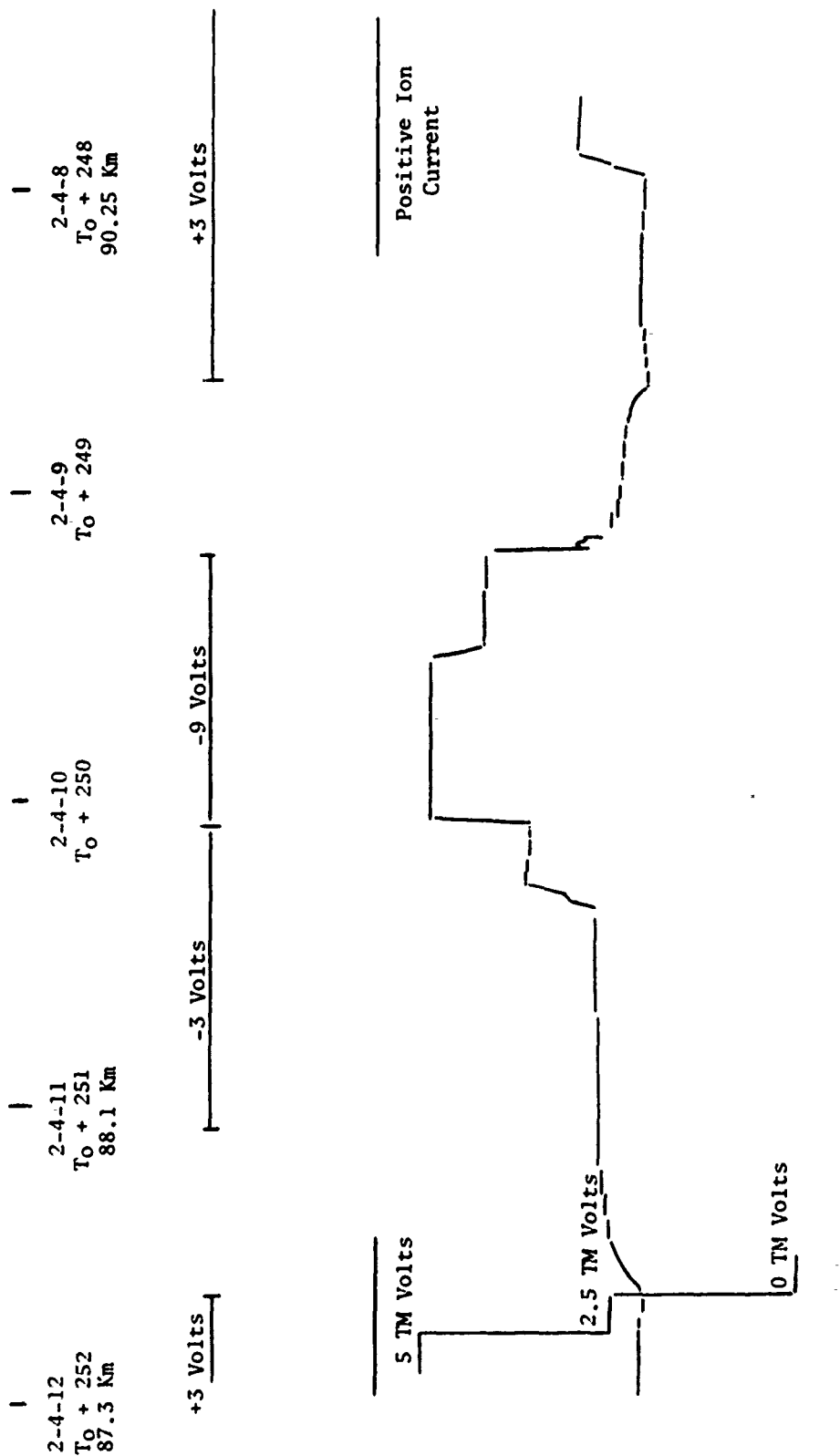


Figure 44 Strip Chart Data on Vehicle Descent Between 90.25 km and 87.3 km. AH 7.890

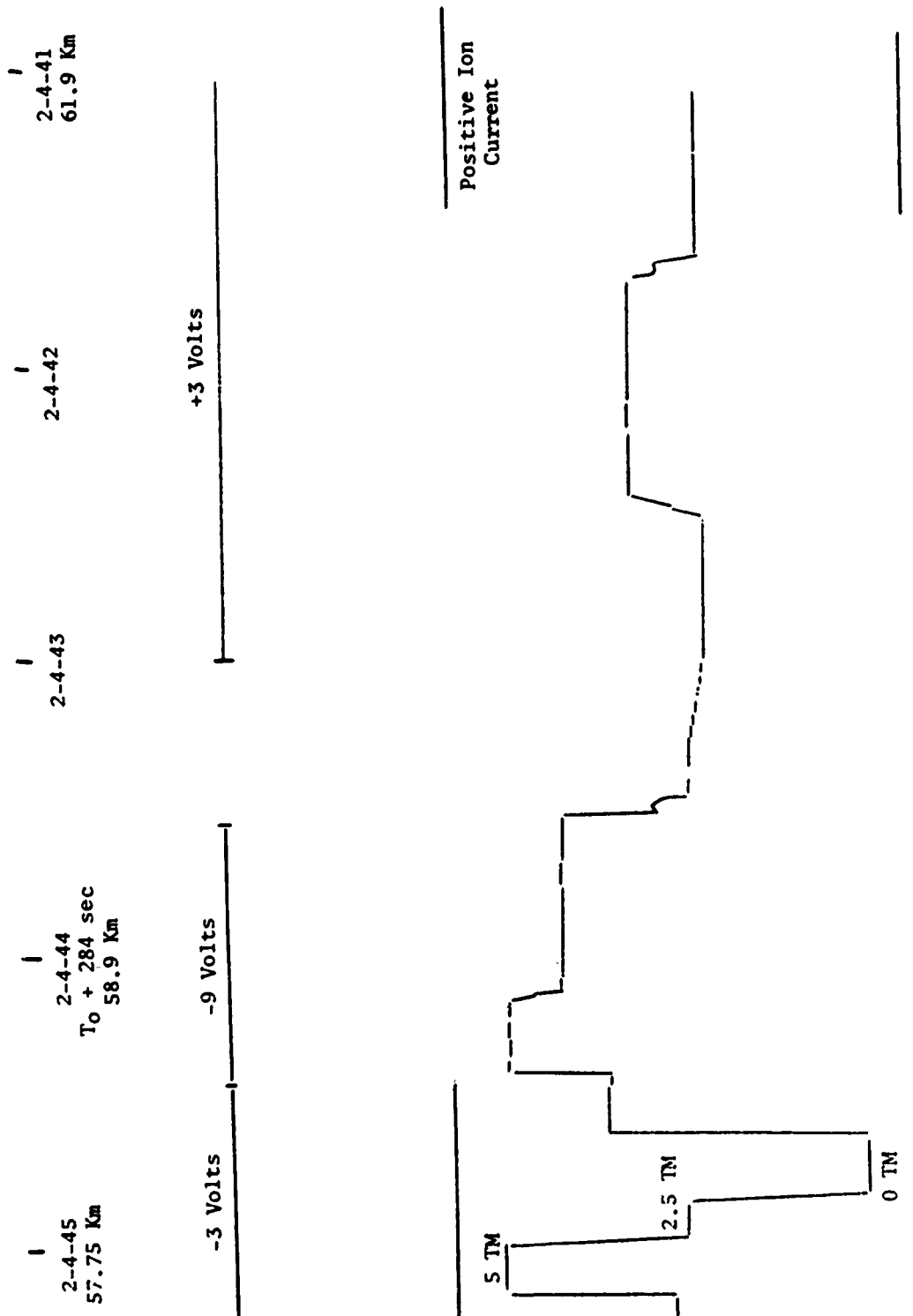


Figure 45 Strip Chart Data on Vehicle Descent Between 61.9 km and 57.75 km. AH 7.890

2-51-59  
T<sub>0</sub> + 59

2-52-00  
T<sub>0</sub> + 60

2-52-01  
T<sub>0</sub> + 61

2-52-02  
T<sub>0</sub> + 62

2-52-03  
T<sub>0</sub> + 63

2-52-04  
T<sub>0</sub> + 64

-9 Volts

-3 Volts

+3 Volts

Electron Current

Positive Ion Current

2 1/2

0

Figure 46 Strip Chart Data Between T<sub>0</sub> + 59 secs and T<sub>0</sub> + 64 secs for AH 7.892

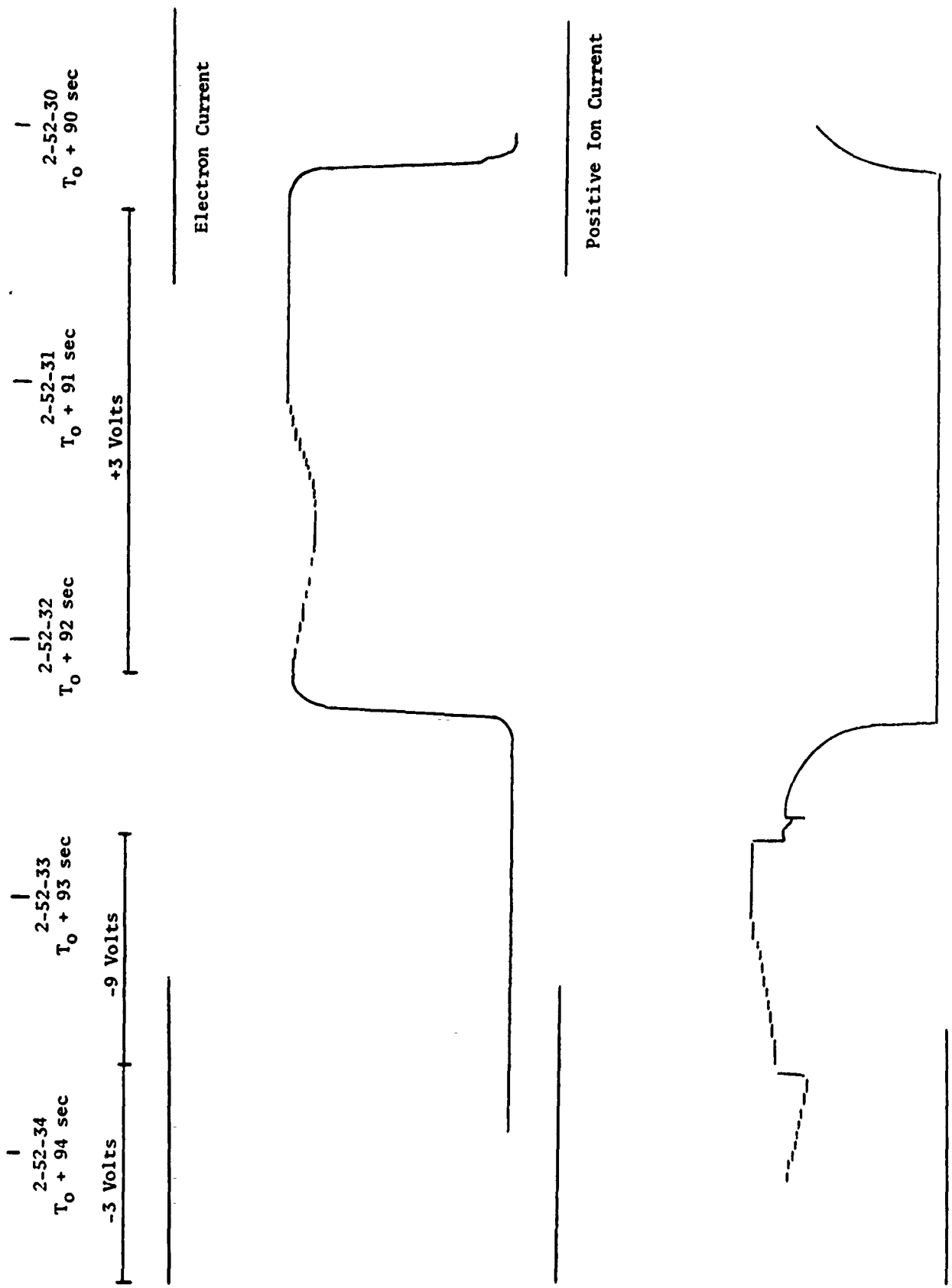


Figure 47 Strip Chart Data Between  $T_0 + 90 \text{ secs}$  and  $T_0 + 94 \text{ secs}$  for AH 7.892

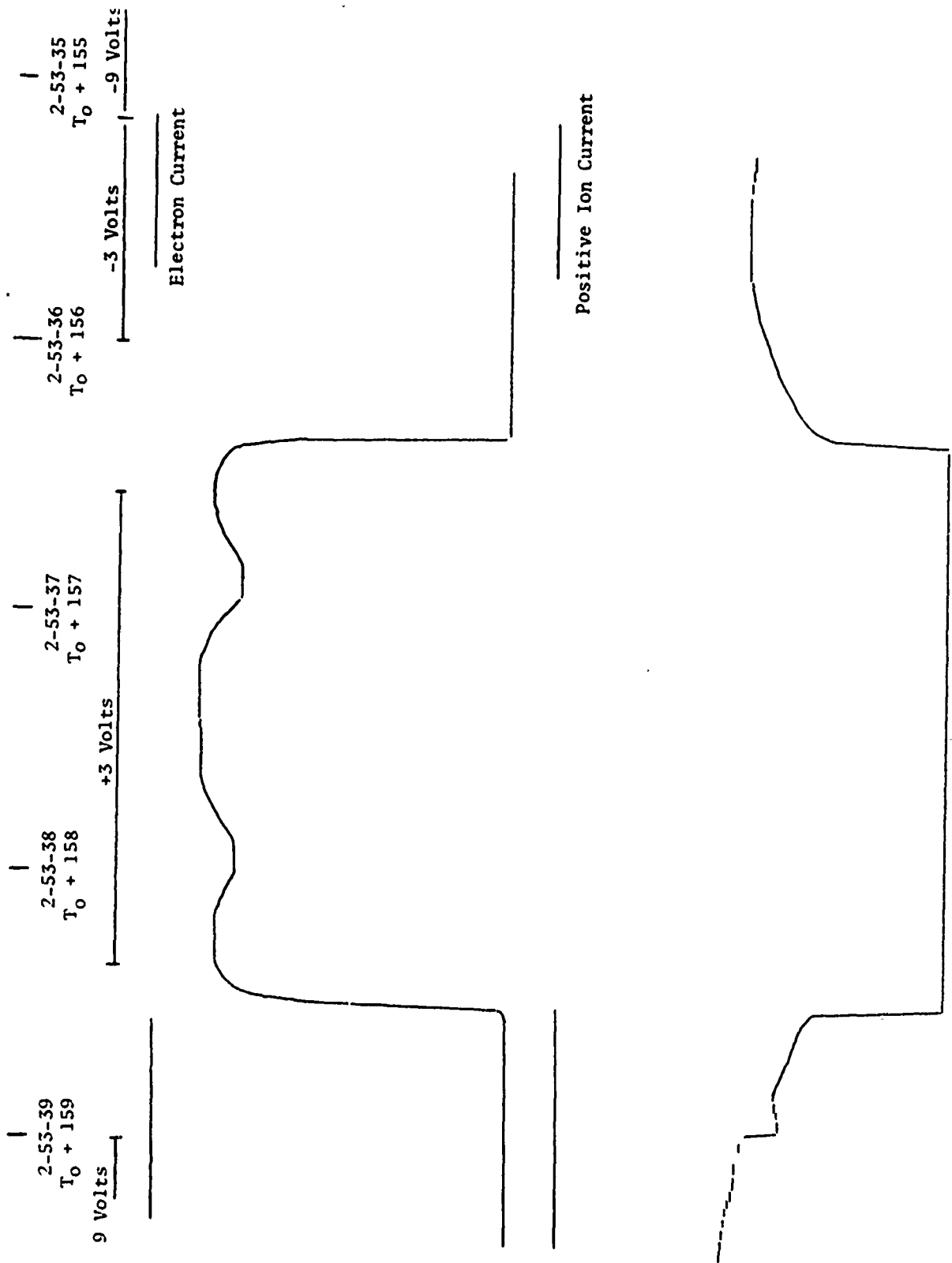


Figure 48 Strip Chart Data Between  $T_0 + 155$  sec and  $T_0 + 159$  sec for AH 7.892

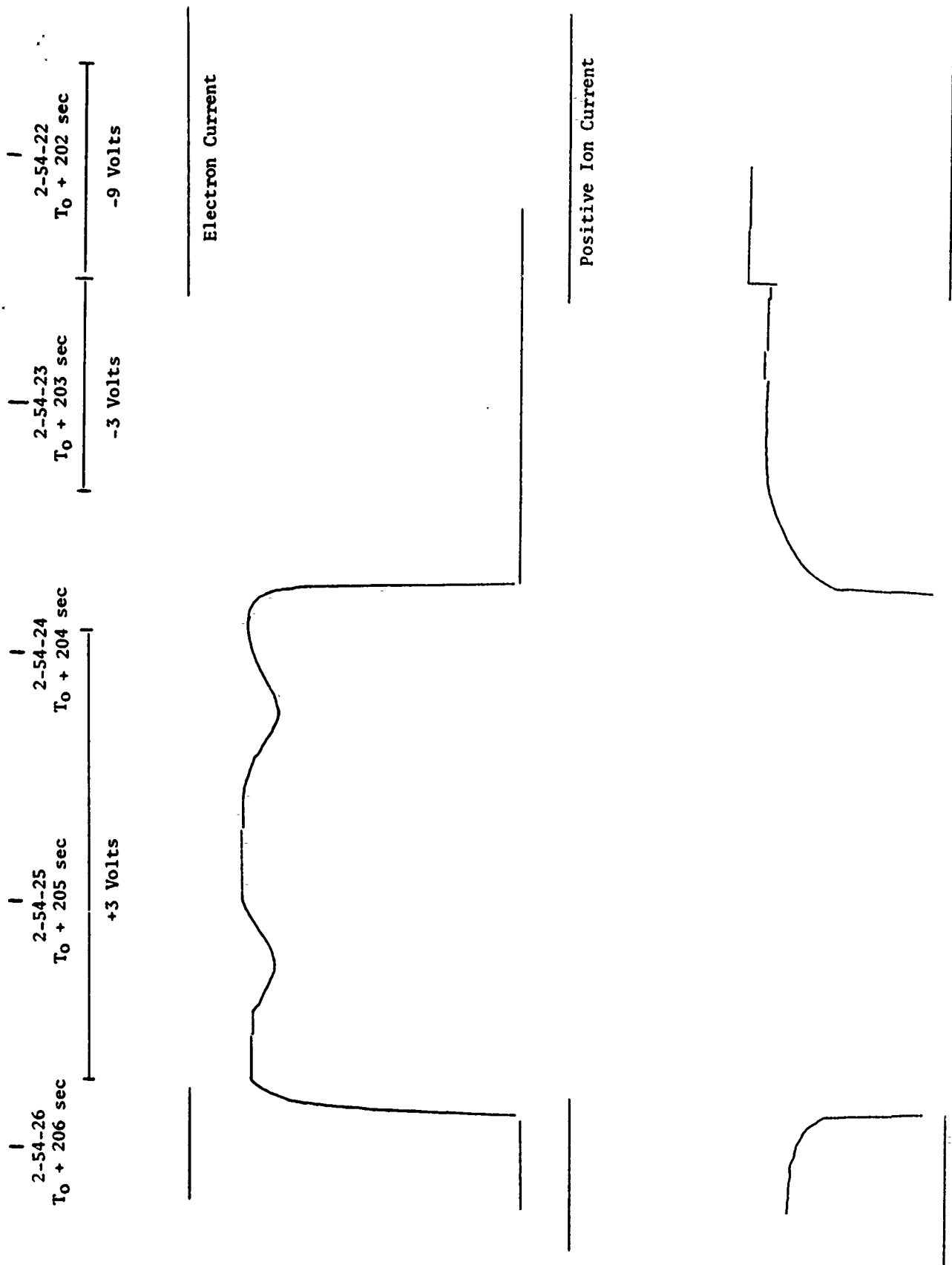


Figure 49 Strip Chart Data Between  $T_0 + 202 \text{ secs}$  and  $T_0 + 206 \text{ sec}$  for AH 7.892

K&E 10 X 10 TO THE CENTIMETER 46 1512  
MADE IN U.S.A.  
 KEUFFEL & ESSLER CO.

Time After Launch (Sec)

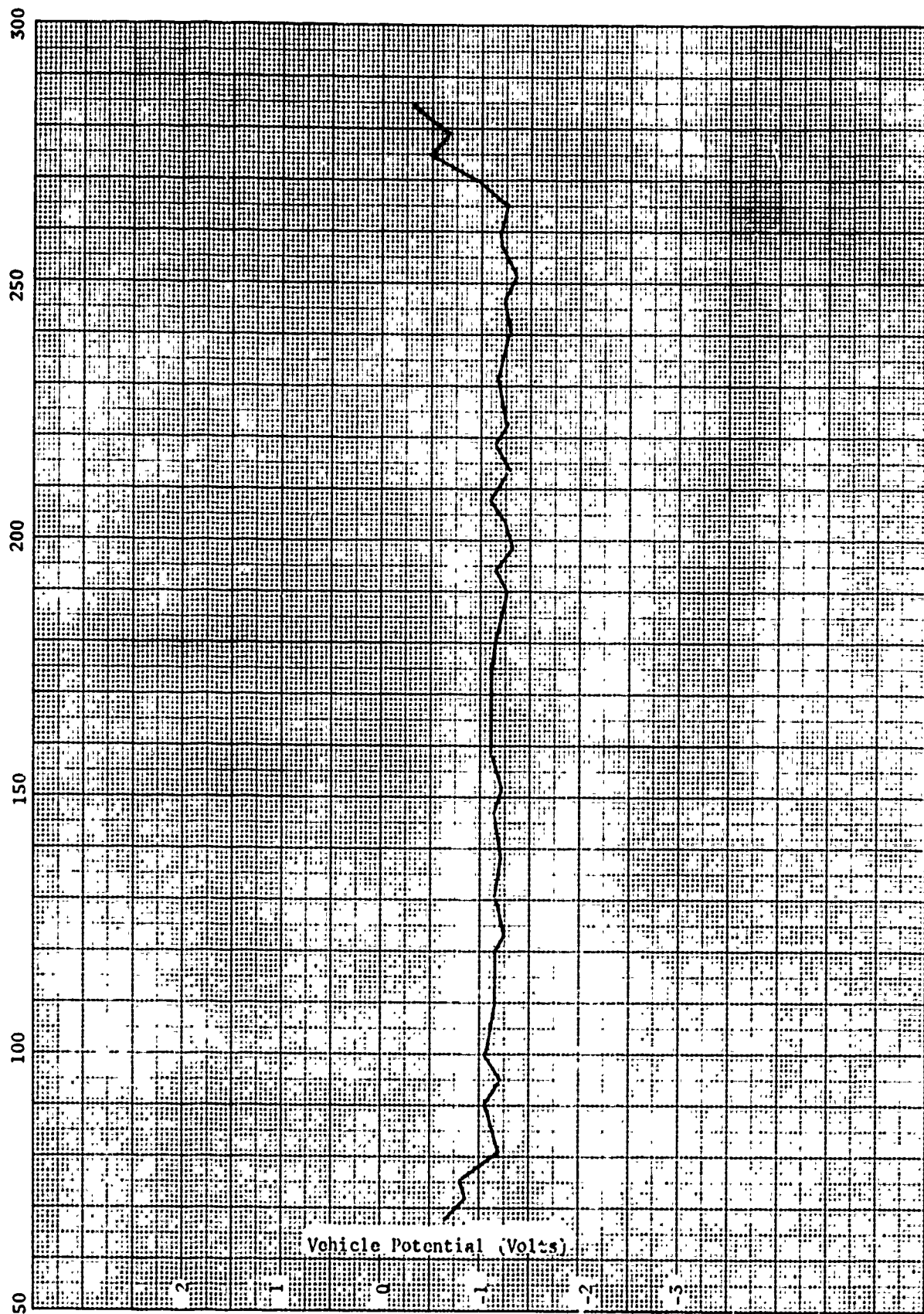


Figure 50 Vehicle Potential Measurement for All 7.892



Electron Current (+3V)  
7.892

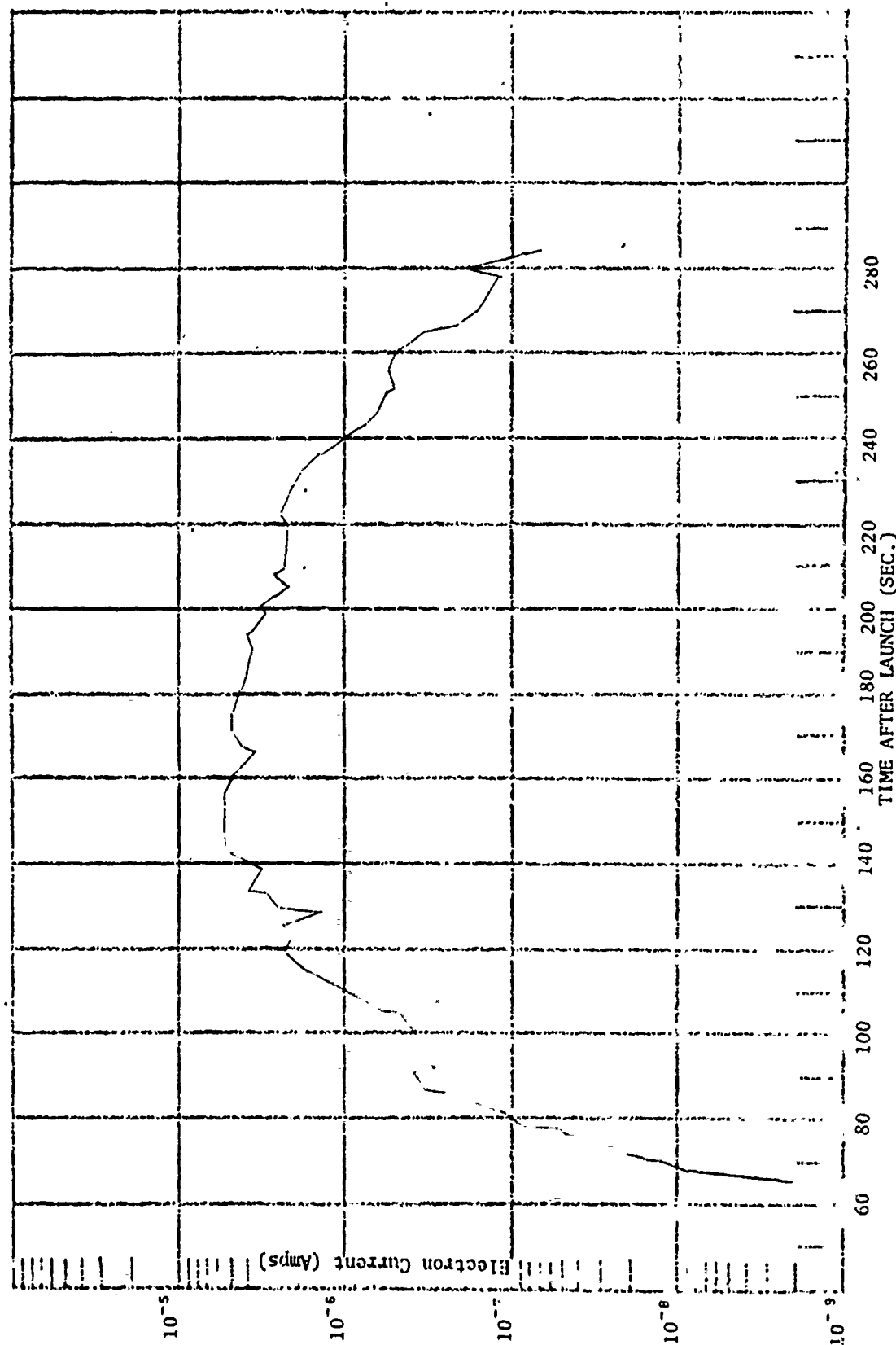


Figure 51 Electron Current Measured at an Applied Probe Voltage of +3 volts as a Function of Time After Launch.  
NIRO 7.892

Positive Ion Current ( $-9^V$ )  
AH 7.892

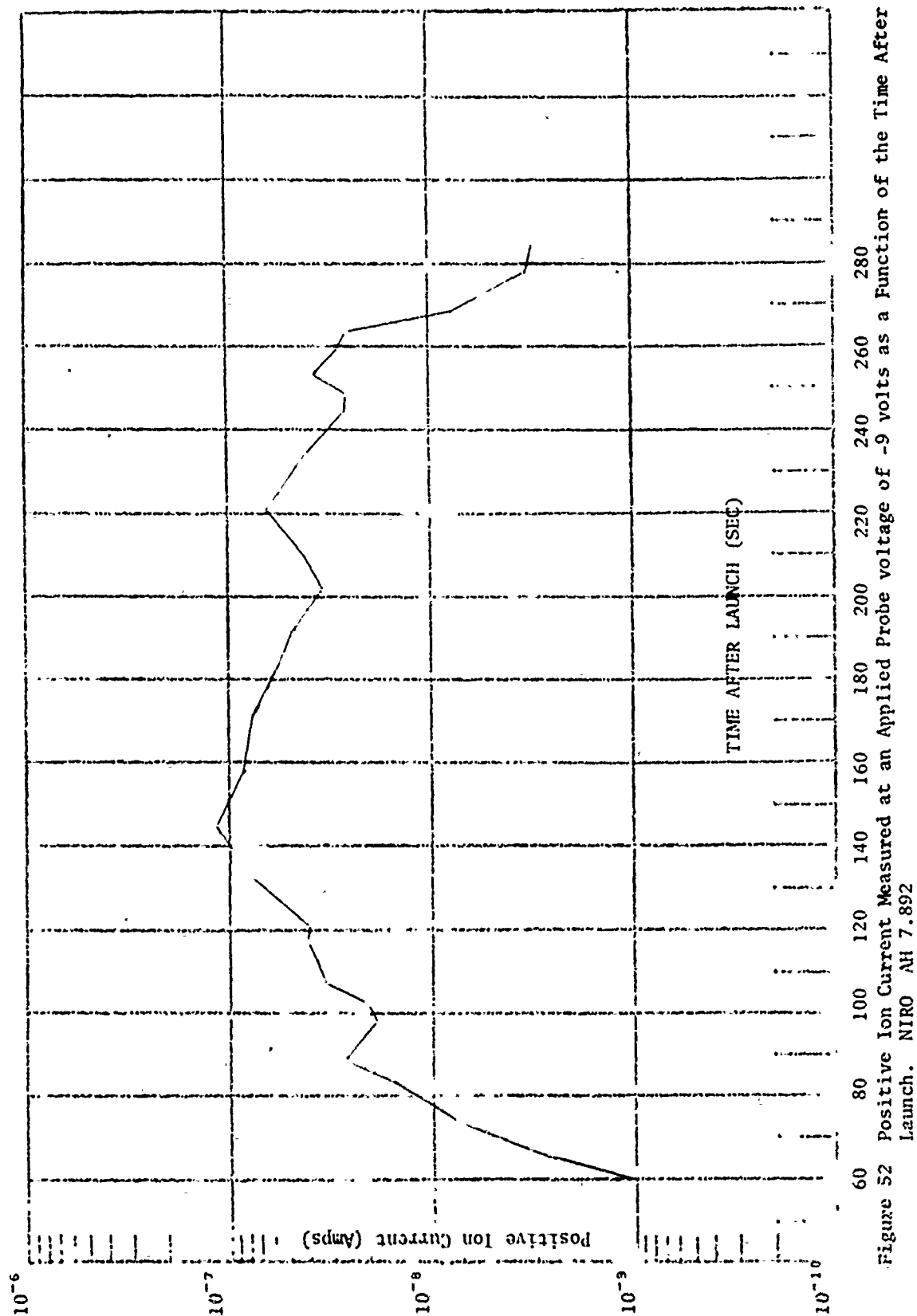


Figure 52 Positive Ion Current Measured at an Applied Probe voltage of  $-9$  volts as a Function of the Time After Launch. NIRO AH 7.892

Positive Ion Current ( $-3^V$ )  
AH 7.892

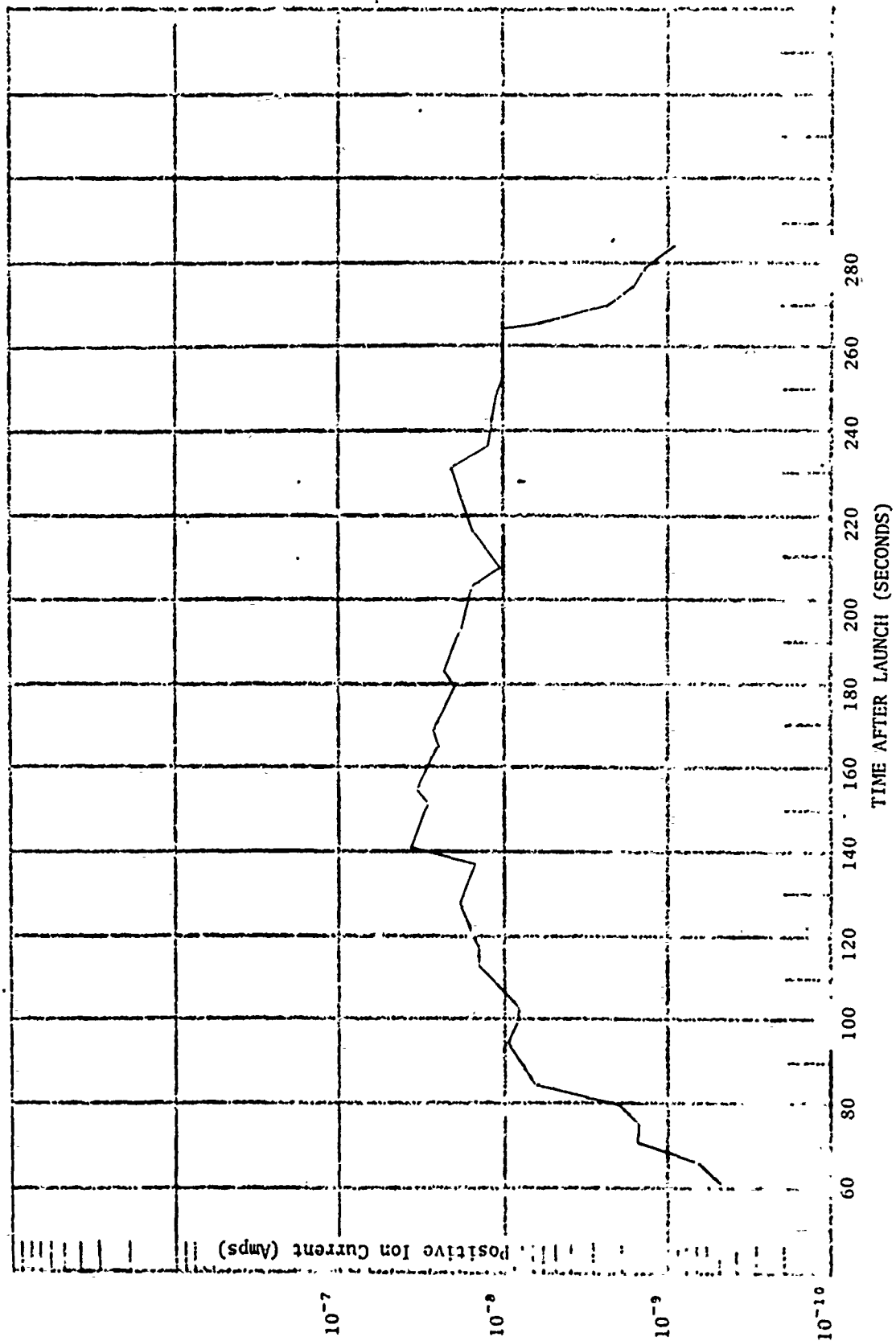


Figure 53 Positive Ion Current Measured at an Applied Probe Voltage of  $-3$  Volts as a Function of Time after Launch. AH 7.892

REF SEMILOGANTH 46 5012  
 4 CIRC 11 11 11 11 11  
 KLOFFEL 1 1 1 1 1 1

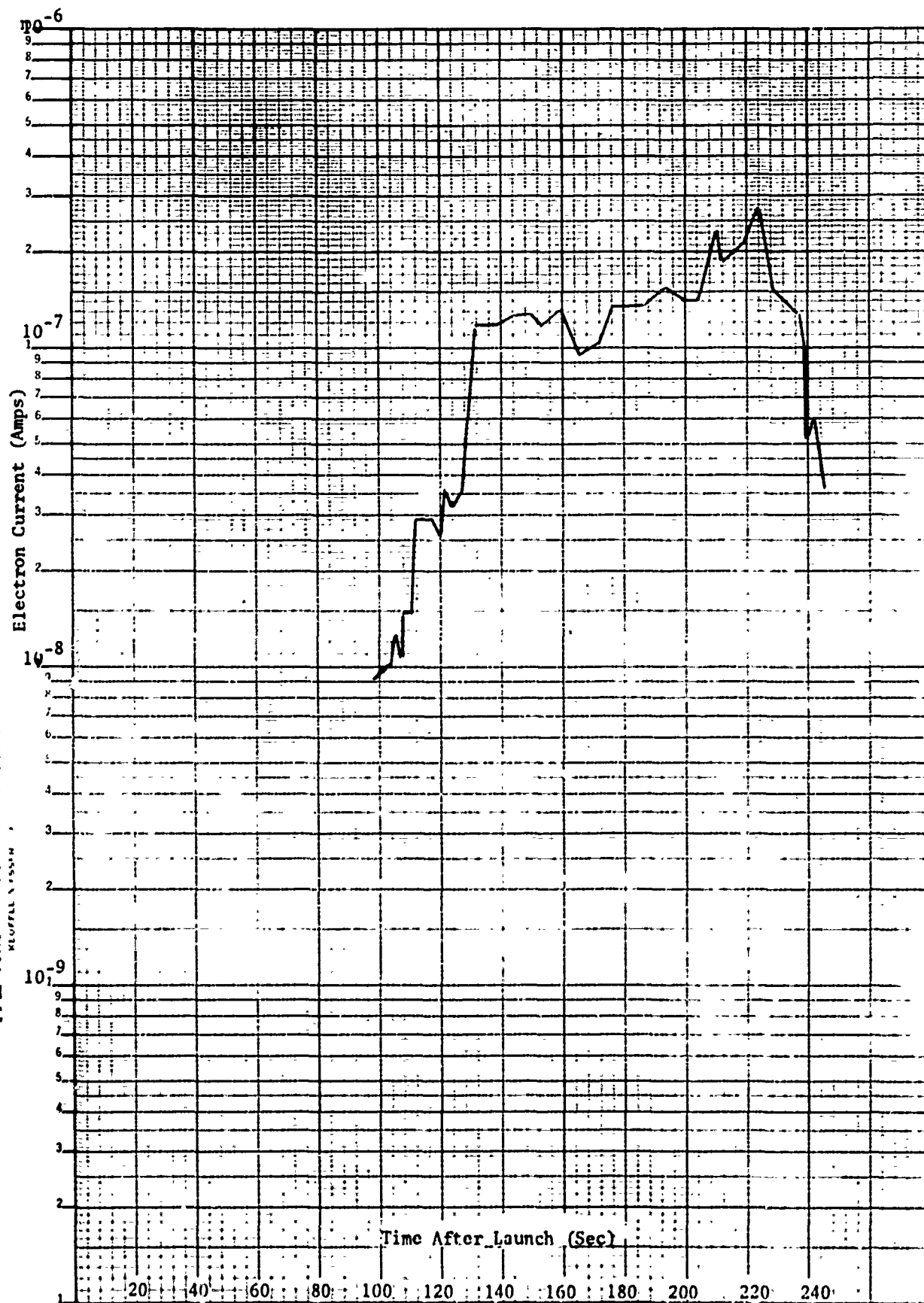


Figure 54 Electron Current Measured +3 volts vs. Time After Launch NIRO 7.902-9

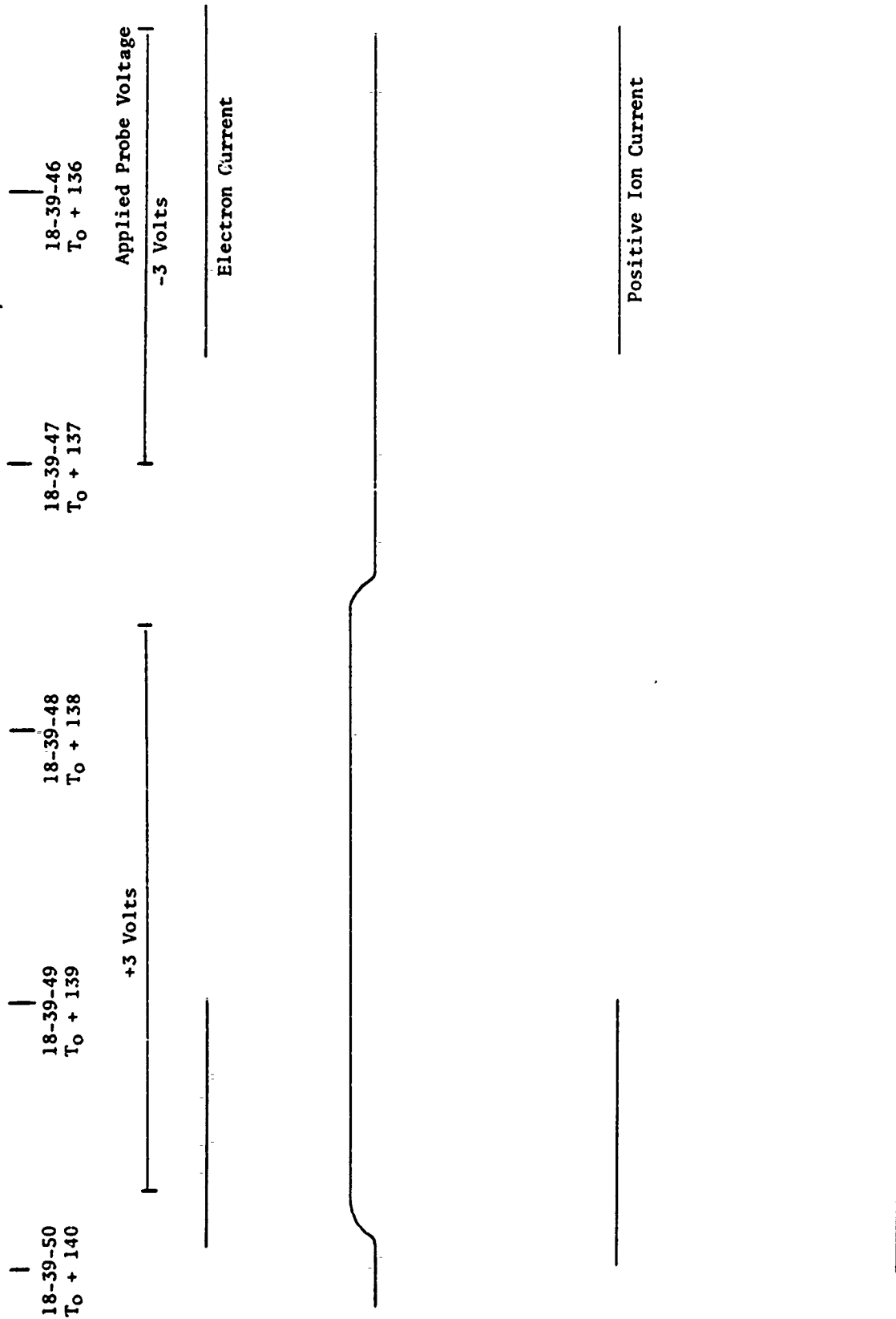


Figure 55 Strip Chart Data Between  $T_0 + 136$  sec and  $T_0 + 140$  sec for AO 7.902-9

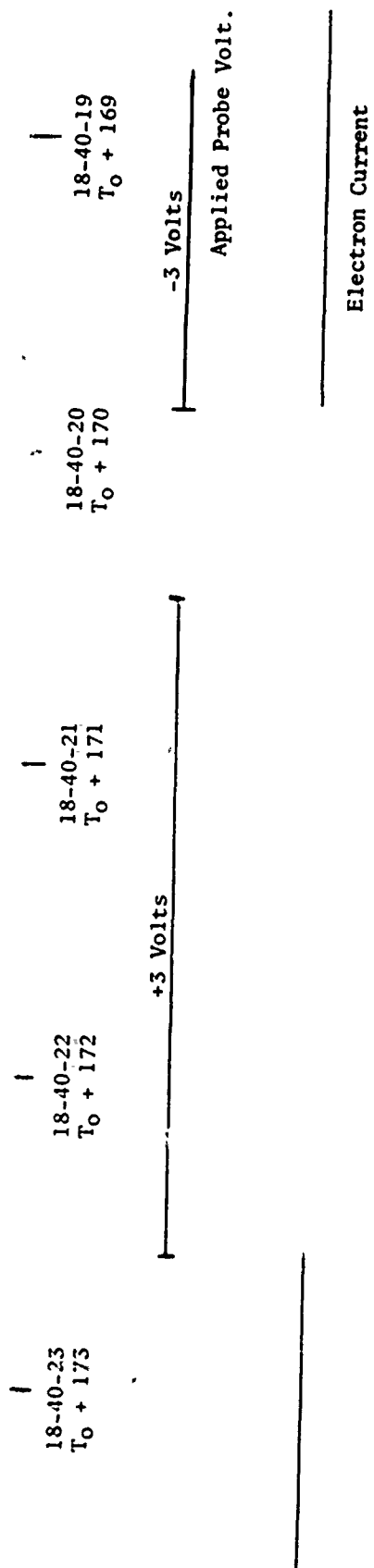


Figure 56 Strip Chart Between  $T_O + 169$  sec and  $T_O + 173$  sec for A0 7.902-9

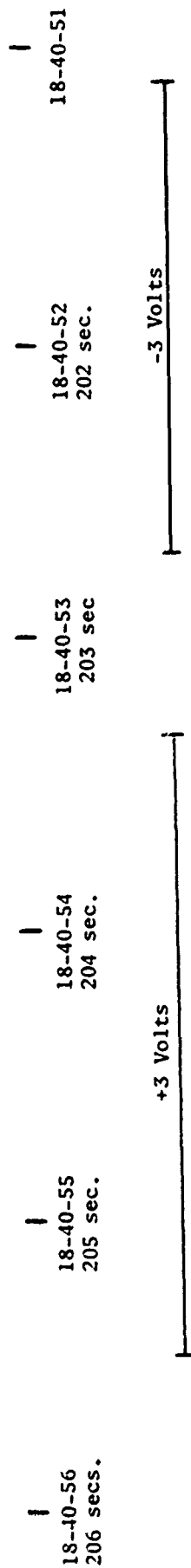


Figure 57 Strip Chart Data Between  $T_0 + 201$  sec and  $T_0 + 206$  sec for AO 7.902-9

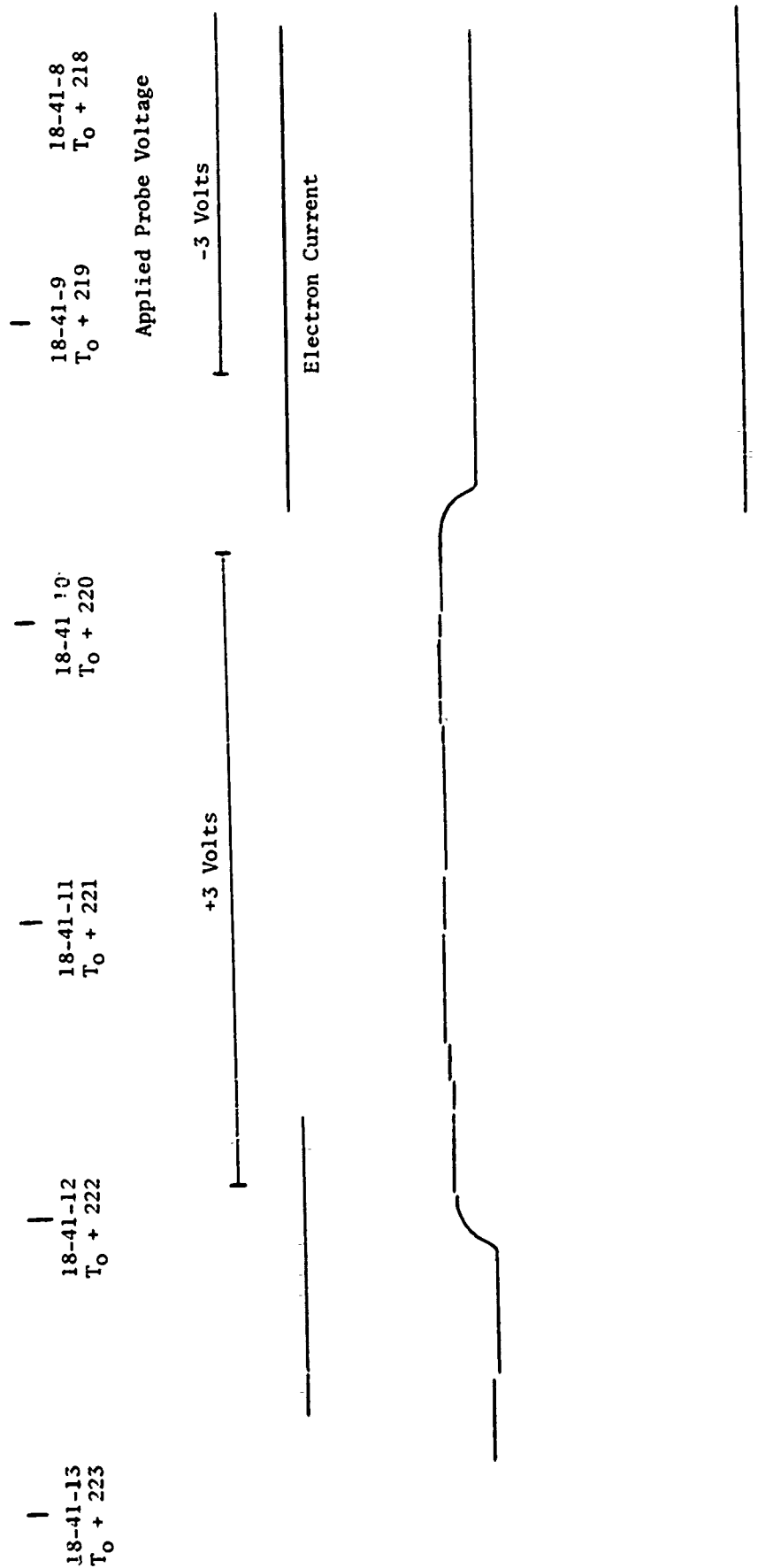


Figure 58 Strip Chart Data Between  $T_0 + 218$  sec and  $T_0 + 223$  sec for A0 7.902-9



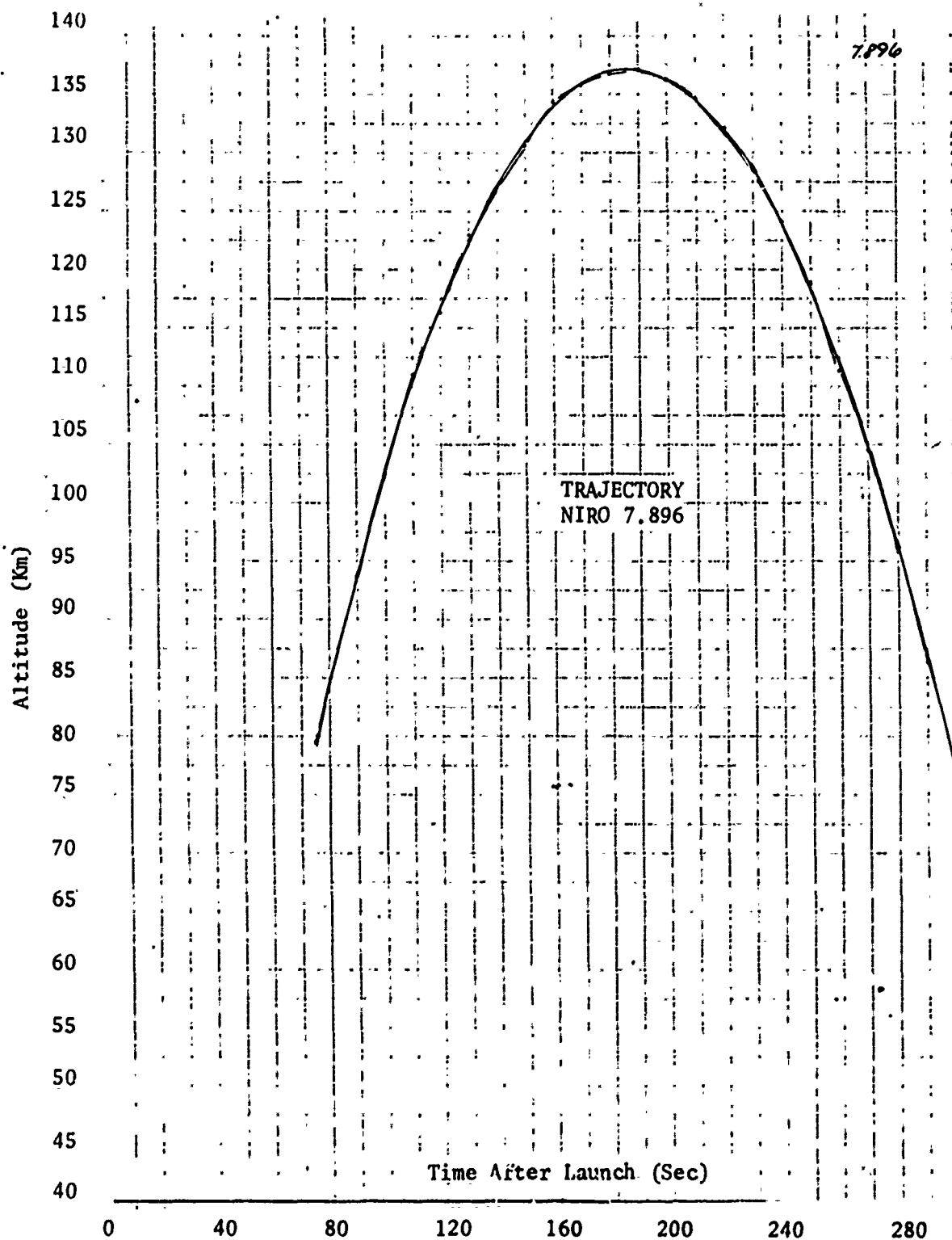


Figure 59 Vehicle Trajectory for NIRO AT 7.896

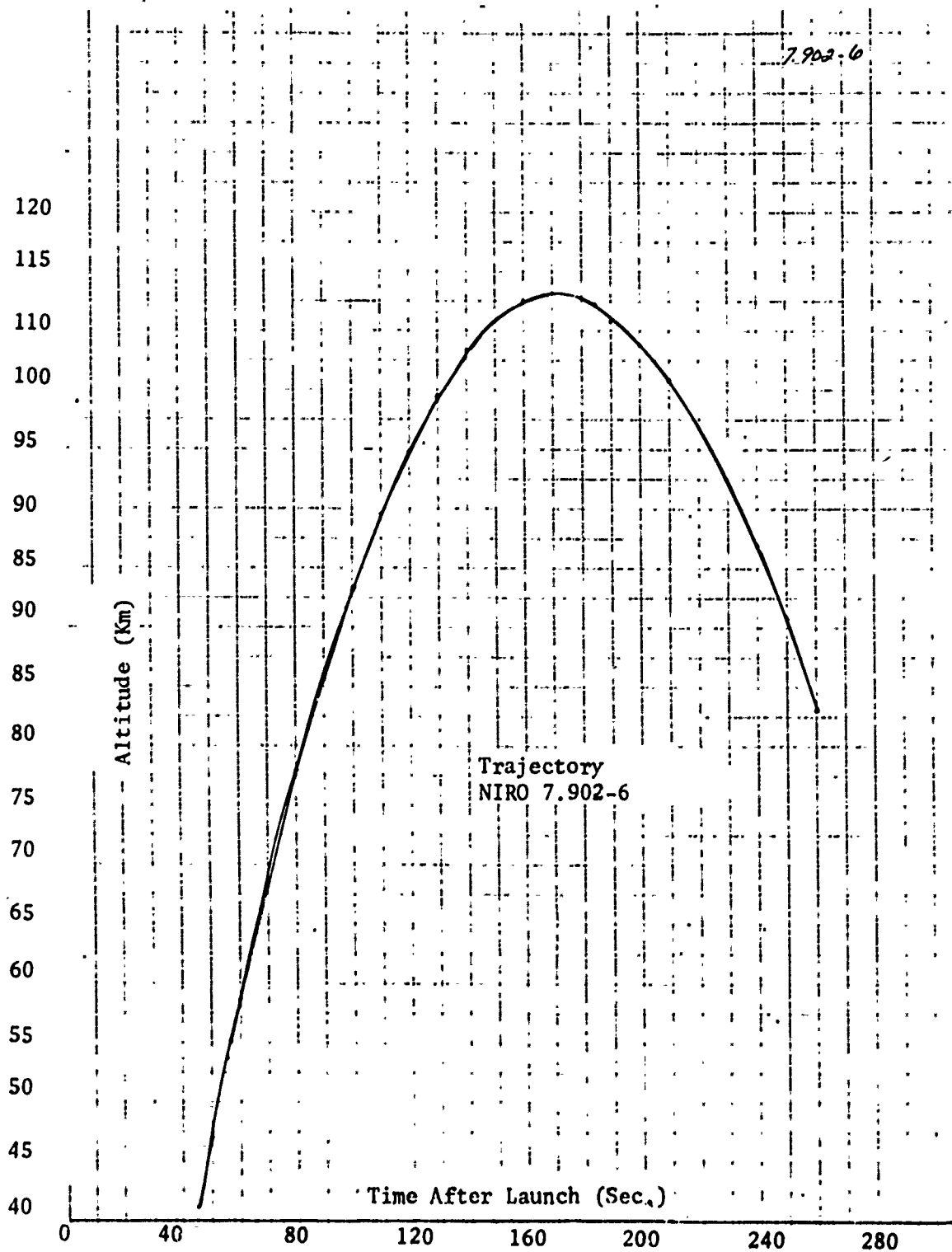


Figure 60 Vehicle Trajectory for NIRO AO 7.902-6

162 10 X 10 TO THE CENTIMETER 46 1512  
 REUFFEL & ESSER CO.

7.902-6  
 Vehicle Potential

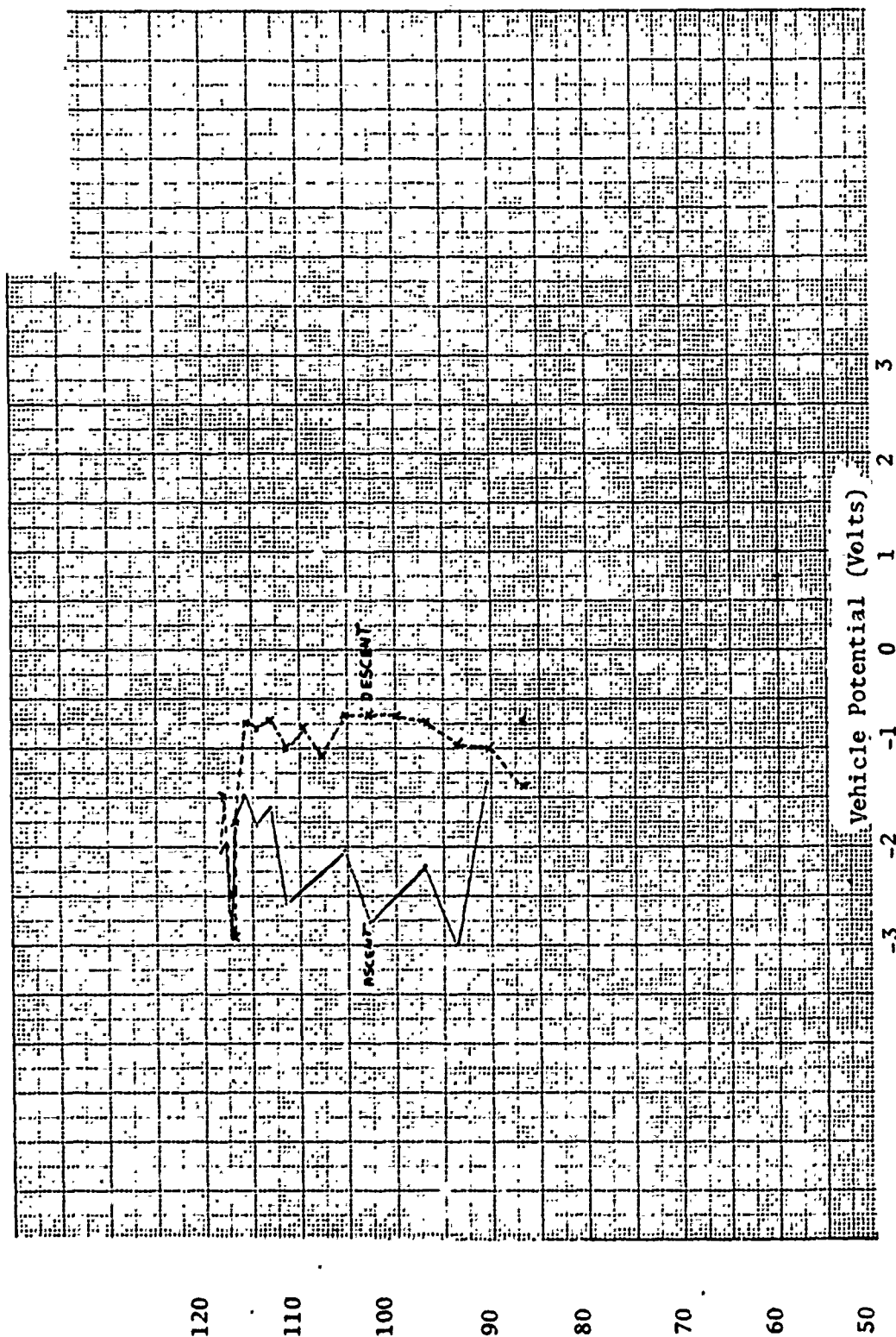


Figure 51 Vehicle Potential Measurement for NIRO AO 7.902-6

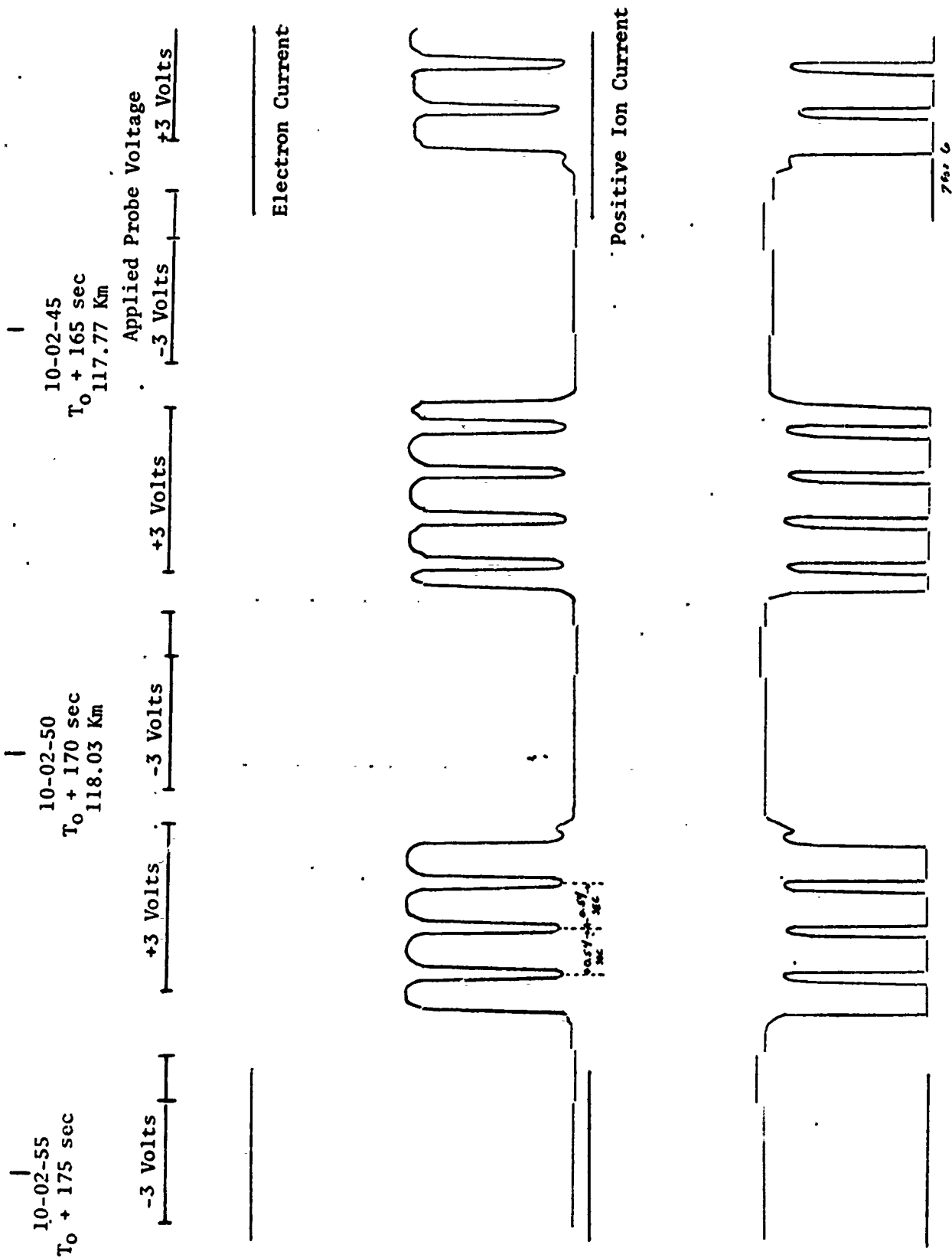


Figure 62 Strip Chart Data Near Rocket Apogee for NIRO AO 7.902-6

10-01-55  
T<sub>0</sub> + 115 sec  
102.35 Km

10-01-50  
T<sub>0</sub> + 110 Sec  
99.52 Km

10-01-45  
T<sub>0</sub> + 105 Sec  
96.46 Km

+3 Volts      -3 Volts      +3 Volts      -3 Volts      +3 Volts

Electron Current

Positive Ion Current

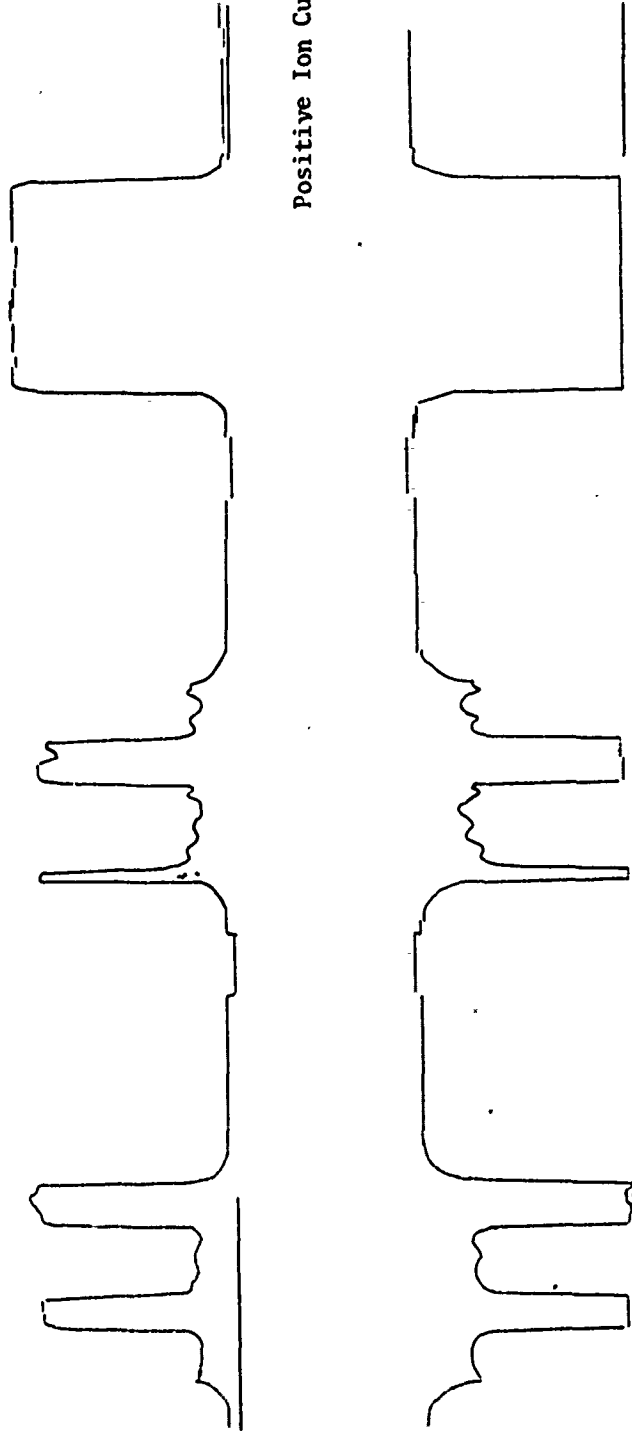
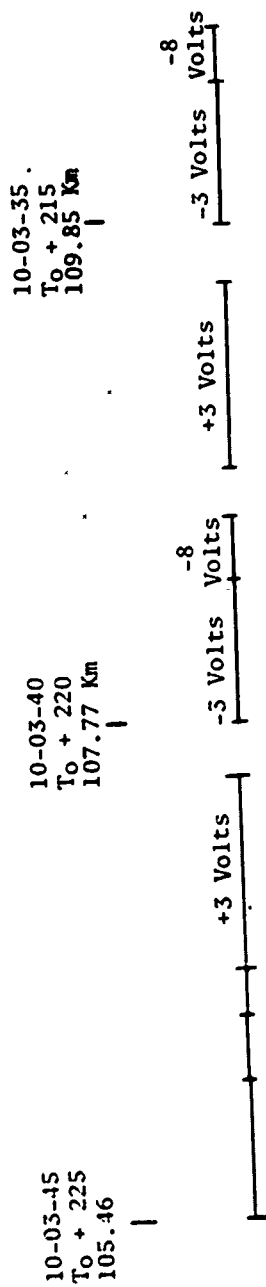
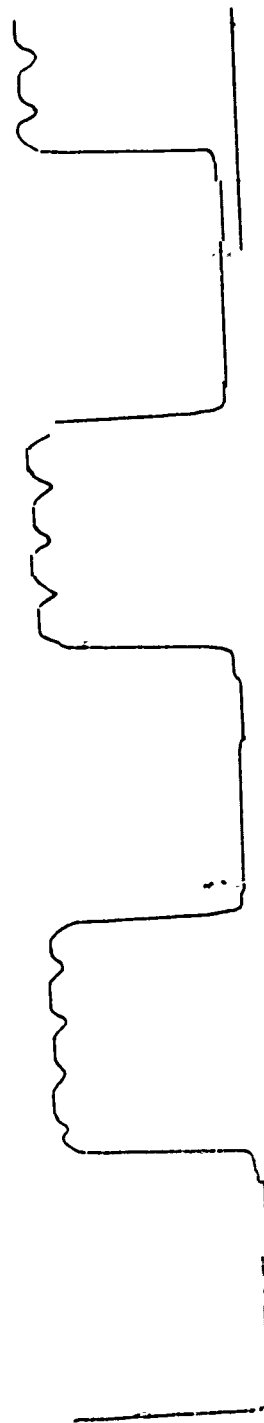


Figure 63 Strip Chart Data Between 96.46 km and 102.35 km for AO 7.902-6



Electron Current



Positive Ion Current

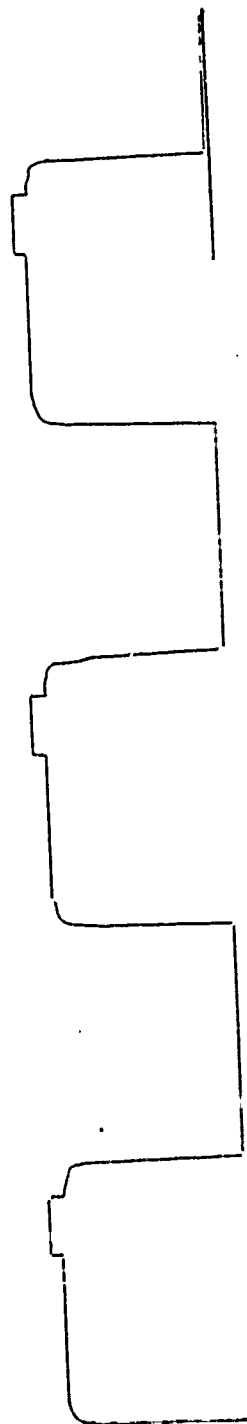


Figure 64 Strip Chart Data Between 109.85 km and 105.46 km on Descent for AO 7.902-6

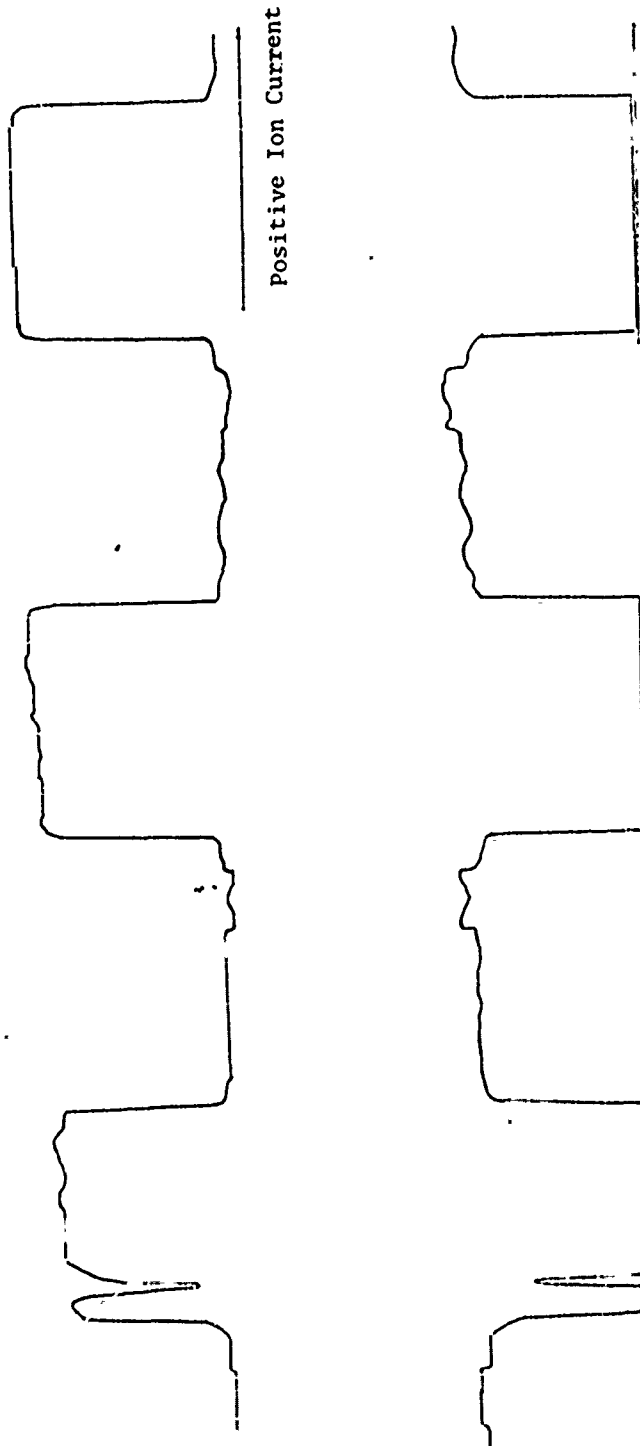
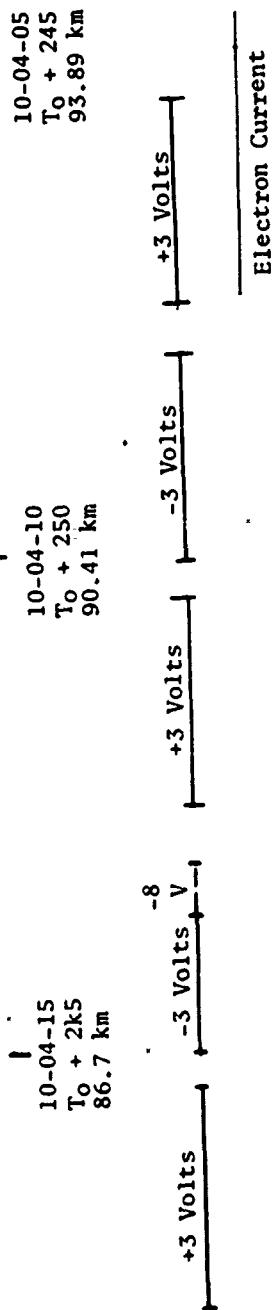


Figure 65 Strip Chart Data Between 93.89 km and 86.7 km on Descent for AO 7.902-6

K02 SEMI LOGARITHMIC  
 4 CYCLES  
 REFERENCE 1000

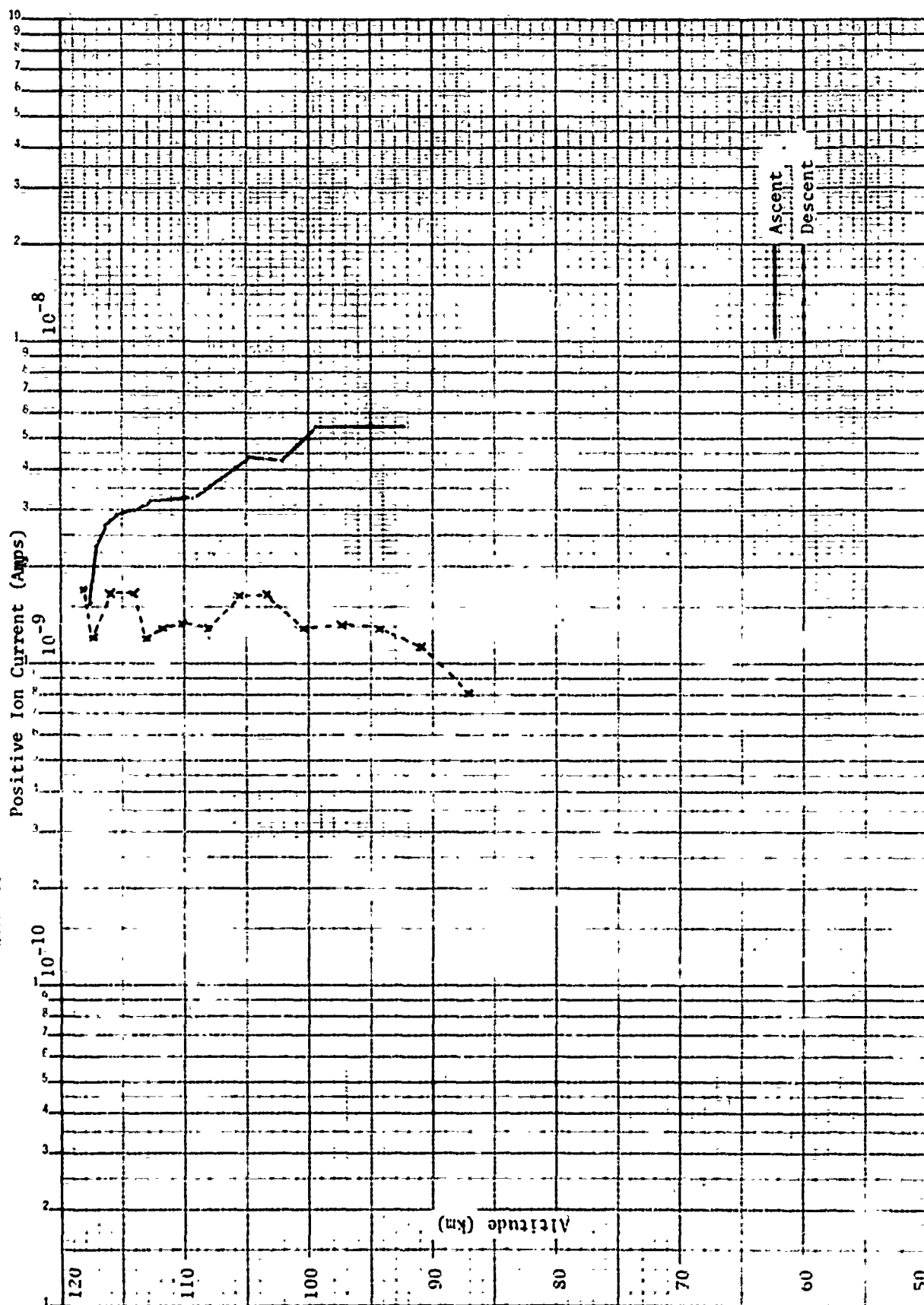


Figure 66 Positive Ion Current Measured at -3 volts for NIRO 7.902-6



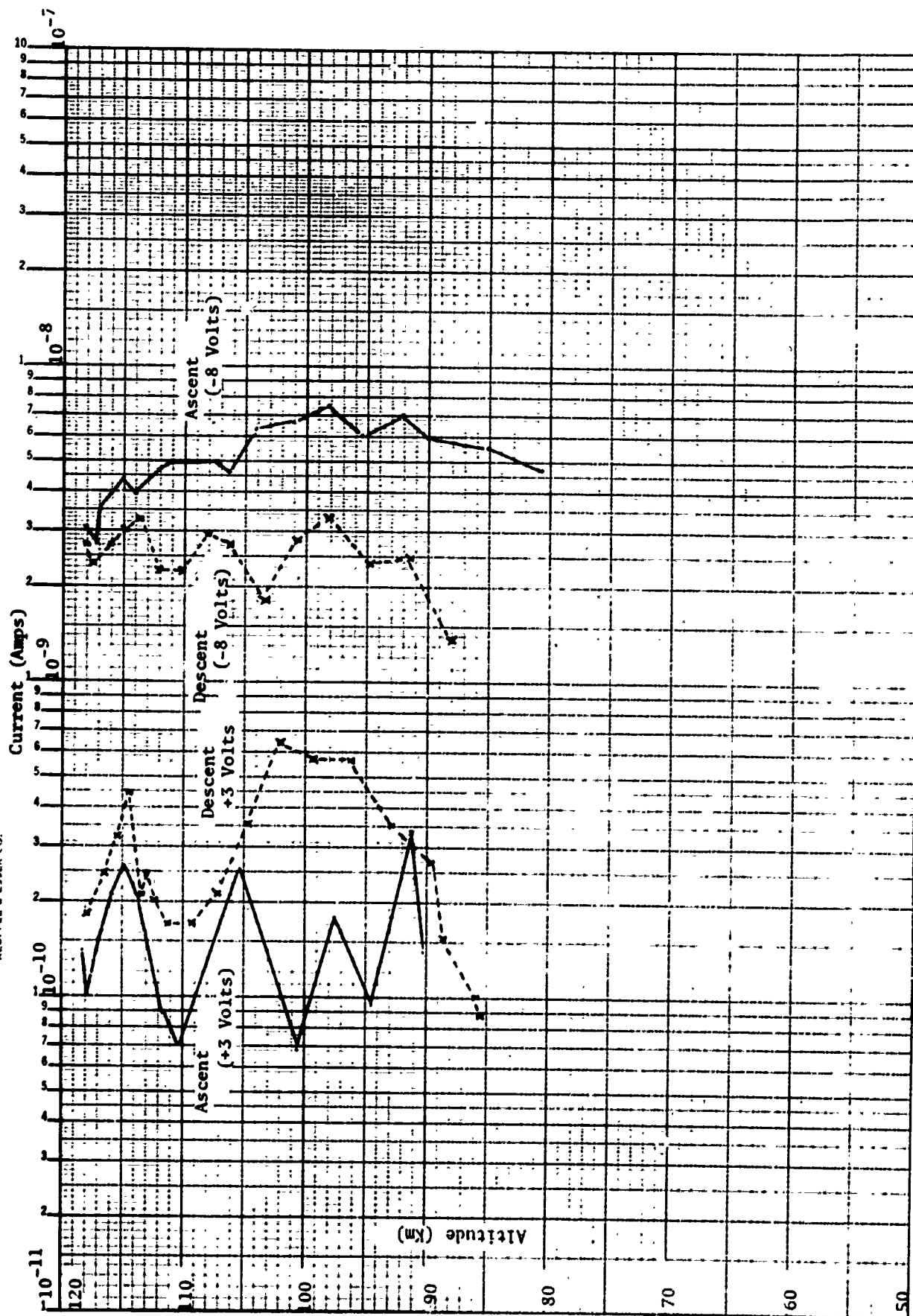


Figure 67 Electron Current (+3V) and positive ion current (-8V) measured by NIRO 7.902-6

K-E 10 X 10 TO THE CENTIMETER 46 1512  
 MADE IN U.S.A.  
 KEUFFEL & ESSER CO.

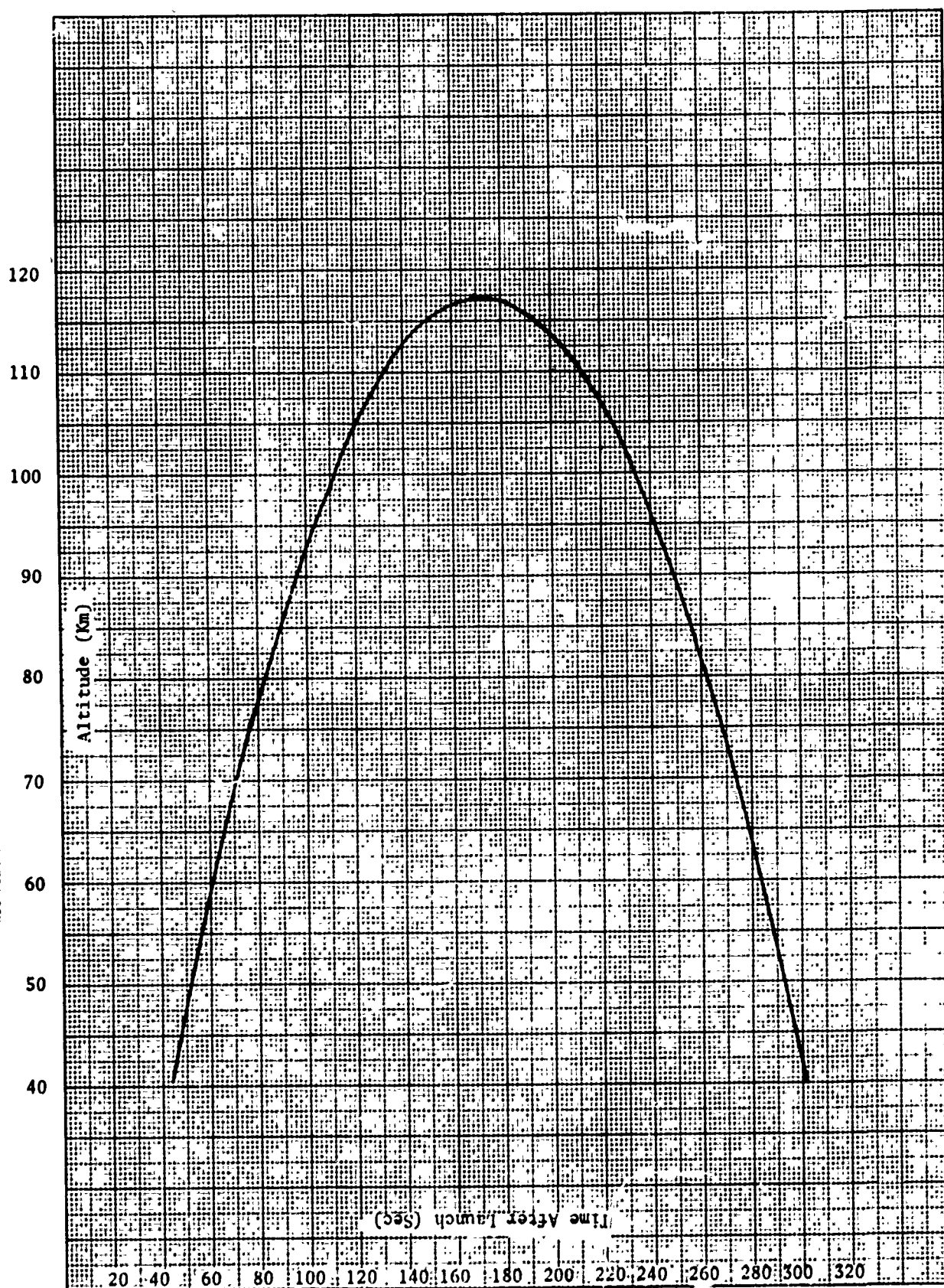


Figure 68 Vehicle Trajectory for NIRO AO 7.101-4

KSE 10 X 10 TO THE CENTIMETER 46 1512  
 MADE IN U.S.A.  
 ALUFFEL & ESSER CO

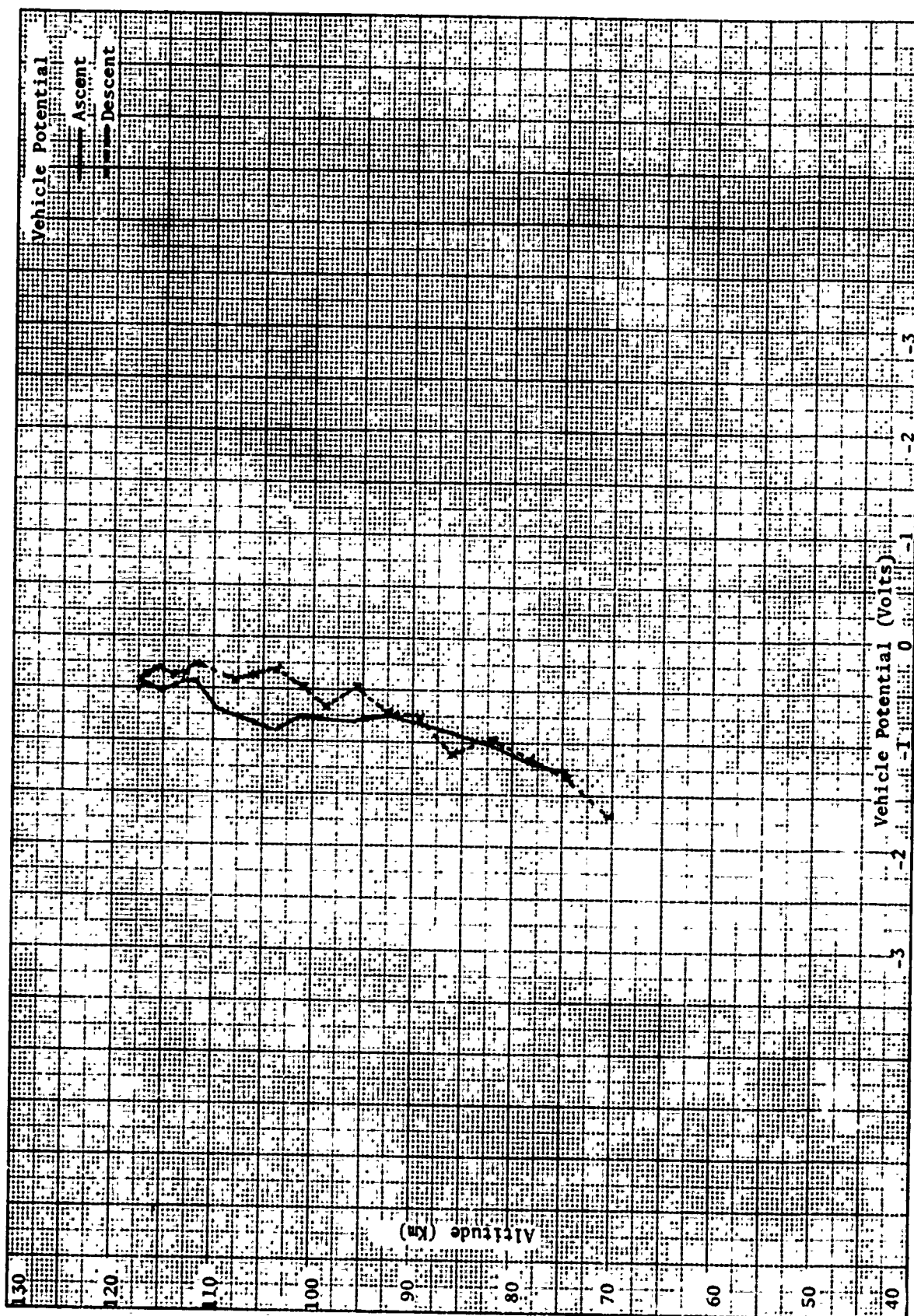


Figure 69 Vehicle Potential Measured During the Flight of NIRO 7.101-4

K02 SEMI-LOGARITHMIC 46 6012  
 45000 100000  
 KEUFFEL & BURET

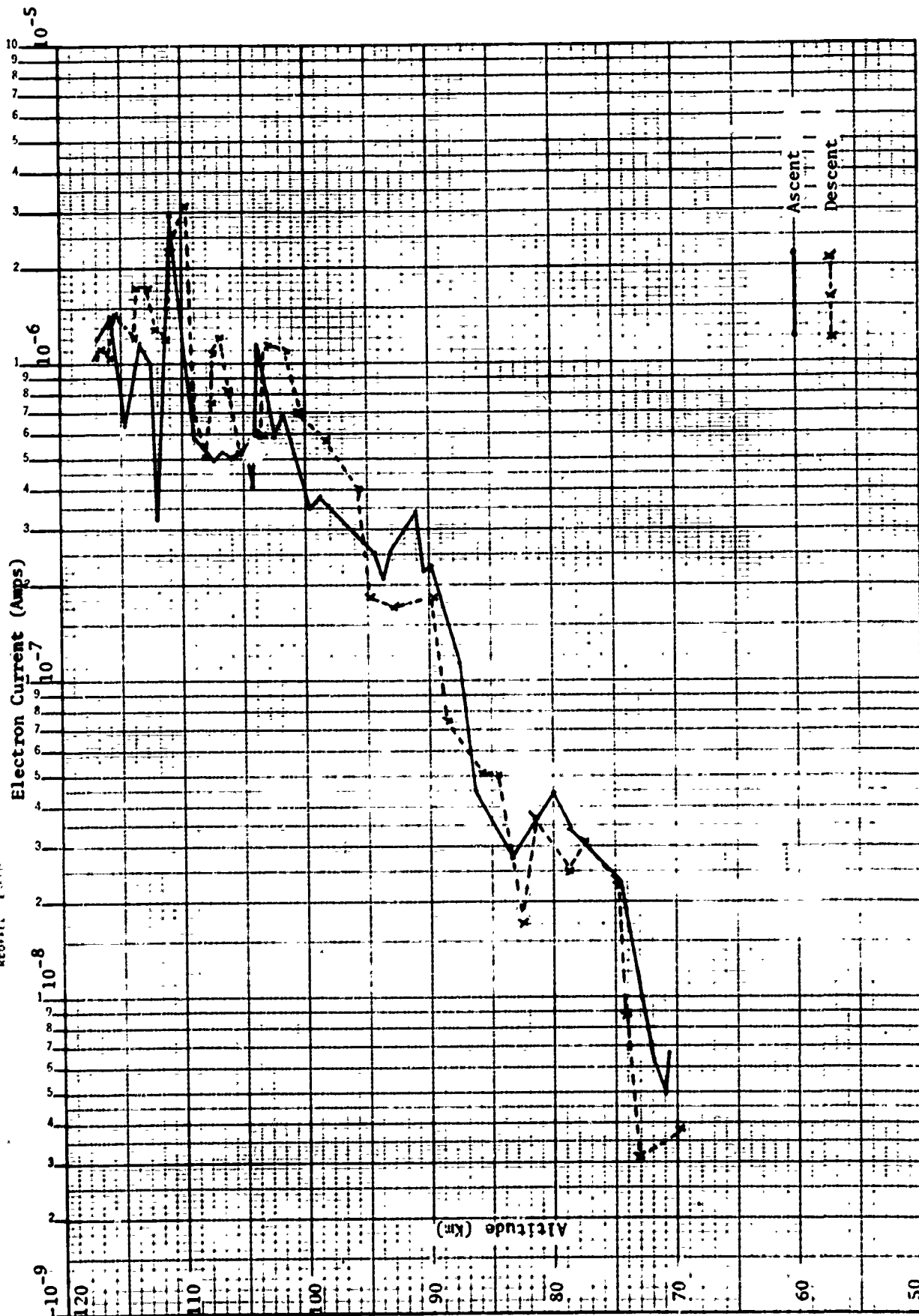


Figure 70 Electron Current Measurements for NIRO AO 7.101-4

K-E SEMI-LOGARITHMIC 46 5492  
 3 CYCLES X 70 DIVISIONS  
 MADE IN U.S.A.  
 KEUFFEL & ESSER CO.

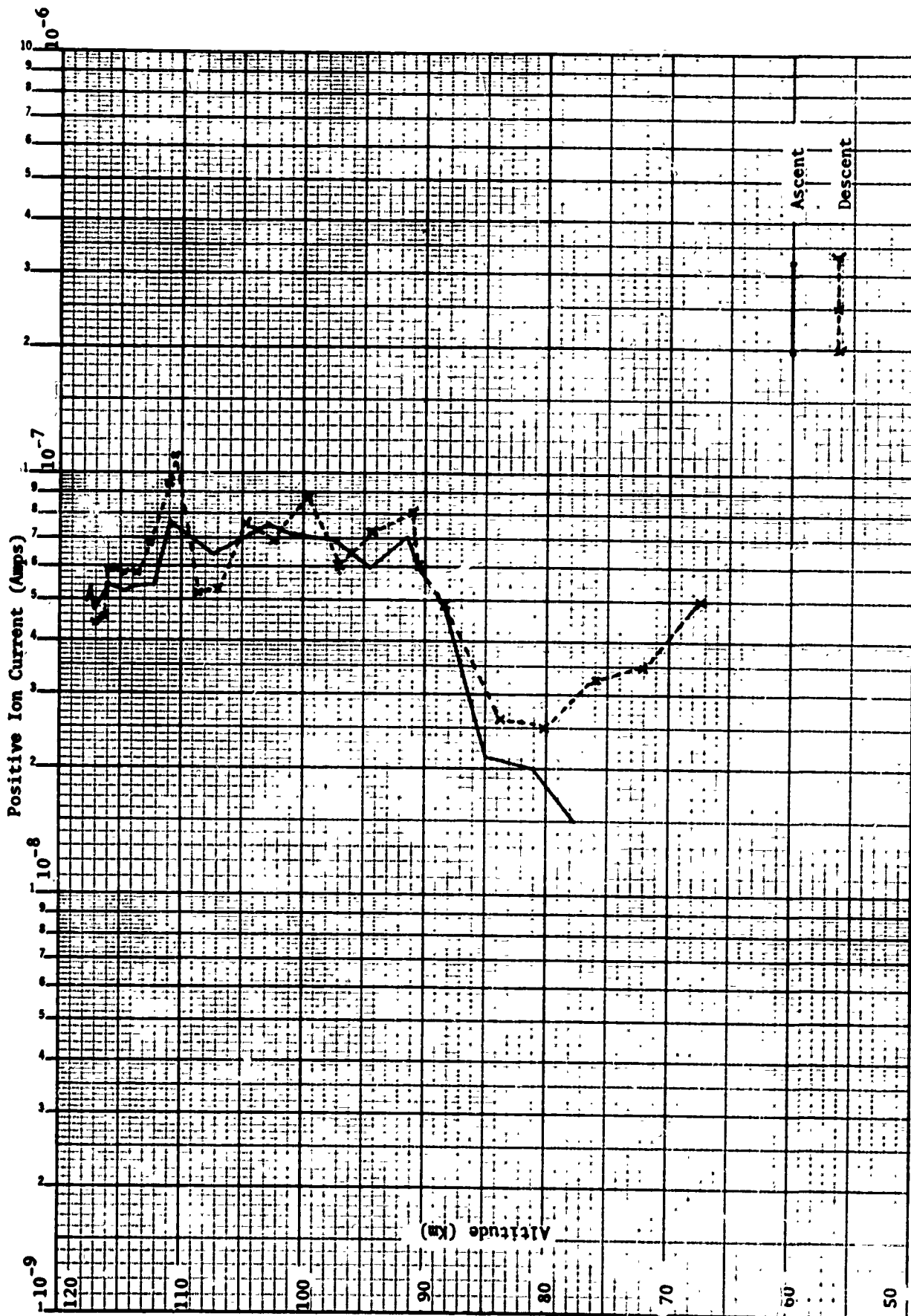


Figure 71 Positive Ion Current Measurements at -9 volts for N100 A0 7.101-4

K&E SEMI-LOGARITHMIC 46 5492  
 3 CYCLES X 70 DIVISIONS  
 MADE IN U.S.A.  
 KEUFFEL & ESSER CO.

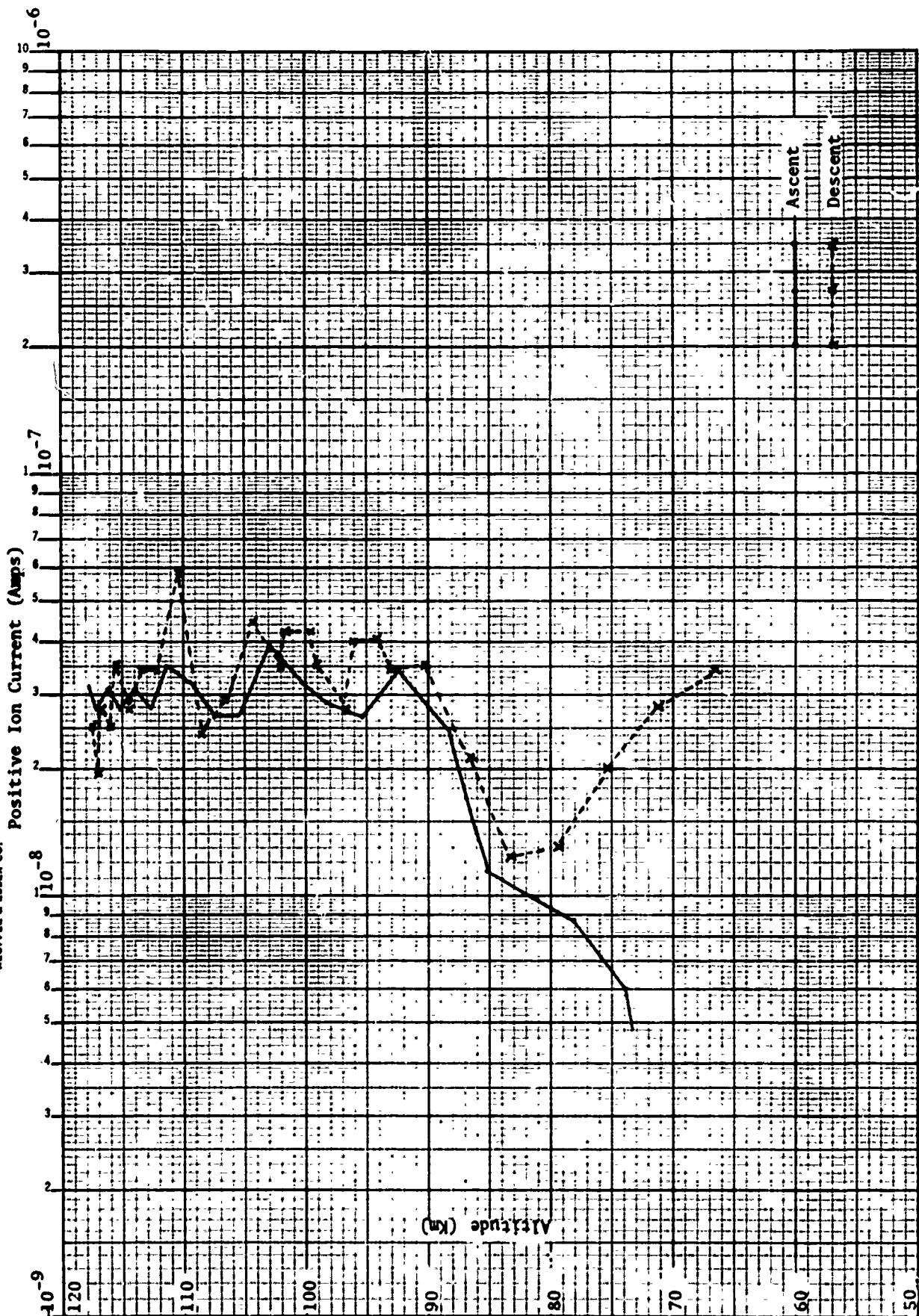


Figure 72 Positive Ion Current Measurements at -3 volts for NIRO AO 7.101-4

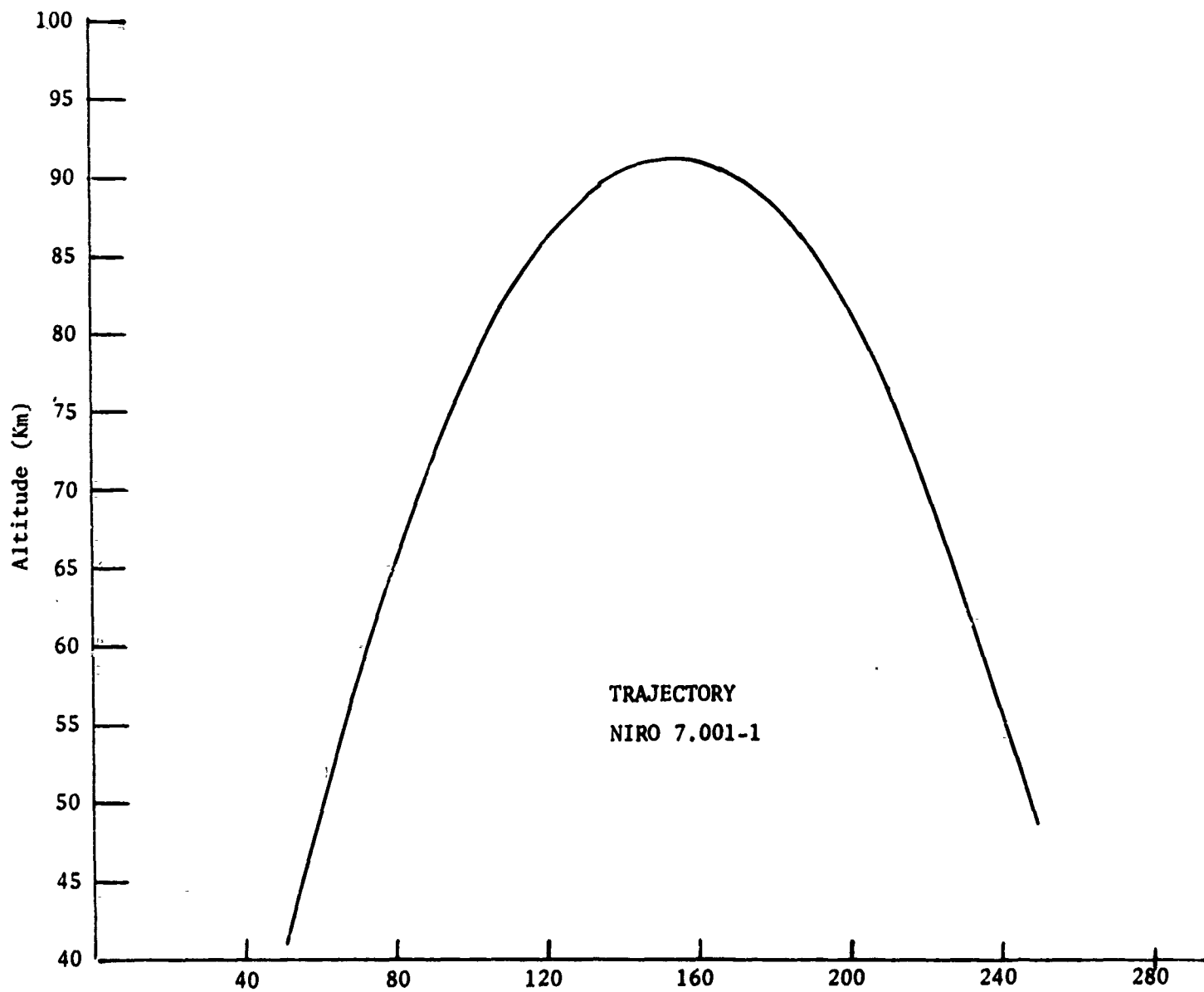


Figure 73 Vehicle Trajectory for NIRO AO 7.001-1



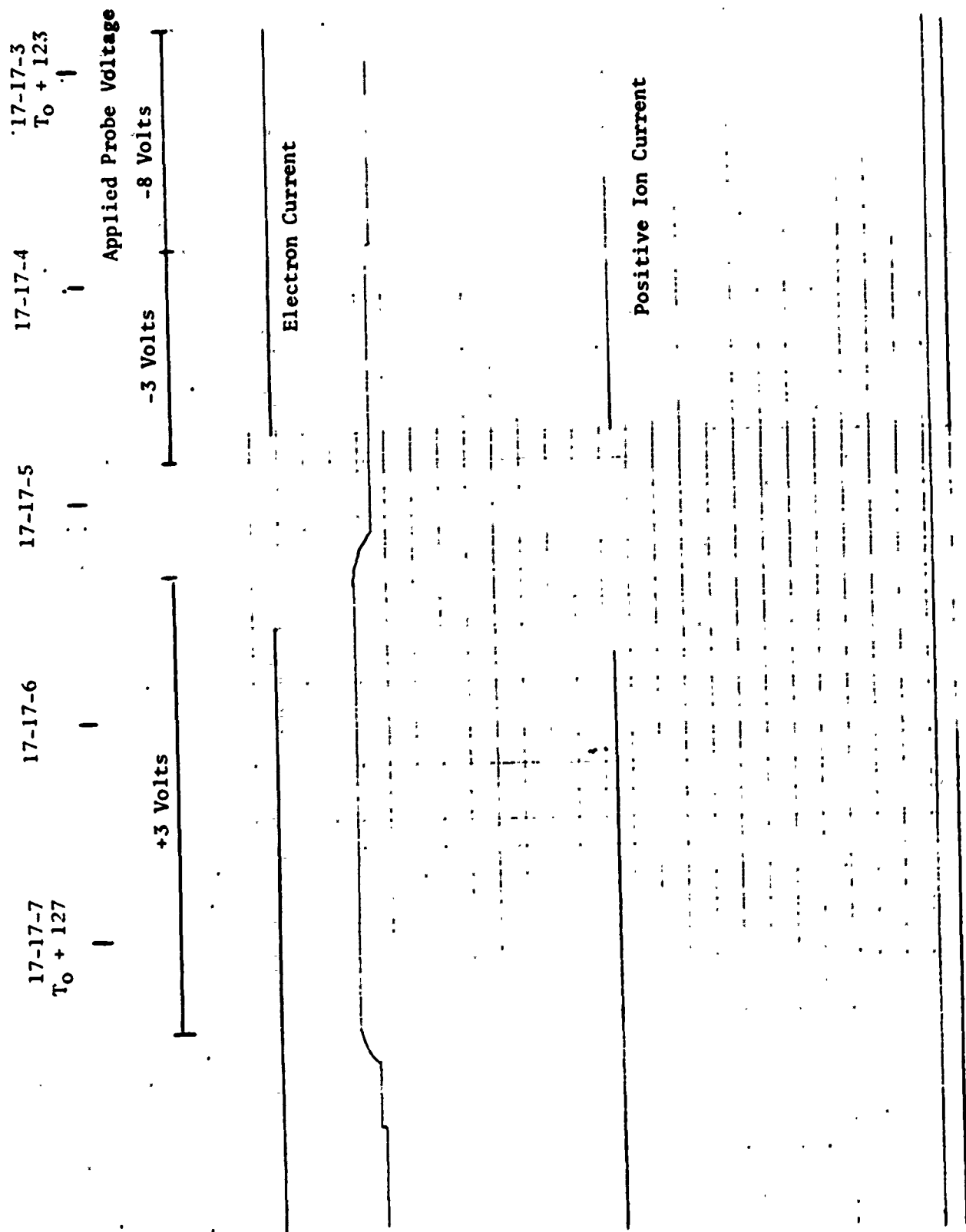


Figure 74 Strip Chart Data Between  $T_0 + 123$  sec and  $T_0 + 128$  sec for NIRO AO 7.001-1



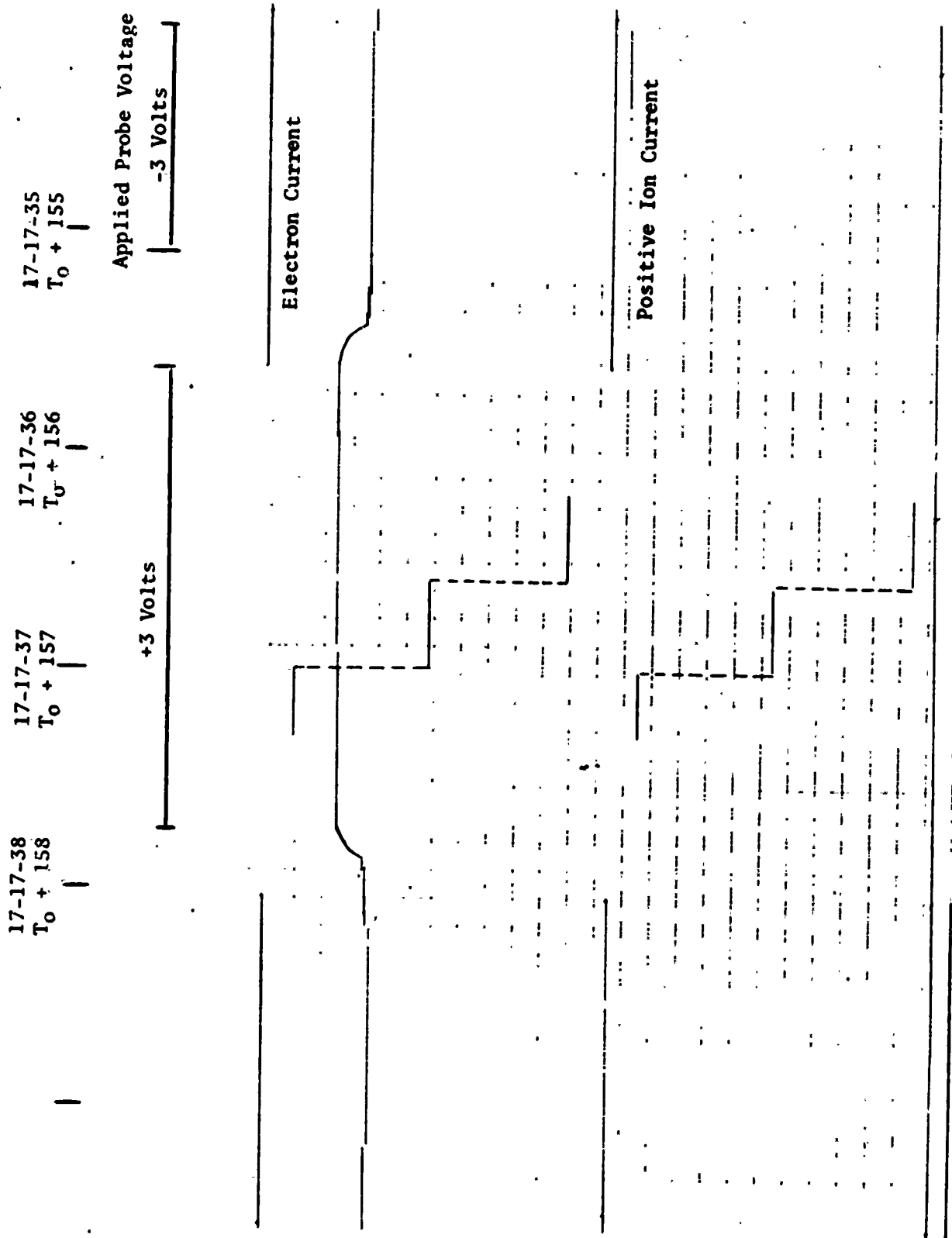


Figure 75 Strip Chart Data Between  $T_0 + 155$  sec and  $T_0 + 159$  sec for NIRO AO 7.001-1

RCE SEMILOG-GRAPHIC 48 0012  
 4 CYCLES X 7.5 VOLTS  
 REUFEL & ENSLER CO.

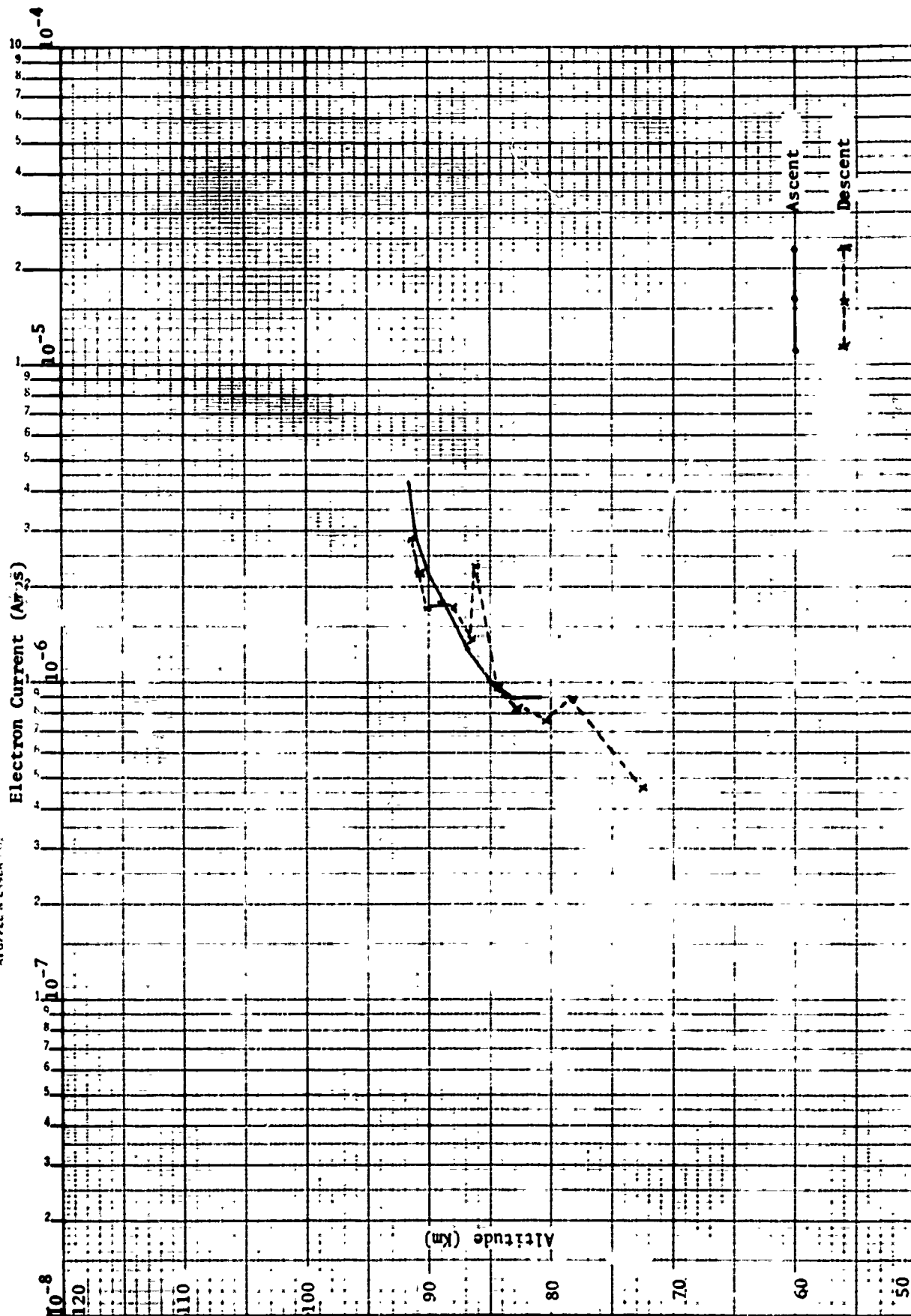


Figure 76 Electron Current Measurements (+3 volts) for NIRO A07.001-1

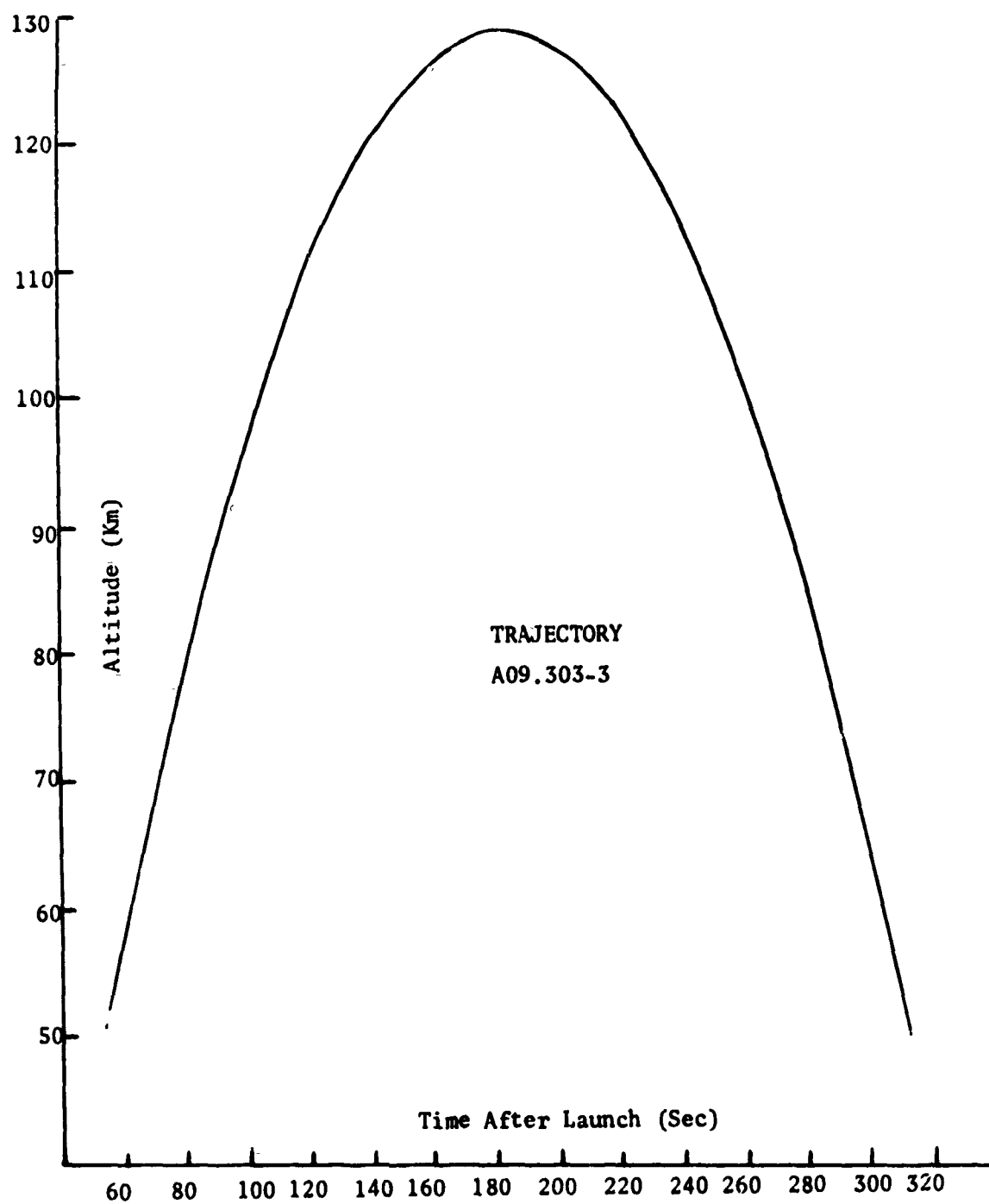


Figure 77 Vehicle Trajectory for Ute-Tomahawk A09.303-3

10 X 10 TO THE CENTIMETER 46 1512  
REUPPEL & ESSER CO.

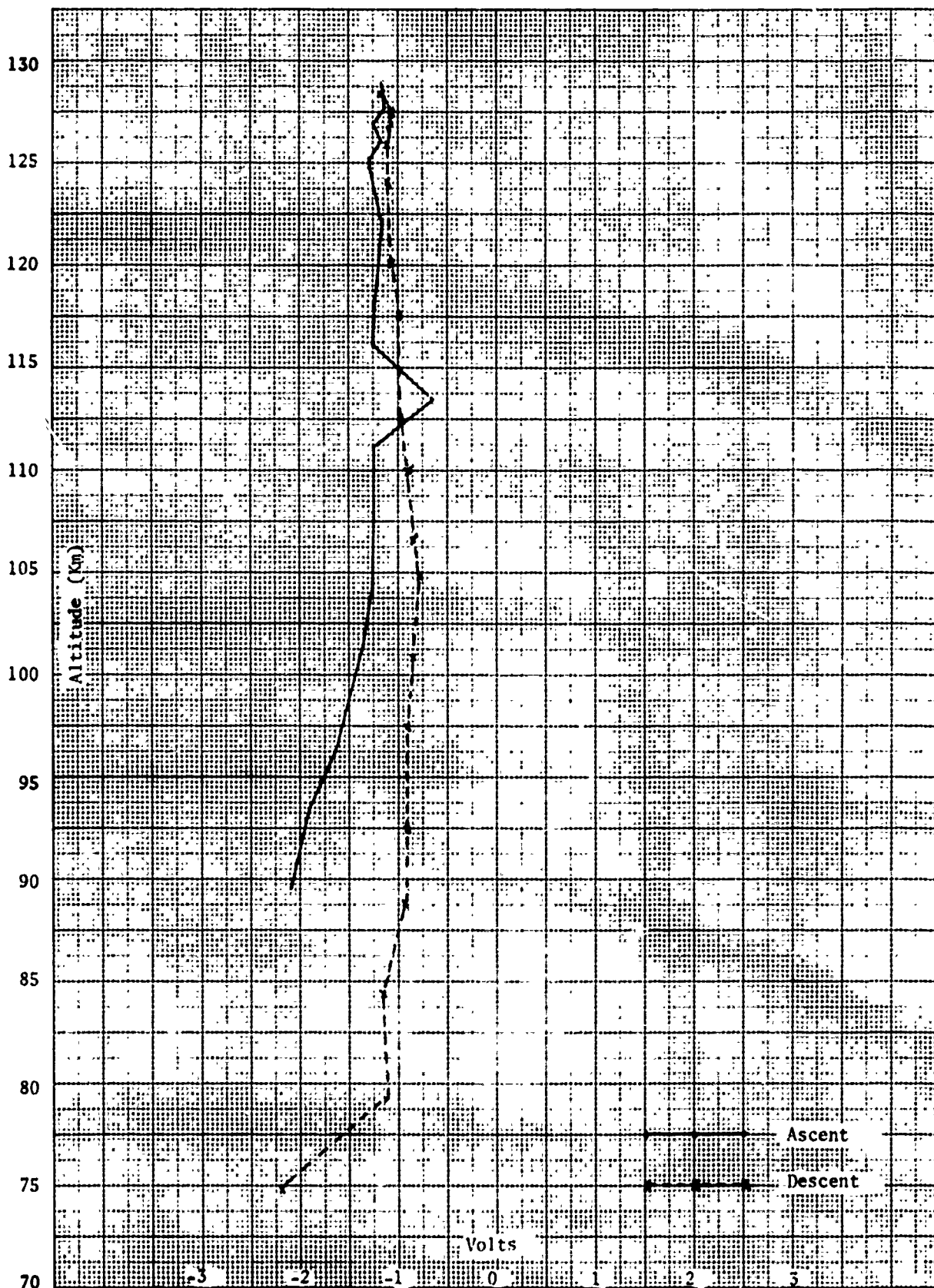


Figure 78 Vehicle Potential Measured by Ute-Tomahawk 9.303-3

K-E SEMI-LOGARITHMIC 46 6012  
4 CYCLES X 70 DIVISIONS  
MADE IN U.S.A.  
NEUFEL & ESSER CO.

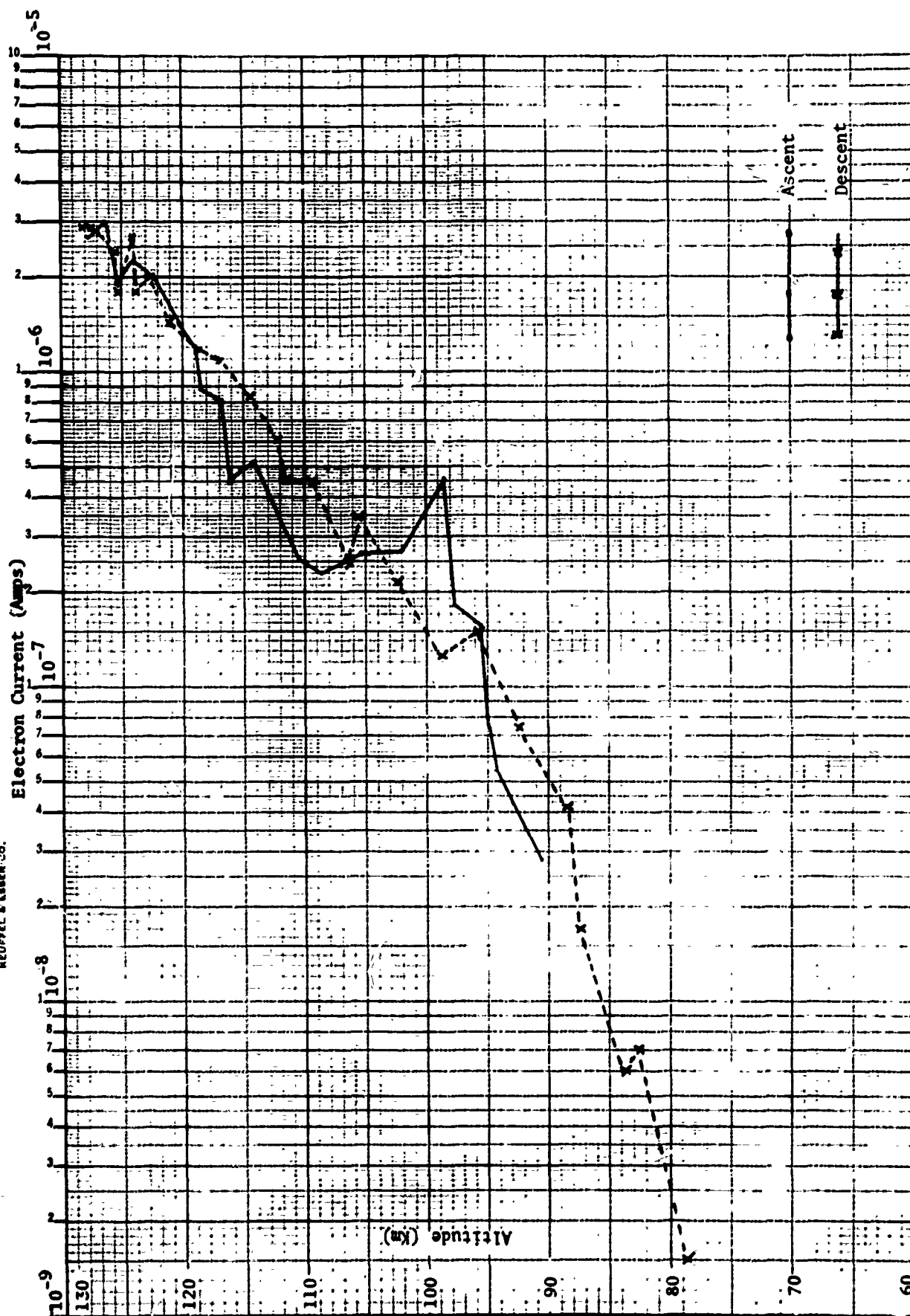


Figure 79 Electron Current Measured at +3 volts for A09.303-3

K&E SEMI-LOGARITHMIC 46 5492  
 5 CYCLES X 70 DIVISIONS  
 KEUFFEL & ESSER CO.

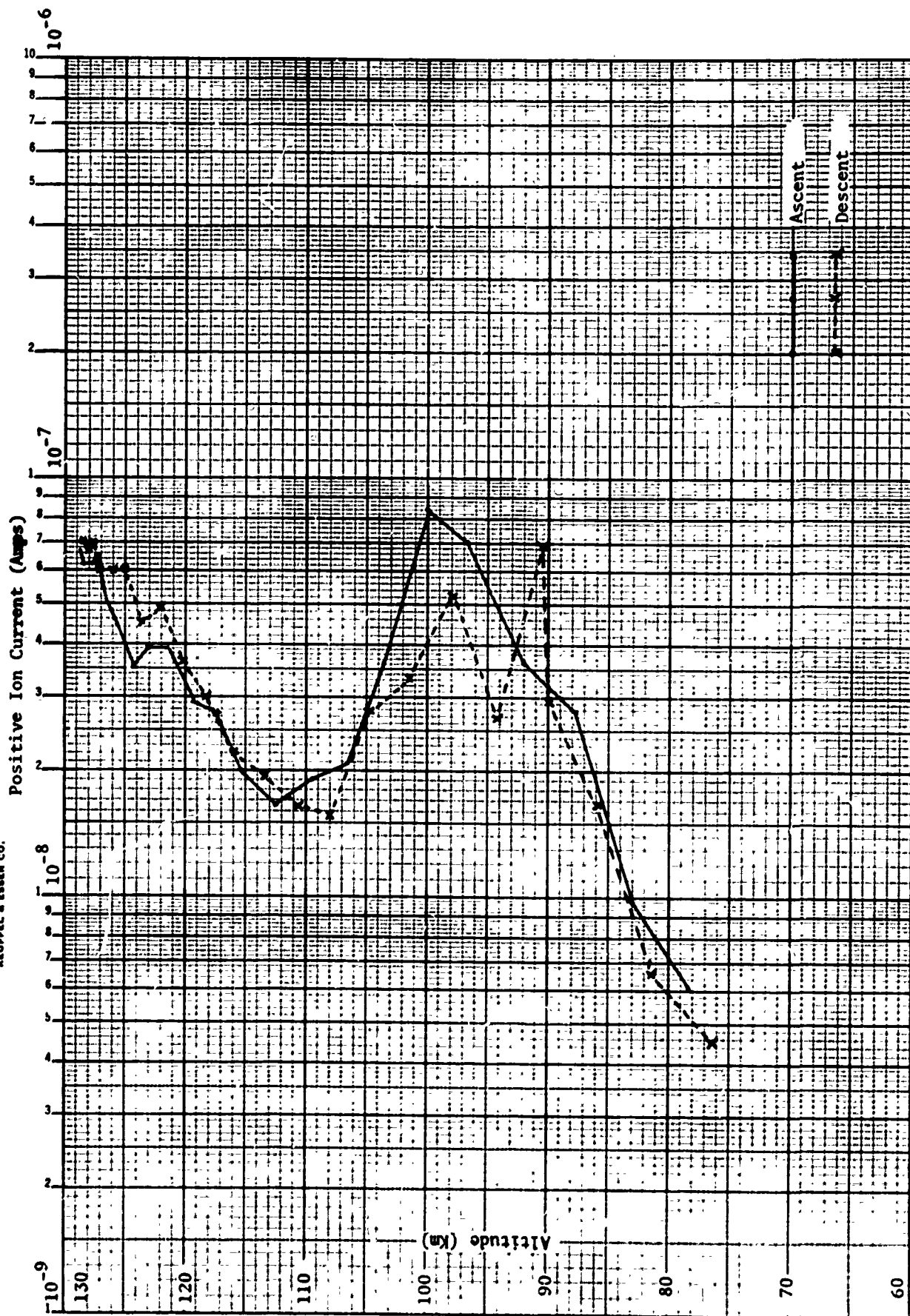


Figure 80 Positive-Ion Current Measured at -9 volts for A09.303-3

ROSE SEV. 1964  
4.5 V. 100 A  
K1001

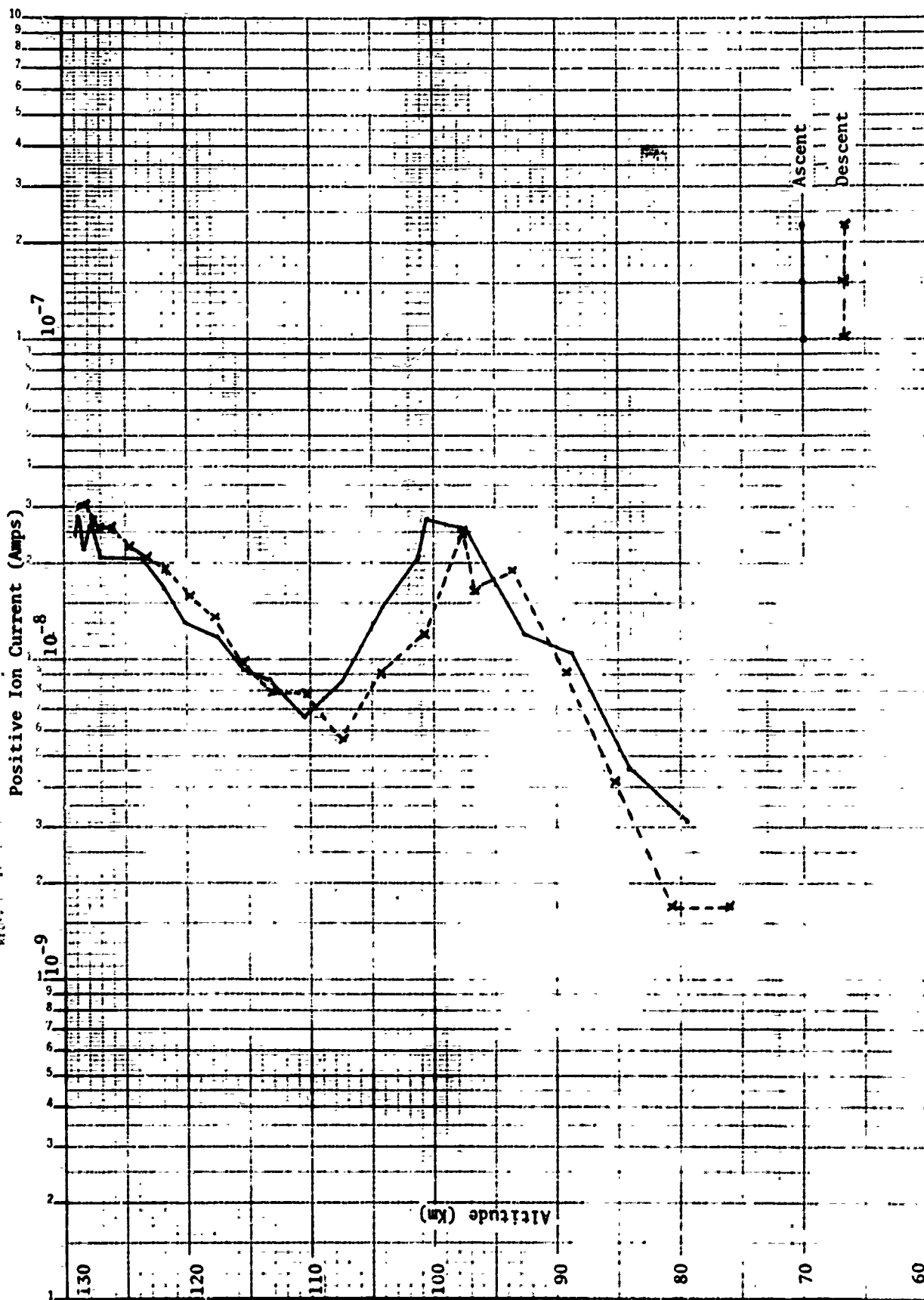


Figure 81 Positive Ion Current (-3 volts) measured by Ute-Tomahawk 9.303-3

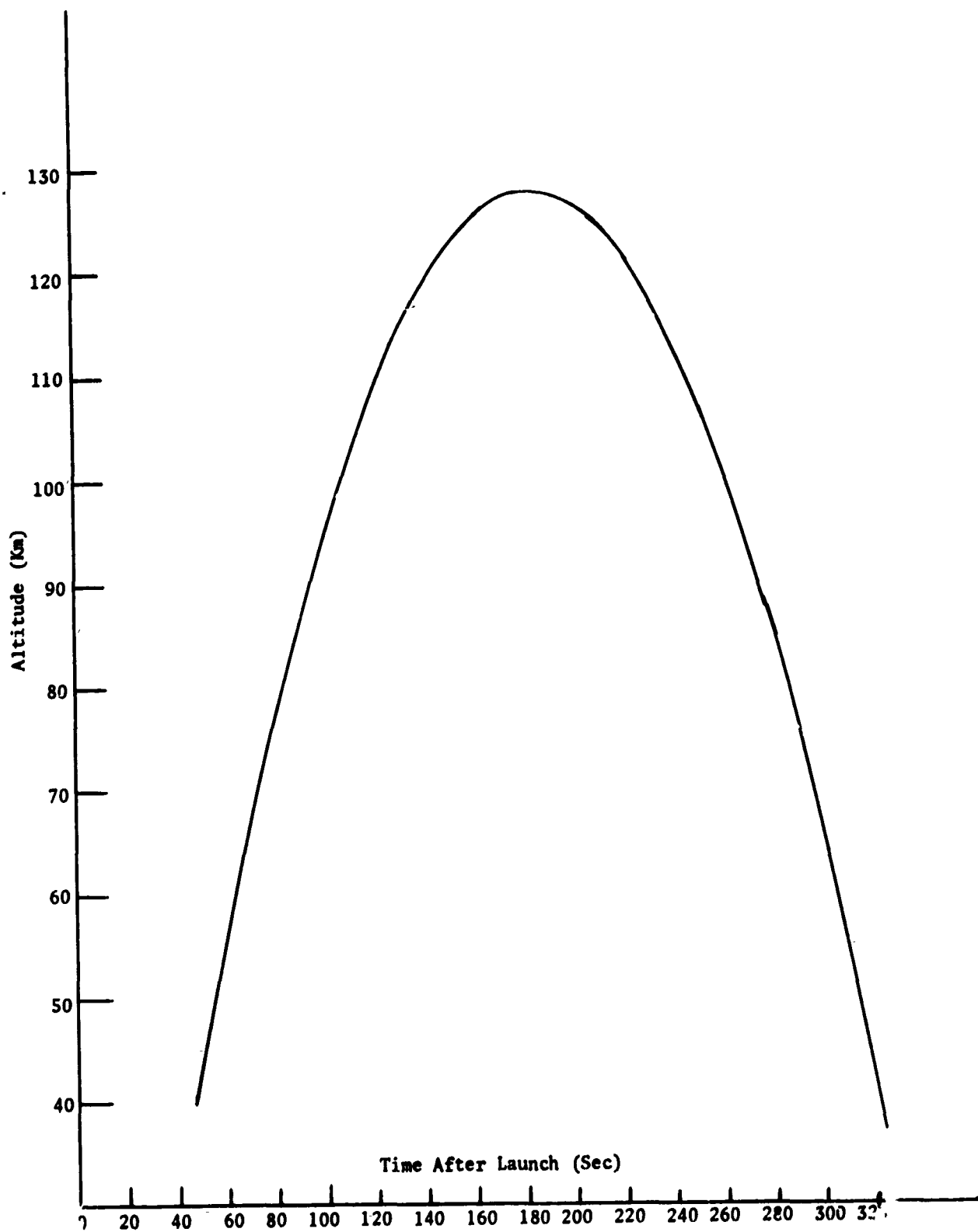


Figure 82 Vehicle Trajectory for AO 9.303-4



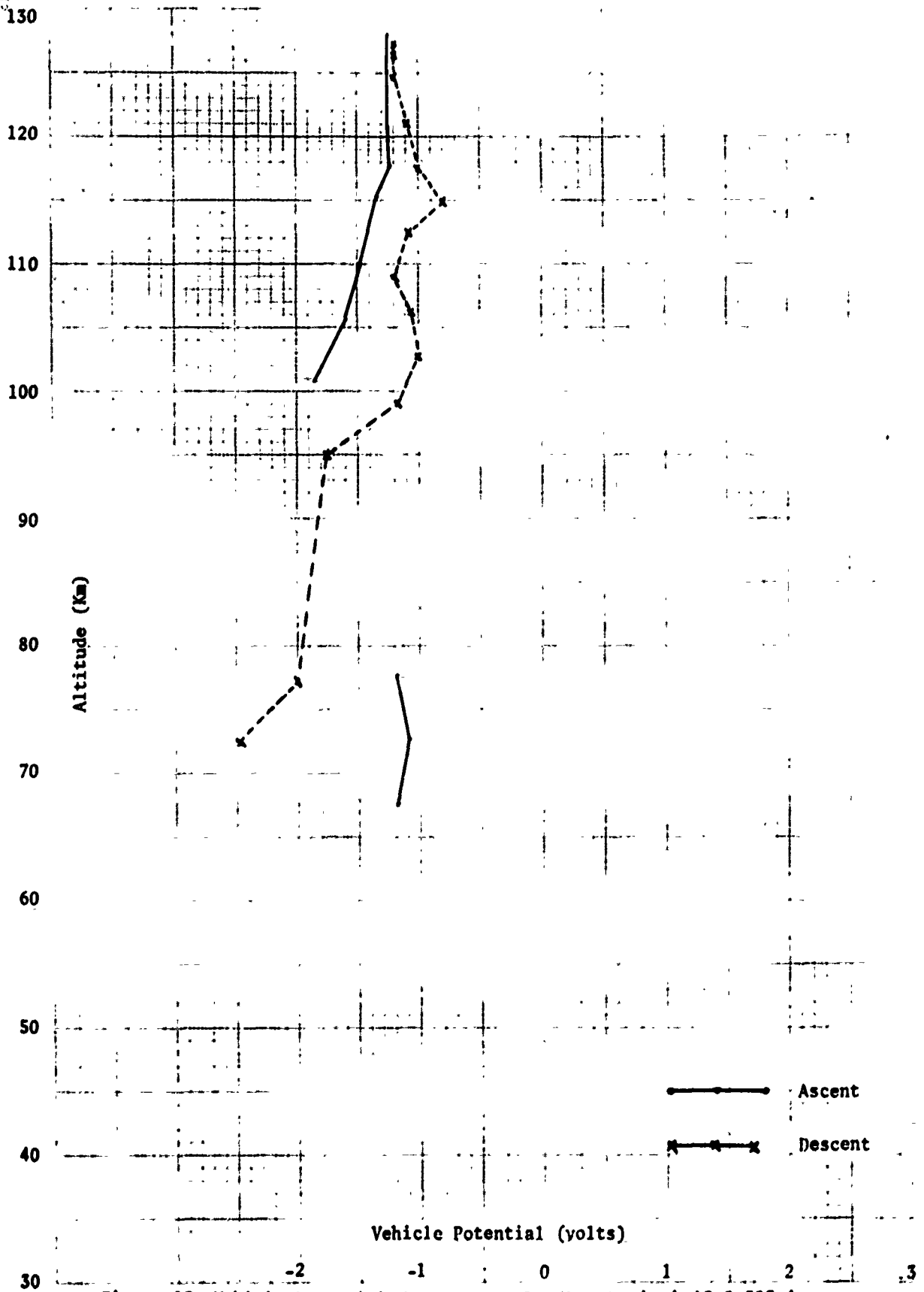


Figure 83 Vehicle Potential Measurement for Ute-Tomahawk AO 9.303-4

10 squares to the inch

K<sub>2</sub> SEMI LOGAR 46 GC12  
 400 100 10 1 0.1 0.01 0.001 0.0001 0.00001 0.000001 0.0000001

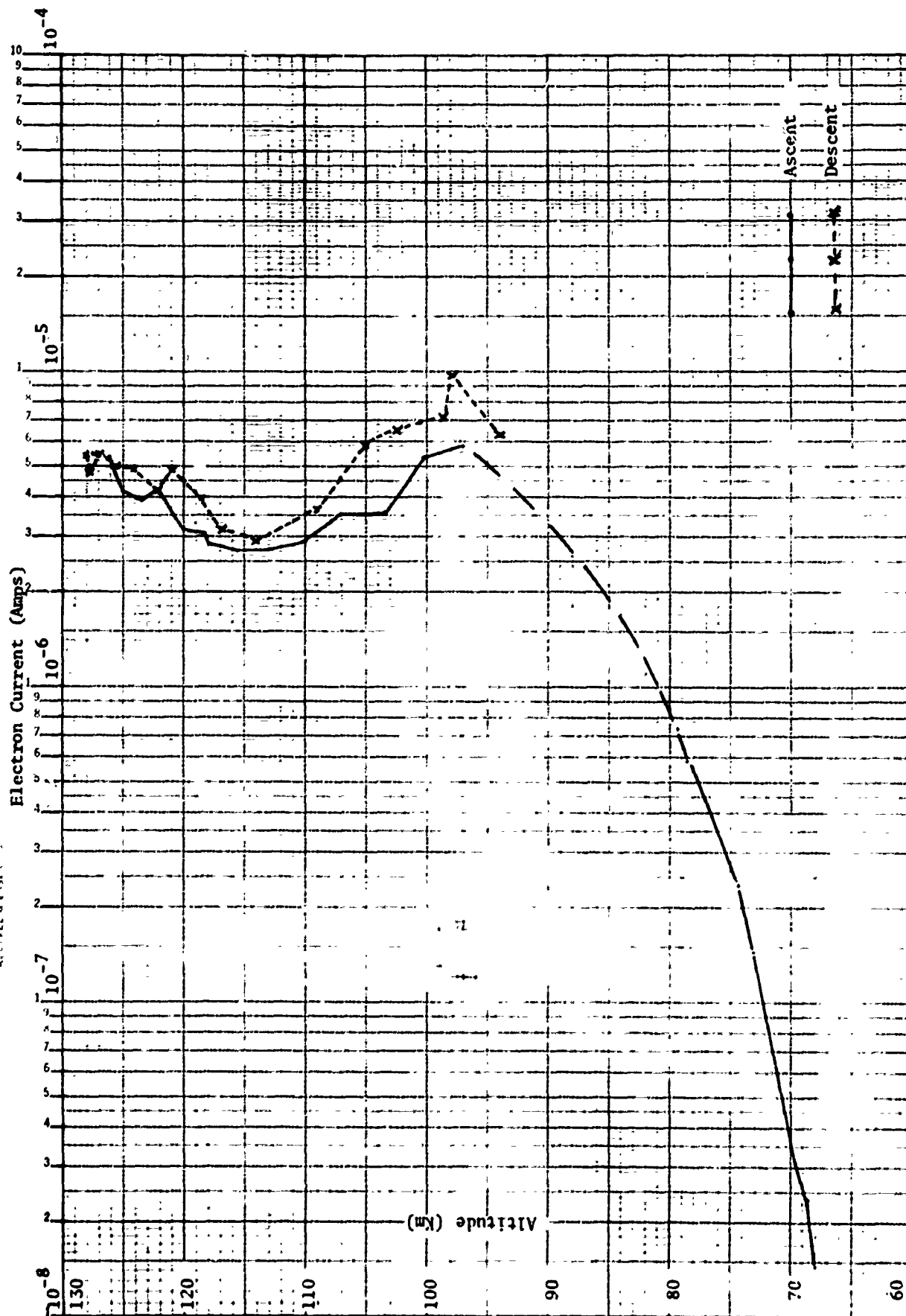


Figure 84 Electron Current Measured at +3 volts for AO 9.303-4

K-E SEMI-LOGARITHMIC 46 6012  
 4 CYCLES X 70 DIVISIONS  
 MADE IN U.S.A.  
 KEUFFEL & ESSER CO.

Positive Ion Current (Amps)

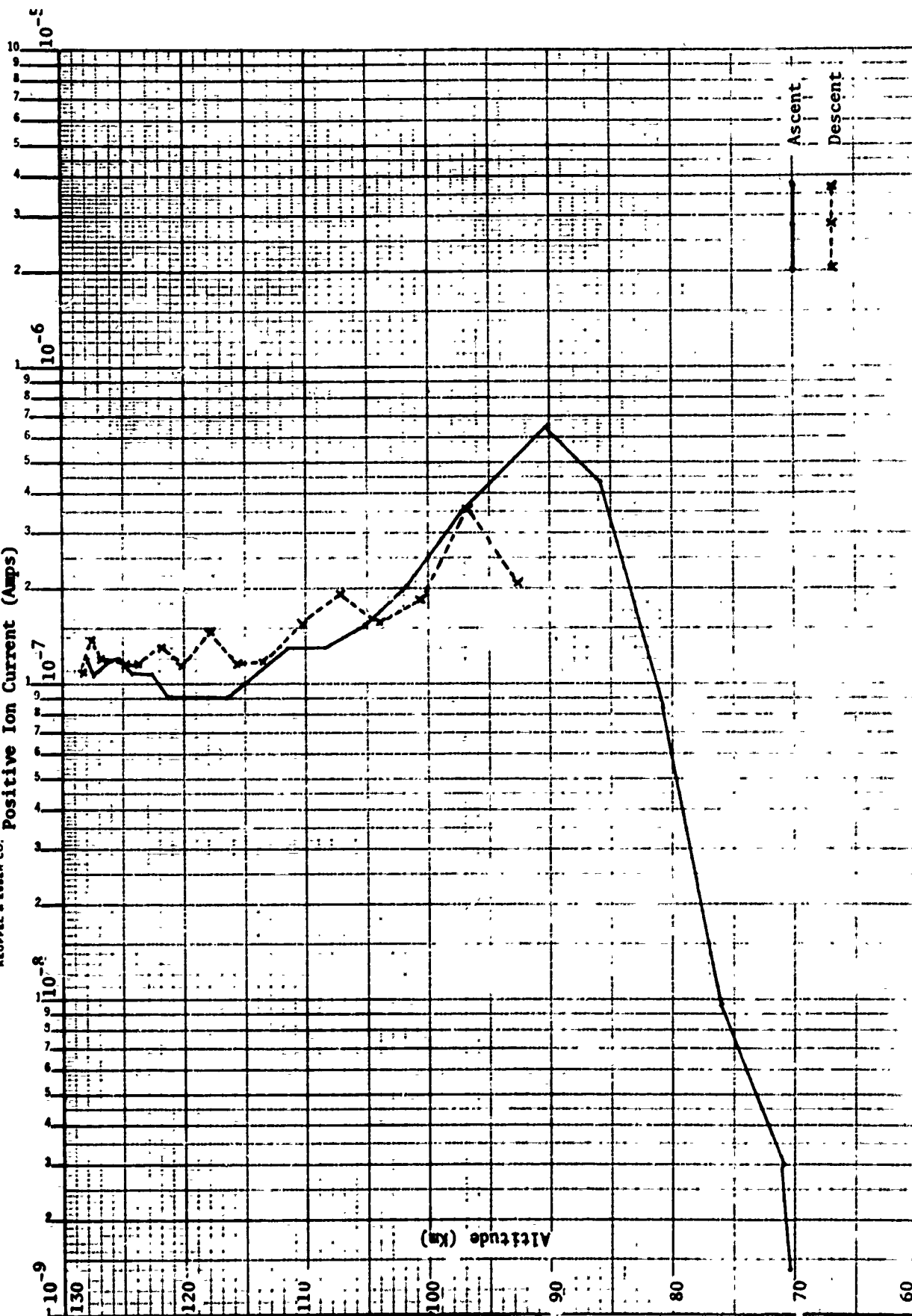


Figure 85 Positive Ion Current Measured at -9 Volts for Ute-Tomahawk AO 9.303-4

Positive Ion Current (Amps)

Altitude (Km)

Ascent

Descent

Altitude (Km)	Ascent (Amps)	Descent (Amps)
130	$1.0 \times 10^{-7}$	$1.0 \times 10^{-7}$
125	$1.0 \times 10^{-7}$	$1.0 \times 10^{-7}$
120	$1.0 \times 10^{-7}$	$1.0 \times 10^{-7}$
115	$1.0 \times 10^{-7}$	$1.0 \times 10^{-7}$
110	$1.0 \times 10^{-7}$	$1.0 \times 10^{-7}$
105	$1.5 \times 10^{-7}$	$1.0 \times 10^{-7}$
100	$1.5 \times 10^{-7}$	$1.0 \times 10^{-7}$
95	$2.5 \times 10^{-7}$	$2.5 \times 10^{-7}$
90	$4.5 \times 10^{-7}$	$1.8 \times 10^{-7}$
85	$3.5 \times 10^{-7}$	-
80	$1.0 \times 10^{-8}$	-
75	$8.0 \times 10^{-9}$	-
70	$7.0 \times 10^{-9}$	-
65	$5.0 \times 10^{-9}$	-

Figure 86 Positive Ion Current Measured at -3 Volts for Ute-Tomahawk A0 9.303-4

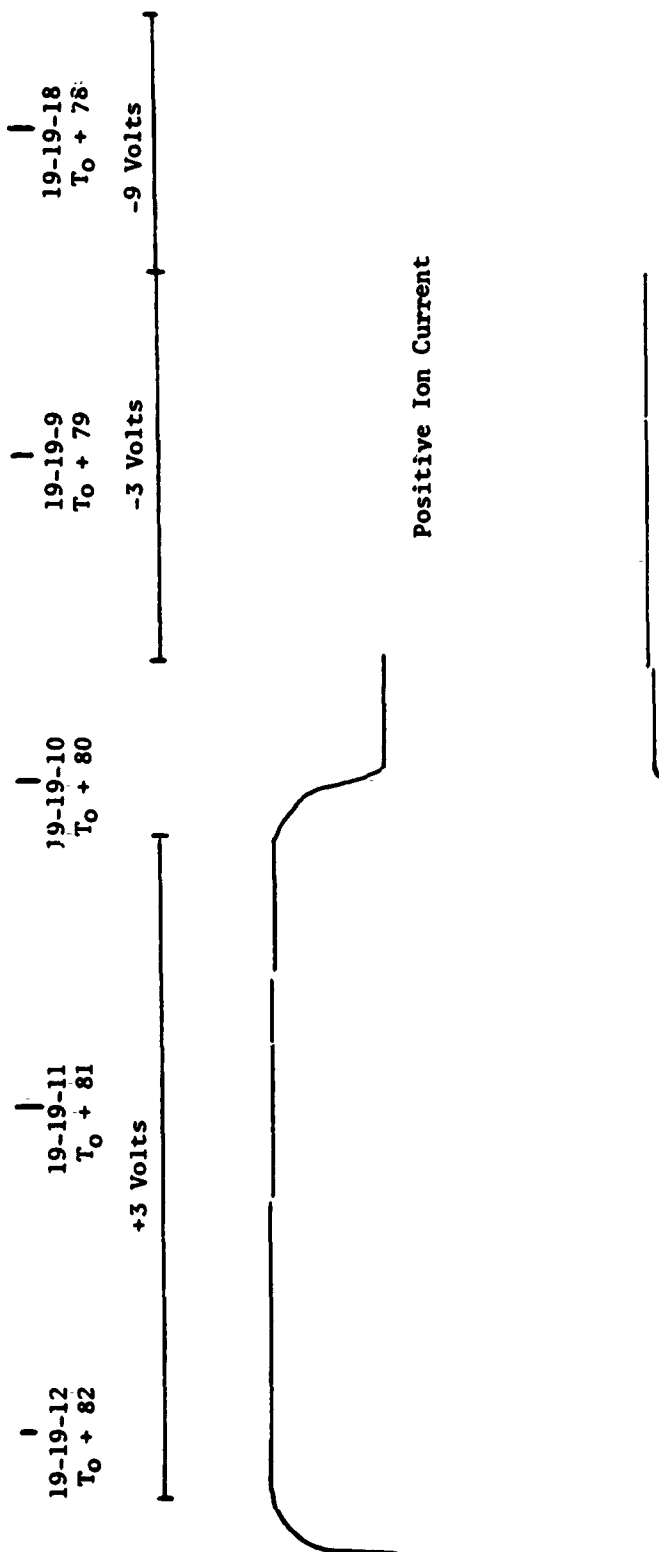


Figure 87 Strip Chart Data Between 75.7 km and 80.6 km on Vehicle Ascent for AO 9.303-4

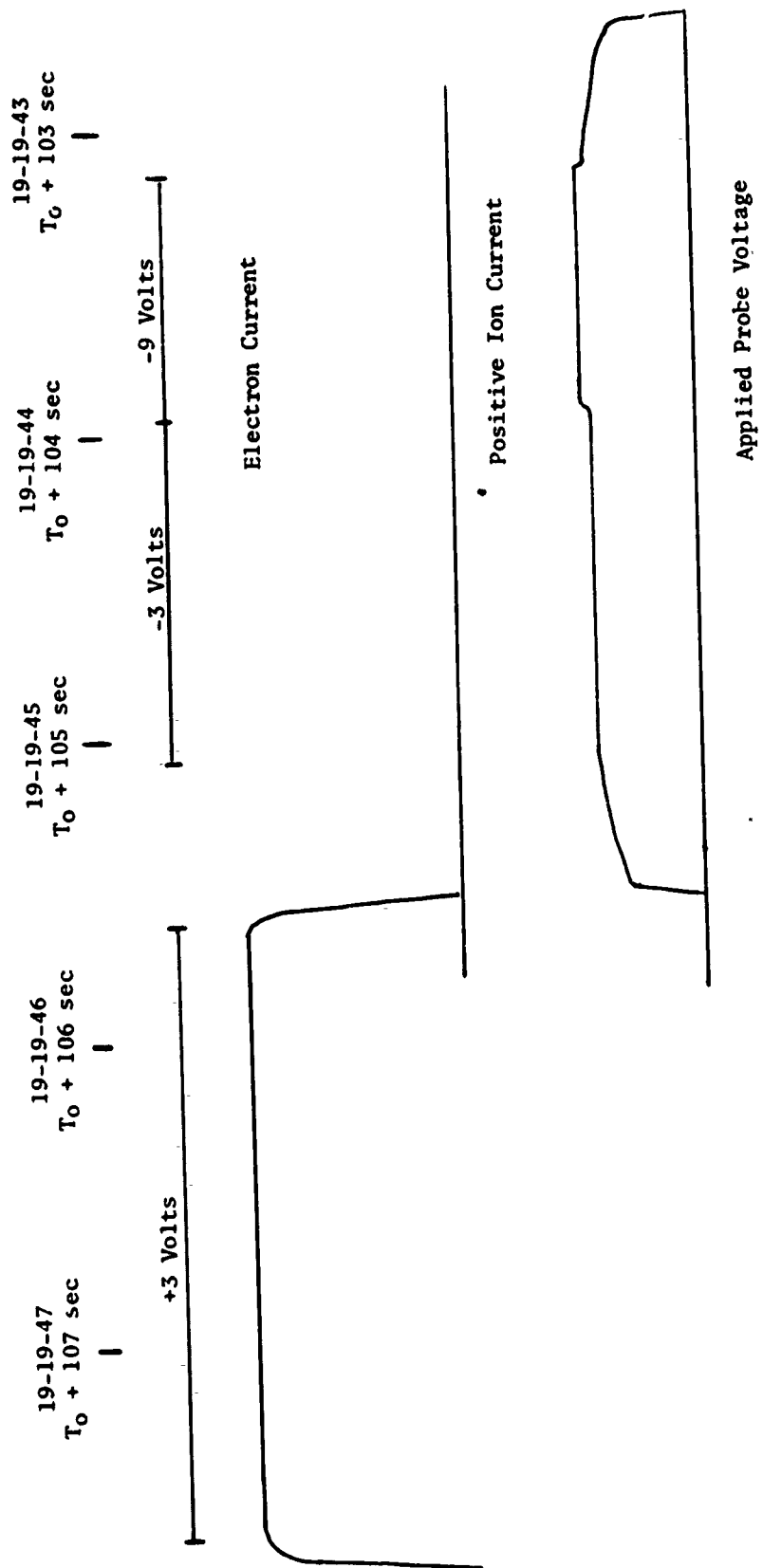


Figure 88 Strip Chart Data Between 97.6 km and 101.32 km on Vehicle Ascent for A0 9.303-4

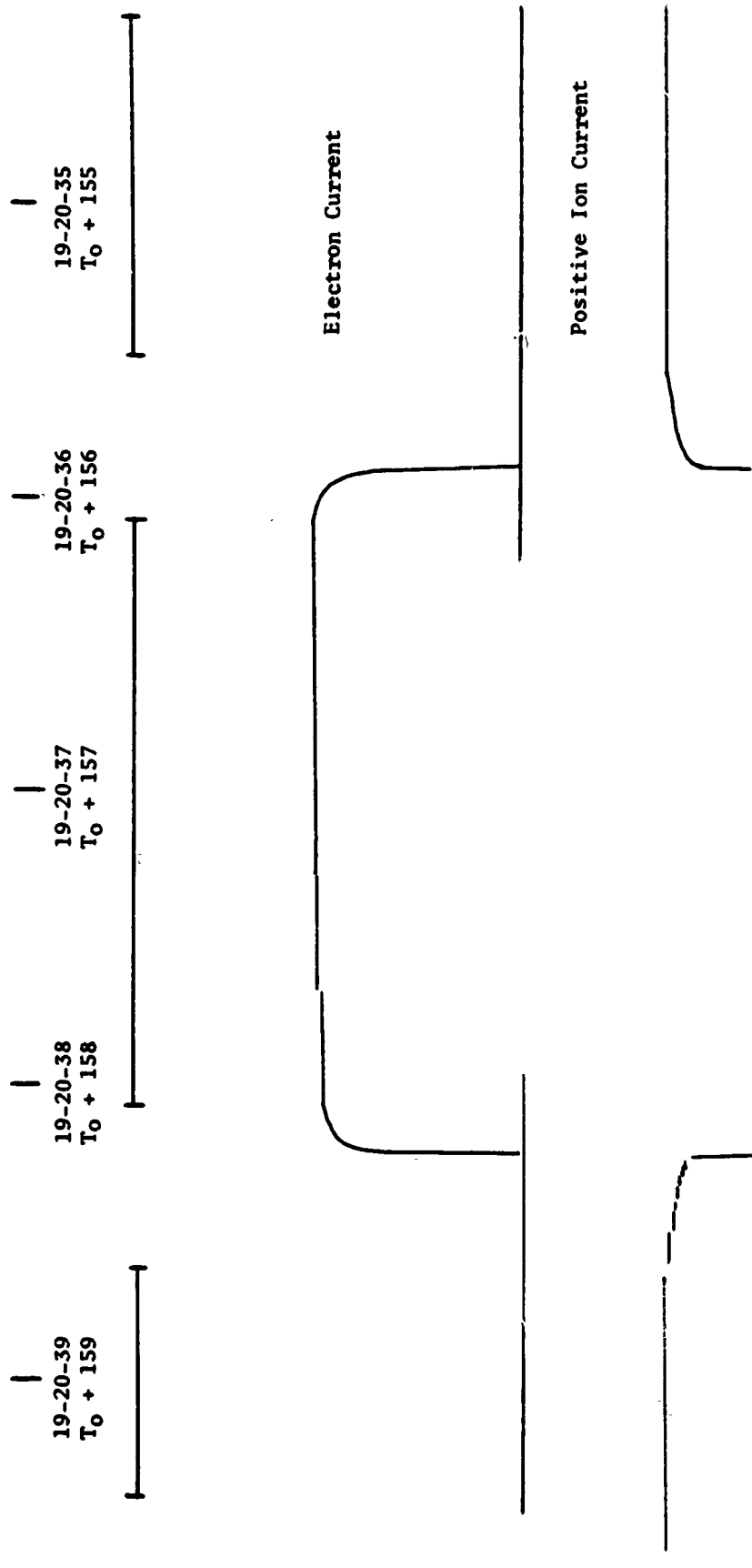


Figure 89 Strip Chart Data Between 124.3 km and 125.5 km on Vehicle Ascent for A0 9.303-4

19-21-21  
 $T_0 + 201$

19-21-22  
 $T_0 + 202$

19-21-23  
 $T_0 + 203$

19-21-24  
 $T_0 + 204$

19-21-25  
 $T_0 + 205$



Electron Current



Positive Ion Current



Figure 90 Strip Chart Data Between 126.67 km and 125.72 km on Vehicle Descent for AO 9.303-4



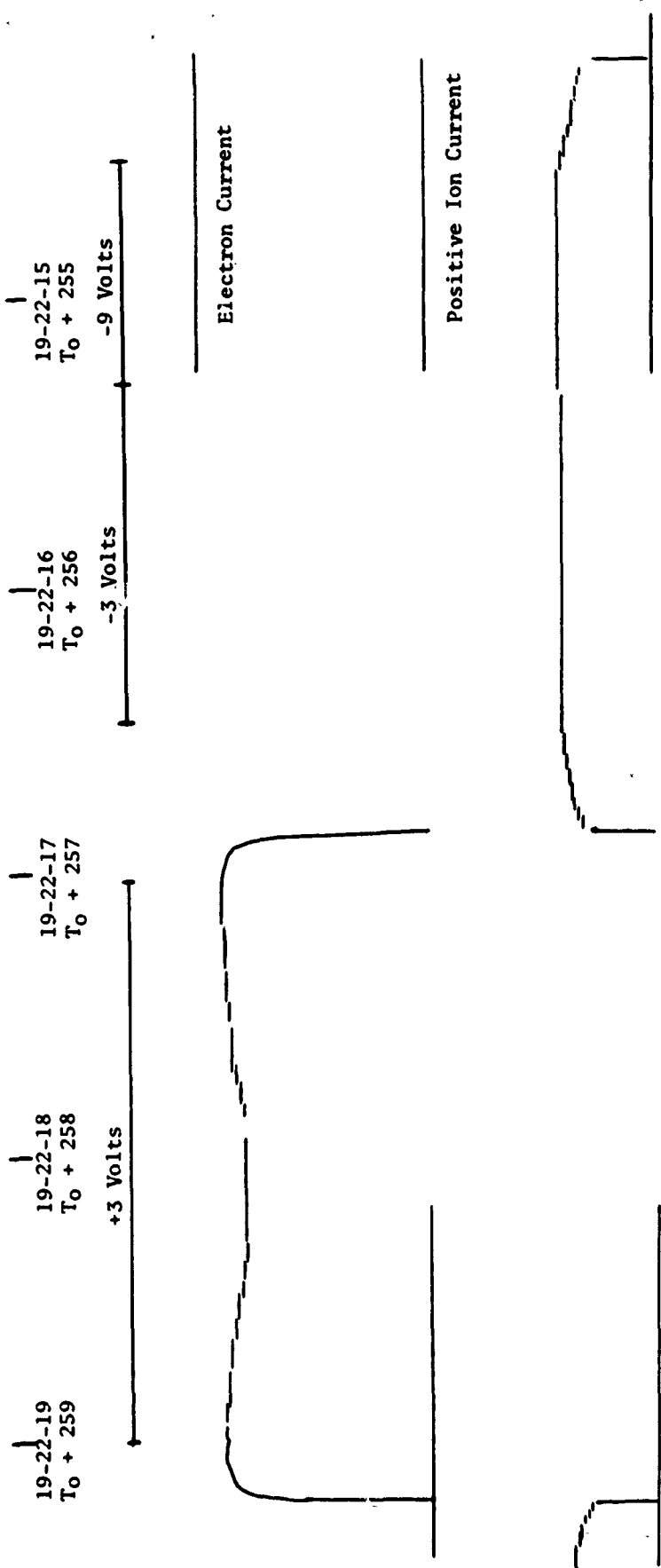


Figure 91 Strip Chart Data Between 103.96 km and 101.17 km during Vehicle Descent for AO 9.303-4

#### REFERENCES

1. Langmuir, I. and H.M. Mott-Smoth, Studies of Electrical Discharges in Gases of Low Pressures, Gen. Elec. Rev., 27, 449, 538, 616, 762, 810, 1924.
2. Smith, L.G., Langmuir Probes for Measurements in the Ionosphere, COSPAR Information Bulletin, No. 17, 37, 1964.
3. Seljaas, K.G., Calibration Manual, Langmuir Probe Model LP68-B Units 1-10 (NIRO SERIES, 33pp., Upper Air Research Laboratory, University of Utah, Salt Lake City, 27 June 1968.
4. Seljaas, K.G., Calibration Manual, Langmuir Probe Model LP68-B, Units 2A, 3A, 5A, 6A, 7A, 9A, and 10A (NIROS SERIES), 28 pp., Upper Air Research Laboratory, University of Utah, Salt Lake City, June 1969.
5. Calibration Manual, Langmuir Probes LP70A-1,2,3, 16 pp., Space Science Laboratory, Utah State University, Logan, February 1972.
6. Calibration Manual, Langmuir Probes LP71B-1,2,3,4, 19 pp., Space Science Laboratory, Utah State University, Logan, February 1972.
7. Calibration Manual, Langmuir Probe LP71B-6, LP71B-7, LP71B-8, LP71B-9, 19 pp., Space Science Laboratory, Utah State University, Logan, September 1973.

#### ACKNOWLEDGEMENTS

Grateful acknowledgements to Beverly Trudell for preparing the figures and to Arnetis Akre for her help in the typing and the preparation of the manuscript.

R.C.W.